STUDIES OF LEPTON AND QUARK INTERACTIONS

by

Ping Wang

Dissertation submitted to the Faculty of the

Virginia Polytechnic Institute and State University

in partial fulfillment of the requirements for the degree of

Doctor of Philosophy

in

physics

APPROVED:

R. E. Marshak, Chairman

A. Abashian

L. N. Chang

L. D. Roper

R. A. Arndt

May, 1985

Blacksburg, Virginia

STUDIES OF QUARK AND LEPTON INTERACTIONS

by

Ping Wang

Committee Chairman, R. E. Marshak

Physics

(ABSTRACT)

Part I

Proposed Experimental Tests of the Right-handed Weak Current

All possible experiments which test the $SU(2)_L \times U(1)_R \times U(1)_{B-L}$ model and $SU(2)_L \times SU(2)_R \times U(1)_{B-L}$ model using the LEP e^+e^- collider and HERA e^-p collider are calculated and the most sensitive experiments are examined.

Part II

Semi-Phenomenological Theory of $(Q\bar{q})$ System

The $(Q\bar{Q})$ and $(Q\bar{q})$ mesons are calculated using a QCD motivated potential model. It is discovered that by including a long distance relativistic correction term derived by Grome, the Coulomb + Linear potential works not only for c and b quarks, but s quark as well. The leptonic decay constants of various $(Q\bar{q})$ mesons together with their masses are predicted. The topponium states are also discussed.

ACKNOWLEDGEMENTS

First and foremost I am grateful to Professor R. E. Marshak's patient guidance during my dissertation work. His inspiring lectures sparked my attention to many interesting phenomena in elementary particle physics.

I am also indebted to Professor L. N. Chang who provided me the opportunity to come to Virginia Tech, and who has given me so much valuable advice.

I would like to thank Professor A. Abashian with whom I have discussed the experimental feasibility. Professor L. D. Roper and Professor R. A. Arndt gave me enormous help with the computer work. Dr. M. Manley helped me with the details of the numerical method used in the second part of this dissertation.

During these years, I have enjoyed many discussions in a free atmosphere with other graduate students in the department, particularly

also read the draft of this dissertion and polished its language.

Before leaving the U.S. for China, I thank many of my friends in the social circle of the department, especially

Their hospitality leave me many happy memories.

Finally, I want to thank some of the secretaries in the department for their helps and kindness, among them .

TABLE OF CONTENTS

List of Figures

Part I

PROPOSED EXPERIMENTAL TEST

OF THE RIGHT-HANDED WEAK CURRENT

INTRODUCTION

It is now generally believed that the weak and electromagnetic interactions are described by the $SU(2)_L xU(1)_Y$ local gauge theory, i.e. the Glashow-Weinberg-Salam (GWS) model. In the past decade, many experiments have tested this model. The neutral current, which is predicted by this theory, was discovered. The Weinberg angle, the only parameter in this theory, has been measured by different experiments, and the results agree with each other within experimental error. All the low energy experiments support the GWS model. The decisive test, however, is the direct observation of W and Z bosons, which mediate the charged and neutral weak currents in the theory, this experiment was done at CERN, with the results:

$$M(W) = 81\pm5 \text{ GeV } [1]$$

$$M(Z) = 91.9\pm1.3\pm1.4 \text{ GeV } [2]$$

which are what the theory predicts within experimental error. Thus the experiments support the GWS model to 100 GeV.

Despite these successes, there are some unsatisfactory features in this model, from both a physical point of view and an aesthetic point of view. In this model, the left-handed fermions are in a $SU(2)_L$ doublet, whereas the right-handed fermions are in a $SU(2)_L$ singlet. The parity breaking is put in by hand. The problem arises: is nature left-handed? Or is nature left-right symmetric (LRS), and the observed parity breaking spontaneous? From the aesthetic point of view, the second answer seems preferable.

In the standard model, the hypercharge quantum number Y has an obscure physical meaning. It depends on the helicity of the fermion as well as whether it is a quark or lepton. This violates full quark-lepton symmetry, in addition to the breaking of left-right symmetry.

In the standard model, there are only left-handed neutrinos, which are massless, but some theories of cosmology suggest that the neutrino has a finite mass. To accommodate the massive neutrinos in the standard model, one must introduce a Yukawa coupling constant for neutrinos which is five orders of magnitude smaller than that for other fermions, which seems unnatural. An alternative is to assume that the neutrino is a Majorana particle. To give the Majorana mass in the standard model, a Higgs triplet is needed. Unlike the Higgs doublet , which gives both the gauge boson masses and fermion masses, the only role of this Higgs triplet is to give mass to the neutrino. This does not seem beautiful.

Because of these reasons, some people have suggested that the standard model is only the low energy limit of a gauge theory with more gauge bosons. The simplest extension of the standard model is a two-Z-boson theory.

If there are two Z bosons, what is the quantum number of the third gauge group? There are many suggestions. But the most promising one is that the third gauge group is B-L. The quantum number B-L has a clear physical meaning, and restores the full quark-lepton symmetry for the hypercharge. We know that B-L symmetry should be broken. By breaking the B-L symmetry, one gets Majorana neutrinos, and the right-handed Majorana neutrino mass is at the mass scale at which B-L symmetry is broken.

We know the first gauge group has to be $SU(2)_L$ to explain all the well known low energy phenomena. The electric charge must be:

$$Q=I_{3L}+I_2+(B-L)/2$$

where I_2 represents the quantum number associated with a right-handed representation of a quark or a lepton. Depending on whether the second group is $SU(2)_R$ or $U(1)_R$, there are two possible models which treat B-L as a local symmetry:

$$SU(2)_L x U(1)_R x U(1)_{B-L} \text{ or } SU(2)_L x SU(2)_R x U(1)_{B-L}$$

First consider the $SU(2)_L x SU(2)_R x U(1)_{B-L}$ model[3]. In this model, the fermion representations for the first generation are:

$$(u,d)_L=(2,1,1/3)$$

$$(u,d)_R=(1,2,1/3)$$

$$(\nu,e)_L=(2,1,1)$$

$$(\nu,e)_R=(1,2,1)$$

and $Q = I_{3L} + I_{3R} + (B-L)/2$. The left-right symmetry suggests that $g_L=g_R$, where g_L is the $SU(2)_L$ gauge coupling constant and g_R is the $SU(2)_R$ gauge coupling contant. However, one can have $g_L \neq g_R$(see below).

From the K_L-K_S mass difference, the limit on M_R is:

$$M_R \geq 1.6 \text{ TeV}.$$

There is no limit for the mass of Z_2 . The ratio of the Z_2 mass to the W_R mass depends on the Higgs structure.

Next we consider the $SU(2)_L x U(1)_R x U(1)_{B-L}$ model. The fermion representations are:

$$(u,d)_L = (2,1,1/3)$$

$$(\nu,e)_L= (2,1,1)$$

$$u_R = (1,1/2,1/3)$$

$$d_R = (1,-1/2,1/3)$$

$$\nu_R = (1,1/2,1)$$

$$e_R = (1,-1/2,1)$$

and $Q = I_{3L} + I_R + (B-L)/2$

In this case there is no reason to assume that $g_L = g_R$, and the value of g_L/g_R can be calculated from the symmetry breaking if $SU(2)_L x U(1)_R x U(1)_{B-L}$ is embedded in a larger group.

Another motivation of two-Z-boson theory is that it may provide evidence for an intermediate mass scale of a larger unification group. In the first grand unification theory proposed by Georgi and Glashow, the unification group is SU(5); it contains the standard group $SU(2)_L x U(1)_Y x SU(3)_C$ as the maximal subgroup. The SU(5) grand unification group does not have a mass scale between M_W (the mass of the left-handed weak gauge boson) and M_X (the grand unification mass scale). It predicts the correct $\sin^2\theta_W$ value. But it also predicts proton decay into $e^+\pi^0$, with a decay rate which is not supported by experiment.

The failure of SU(5) forces one to consider other grand unification groups. It has been known for some time that SO(10) is an alternative to SU(5). It has the property of being a simple group that contains $SU(2)_L$, $U(1)_Y$ and $SU(3)_C$ as subgroups. Also, it has some advantages: 1) The 16 dimensional representation of SO(10) accommodates all the 15 quark and lepton states plus a right-handed neutrino state so that the full quark-lepton symmetry is restored. 2) The inclusion of ν_R in the 16 dimensional representation of SO(10) implies a Majorana neutrino mass, in contrast to the massless neutrino in minimal SU(5). 3) B-L is a generator of the SO(10) group (in SU(5) it is only globally conserved).

The gauging of B-L or the gauging of quark-lepton symmetry is achieved by requiring the group $U(1)_{B-L}$ to be a subgroup of the grand unification group. The gauging of B-L and its spontaneous breaking opens up many new possibilities. These theories can be tested at energies above 100 GeV.

Among all the chains of SO(10) descending to the standard group $SU(2)_L x U(1)_Y x SU(3)_C$, Chang et al. [4] found that if one imposes a minimality condition (using the lowest dimensional Higgs at each symmetry-breaking stage) and the phenomenological requirement :

$$\tau_p \to e^+ \pi^0 \geq 2 \times 10^{32} \text{ years}$$

$$\sin^2\theta_W(M_W) = 0.22 \pm 0.02$$

$$\alpha_s(M_W) = 0.10 \sim 0.12$$

then there is a unique chain which allows interesting physics at relatively low energies. This chain is :

$$\begin{aligned} SO(10) &\xrightarrow{M_U} SU(2)_L x SU(2)_R x SU(4)_C x P \xrightarrow{M_P} SU(2)_L x SU(2)_R x SU(4)_C \\ &\xrightarrow{M_R^+} SU(2)_L x U(1)_R x U(1)_{B-L} x SU(3)_C \xrightarrow{M_R^0} SU(2)_L x U(1)_Y x SU(3)_C \end{aligned} \qquad (1)$$

where M_U is the mass scale at which SO(10) is spontaneously broken to $SU(2)_L x SU(2)_R x SU(4)_C x P$. Similarly, M_P, M_R^+, and M_R^0 are the mass scales at which the symmetries are spontaneously broken from one level to the next. The symbol P means the symmetry under D parity transformation. This symmetry is broken at mass scale M_P . D parity is defined as the element of SO(10) group:

$$D = \Sigma_{23}\Sigma_{67}$$

where $\Sigma_{\mu\nu}$ ($\mu,\nu,\ldots 10$) are the 45 totally antisymmetric generators of SO(10). Under the operator D, the fermions transform as:

$$f_L \xrightarrow{D} f_L^C = (C\bar{f})_L \tag{2}$$

In this chain, $g_L = g_R$ is valid only above the M_P mass scale. When the symmetry is broken down to $SU(2)_L xSU(2)_R xU(1)_{B-L} xSU(3)_C$, $g_L \neq g_R$.

The mass scales at which the symmetry breaking happens are:

$$\log M_U = 16.6 \sim 16.1$$

$$\log M_P = 14.0$$

$$5 \leq \log M_{R^+} \leq 7$$

$$M_{R^0} \simeq M_W$$

The second neutral Z boson is expected to be in the range of 300 to 1000 GeV. There are many physical consequences. Among them, the branching ratio for $K_L^0 \rightarrow \mu^+ e^-$ is approximately $10^{-8} \sim 10^{-12}$, the n-$\bar{n}$ osillation time $\tau_{n\bar{n}} \simeq 10^8 \sim 10^9$ sec. The proton life time $\tau_p \simeq 6.5 \times 10^{35 \pm 0.9} (\Lambda_{\overline{MS}} / 160\text{Mev})^4$ years, and

$$B.R.(p \rightarrow e^+ \pi^0) = B.R.(p \rightarrow \nu \pi^+)$$

In this symmetry breaking chain, at the symmetry level $SU(2)_L xU(1)_R xU(1)_{B-L}$, the coupling constant of $SU(2)_L$ and $U(1)_R$ are related, at the energy scale M_W , by the renormalizion group equation:

$$\begin{aligned} \varepsilon^2 &\equiv g_L^2(M_W) \;/\; g_R^2(M_W) \\ &= 1 + (11/6/\pi)\; \alpha(M_W)/\sin^2\theta_W(M_W)\; \log(M_P/M_W) \end{aligned} \tag{3}$$

In this symmetry breaking chain, $\log M_P = 14.0$, so that $\varepsilon(M_W) \simeq 1.09$. Later on, this value will be used for numerical calculations of the $SU(2)_L xU(1)_R xU(1)_{B-L}$ model predictions.

We see that the unique chain predicted by this new SO(10) model descends through the subgroup $SU(2)_L xU(1)_R xU(1)_{B-L}$ but not the group $SU(2)_L xSU(2)_R xU(1)_{B-L}$, with a well-defined range of $M_R 0$. Consequently, the experimental tests of the group $SU(2)_L xU(1)_R xU(1)_{B-L}$ and $SU(2)_L xSU(2)_R xU(1)_{B-L}$ that we are considering in the following will give us a broader range of physical possibilities than the unique chain of SO(10).

EXPERIMENTAL TESTS ON THE ELECTRON-POSITRON COLLIDER(LEP)

The-two-Z boson model embeds the standard model, i.e. at energy of 100 GeV it breaks down spontaneously to the $SU(2)_L xU(1)_Y$ group. The two-Z-boson model and the standard model agree on all the low energy phenomena predictions. The way to distinguish them is to go to energies above 100 GeV.

There are two new generation accelerators under construction which will be able to test the physics beyond the standard model, in particular to test if there is a second Z boson. They are the e^+-e^- collider LEP, and the e-p collider HERA. In this section we will consider the possible experiments at LEP.

The LEP e^+-e^- collider will eventually have 260 GeV in c.m. (center of mass) energy, or 130 GeV for each beam. The beams can be polarized. There are many measurements that can be done with it. Some of them will be sensitive to the second Z boson if its mass is in the neighborhood of ~ 300GeV.

Because the lower limit of the W_R mass is 1.6 TeV, which is very heavy compared to the LEP energy, and any leptonic process involving W_R, in the tree level, also involves the right-handed neutrino, which is very massive, the way to test the right-handed current in the e^+-e^- process is to look for the effects due to the second Z boson.

In e^+-e^- collisions, there are two types of final products which can be measured: e^+-e^- and f^+-f^- (where f is any fermion other than electron).

Let us first consider the process $e^+e^-\to e^+e^-$.

This process is calculated from the Feynman diagrams in Fig 1. The initial beams can be naturally polarized, i.e., the e^+ beam and e^- beam are transversly polarized, parallel and anti-parallel respectively to the magnetic field of the accelerator. In this case, the final state e^+e^- distribution along different azimuthal angles can be measured. The collider is designed so that the beams can also be longitudinally polarized.

Considering all the possible polarizations, the differential cross sections are for:

naturally polarized beam

$$\begin{aligned}\frac{d\sigma}{d\Omega}=(E^2/8\pi^2)\sum_{i,j=1}^{N}&[(g_V^ig_V^j+g_A^ig_A^j)^2(1+\cos^4\tfrac{\theta}{2})+(g_V^ig_A^j+g_V^ig_A^j)^2(\cos^4\tfrac{\theta}{2}-1)]\\&[1/(4E^2\sin^2\tfrac{\theta}{2}+M_{Z_i})(4E^2\sin^2\tfrac{\theta}{2}+M_{Z_j})]\\&+[(g_V^ig_V^j+g_A^ig_A^j)\frac{1+\cos^2\theta}{2}+(g_V^ig_A^j+g_A^ig_V^j)\cos\theta\\&+(g_V^ig_V^j-g_A^ig_A^j)(g_V^ig_V^j+g_A^ig_A^j)\frac{\sin^2\theta\cos2\phi}{2}]\\&\mathrm{Re}[1/(4E^2-M_{Z_i}^2+iM_{Z_i}\Gamma_i)(4E^2-M_{Z_j}^2-iM_{Z_j}\Gamma_j)]\\&-\{2[(g_V^ig_V^j+g_A^ig_A^j)+(g_V^ig_A^j+g_A^ig_V^j)^2]\cos^4\tfrac{\theta}{2}\\&+[(g_V^ig_V^j+g_A^ig_A^j)(g_V^ig_V^j-g_A^ig_A^j)+(g_V^ig_A^j+g_A^ig_V^j)(g_A^ig_V^j-g_V^ig_A^j)]\\&\frac{\sin^2\theta\cos2\phi}{2}\,\mathrm{Re}[1/(4E^2\sin^2\tfrac{\theta}{2}+M_{Z_i}^2)(4E^2-M_{Z_j}^2-iM_{Z_j}\Gamma_j)]\end{aligned}\qquad(4)$$

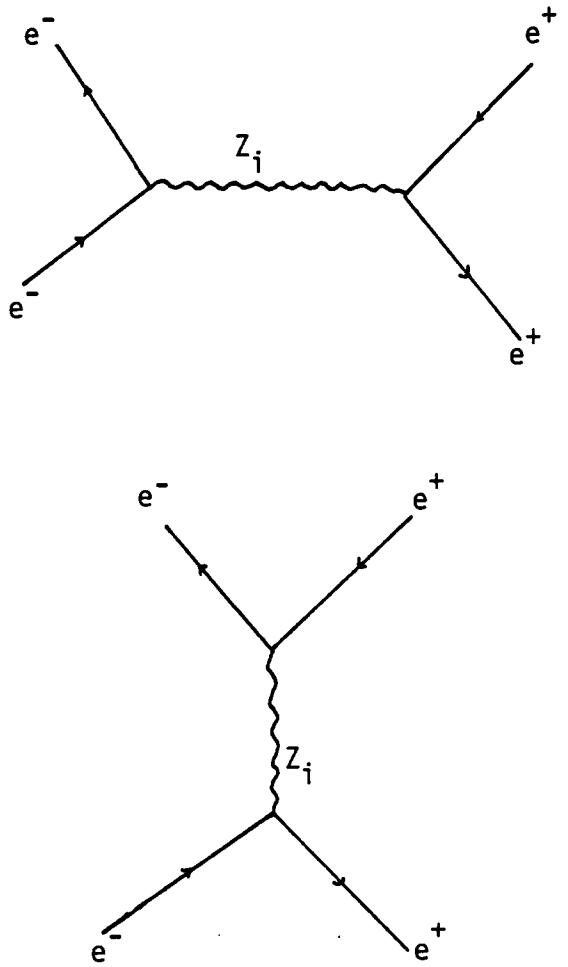

Figure 1

$e^+(L)e^-(L)\rightarrow e^+e^-$

$$\frac{d\sigma}{d\Omega}=(E^2/4\pi^2)\sum_{i,j=1}^{N}(g_V^i-g_A^i)^2(g_V^j-g_A^j)^2\cos^4\frac{\theta}{2} \qquad (5)$$
$$[1/(4E^2\sin^2\frac{\theta}{2}+M_{Z_i}^2)(4E^2\sin^2\frac{\theta}{2}+M_{Z_j}^2)]$$

$e^+(R)e^-(R)\rightarrow e^+e^-$

$$\frac{d\sigma}{d\Omega}=(E^2/4\pi^2)\sum_{i,j=1}^{N}(g_V^i+g_A^i)^2(g_V^j+g_A^j)^2\cos^4\frac{\theta}{2} \qquad (6)$$
$$[1/(4E^2\sin^2\frac{\theta}{2}+M_{Z_i}^2)(4E^2\sin^2\frac{\theta}{2}+M_{Z_j}^2)]$$

$e^+(L)e^-(R)\rightarrow e^+e^-$

$$\frac{d\sigma}{d\Omega}=(E^2/4\pi^2)\sum_{i,j=1}^{N}[(g_V^i)^2-(g_A^i)^2][(g_V^j)^2-(g_A^j)^2] \qquad (7)$$
$$[1/(4E^2\sin^2\frac{\theta}{2}+M_{Z_i}^2)(4E^2\sin^2\frac{\theta}{2}+M_{Z_j}^2)]$$
$$+(g_V^i-g_A^i)^2(g_V^j-g_A^j)^2\cos^4\frac{\theta}{2}$$
$$+\{(g_V^i-g_A^i)^2(g_V^j-g_A^j)^2\cos^4\frac{\theta}{2}+[(g_V^i)^2-(g_A^i)^2][(g_V^j)^2-(g_A^j)^2]\sin^4\frac{\theta}{2}\}$$
$$\mathrm{Re}[1/(4E^2-M_{Z_i}^2+iM_{Z_i}\Gamma_i)(4E^2-M_{Z_j}^2-iM_{Z_j}\Gamma_j)]$$

$e^+(R)e^-(L) \to e^+e^-$

$$\frac{d\sigma}{d\Omega} = (E^2/4\pi^2) \sum_{i,j=1}^{N} [(g_V^i)^2-(g_A^i)^2][(g_V^j)^2-(g_A^j)^2]$$
$$[1/(4E^2\sin^2\frac{\theta}{2}+M_{Z_i}^2)(4E^2\sin^2\frac{\theta}{2}+M_{Z_j}^2)]$$
$$+(g_V^i+g_A^i)^2(g_V^j+g_A^j)^2\cos^4\frac{\theta}{2} \qquad (8)$$
$$\mathrm{Re}[1/(4E^2\sin^2\frac{\theta}{2}+M_{Z_i}^2)(4E^2-M_{Z_j}^2-iM_{Z_j}\Gamma_j)]$$
$$\{(g_V^i+g_A^i)^2(g_V^j+g_A^j)^2\cos^4\frac{\theta}{2}+[(g_V^i)^2-(g_A^i)^2][(g_V^j)^2-(g_A^j)^2]\sin^4\frac{\theta}{2}\}$$
$$\mathrm{Re}[1/(4E^2-M_{Z_i}^2+iM_{Z_i}\Gamma_i)(4E^2-M_{Z_j}^2-iM_{Z_j}\Gamma_j)]$$

In the above expressions, E is the energy per beam, N is the number of neutral gauge bosons in the model that we are considering, including the photon. For the GWS model, N=2. For the two-Z-boson models, N=3; and M_{Z_i} is the mass of the ith neutral gauge boson, where Γ_i is its width; the coupling of Z_i to the vector part of the neutral weak current is g_V^i and g_A^i is the coupling of Z_i to the axial vector part of the neutral weak current.

In the standard model, N=2

$$g_V^{(1)} = e = g\sin\theta_W$$
$$g_A^{(1)} = 0$$
$$g_V^{(2)} = g(-1/4+\sin^2\theta_W)/\cos\theta_W$$
$$g_A^{(2)} = -g/4/\cos\theta_W.$$

Whereas in the $SU(2)_L xSU(2)_R xU(1)_{B-L}$ model, N=3 and $g_V^{(1)}$, $g_A^{(1)}$, $g_V^{(2)}$, $g_A^{(2)}$ are the same as in the standard model, however,

$$g_V^{(3)} = (-1/4+\sin^2\theta_W) \ /\cos\theta_W/\surd/(1-2\sin^2\theta_W)$$

$$g_A^{(3)} = (1/4)(1-2\sin^2\theta_W) \ /\cos\theta_W/\surd \ (1-2\sin^2\theta_W)$$

In the $SU(2)_L xU(1)_R xU(1)_{B-L}$ model, the $g_V^{(1)}$, $g_A^{(1)}$, $g_V^{(2)}$, $g_A^{(2)}$ are also the same as in the standard model, however,

$$g_V^{(3)} = (-1/4\cos\theta_W) \ [\surd(\cos^2\theta_W-\varepsilon^2 \ \sin^2\theta_W)/\varepsilon$$

$$-2\varepsilon\sin^2\theta_W/ \ \surd(\cos^2\theta_W-\varepsilon^2\sin^2\theta_W)]$$

$$g_A^{(3)} = (-1/4\cos\theta_W) \ \surd(\cos^2\theta_W-2\varepsilon^2\sin^2\theta_W) \ /\varepsilon$$

where $\varepsilon = g_L / g_R$. Assuming the parameters of the $SU(2)_L xU(1)_R xU(1)_{B-L}$ and $SU(2)_L xSU(2)_R xU(1)_{B-L}$ are:

$$M(Z_R) = 300 \text{ Gev}$$

$$\sin^2\theta_W = 0.22$$

and for $SU(2)_L xU(1)_R xU(1)_{B-L}$, $g_R/g_L=1.09$. the numerical results are given in Figures 2 to 7. Throughout this paper, we shall use the same parameters for all the numerical calculations.

Here some comment is needed. For the difference between the cross sections of $e^+(L)e^-(R) \rightarrow e^+e^-$ and $e^+(R)e^-(L) \rightarrow e^+e^-$, the $SU(2)_L xSU(2)_R xU(1)_{B-L}$ model predicts a large deviation from the standard model, whereas the $SU(2)_L xU(1)_R xU(1)_{B-L}$ model does not. The reason for this is that the coupling of Z_2 to the electron current behaves differently in different two-Z-boson models.

In $SU(2)_L xSU(2)_R xU(1)_{B-L}$

$$g_L = g_V^{(3)}+g_A^{(3)} = 0.147$$

$$g_R = g_V^{(3)}-g_A^{(3)} = -0.227$$

whereas in SU(2)xU(1)xU(1)

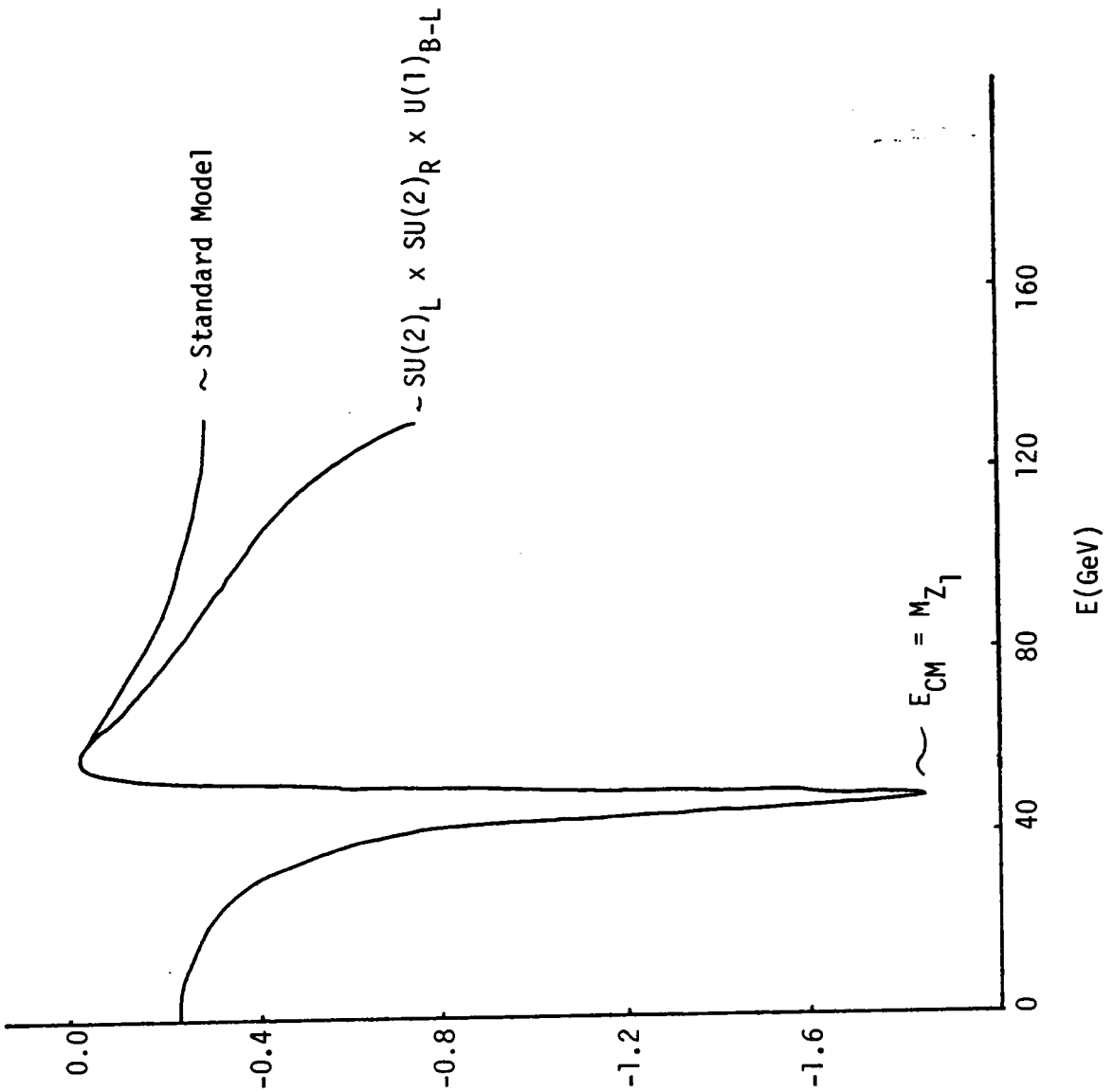

$e^+e^- \to e^+e^-$ naturally polarized beam

$$A = \frac{d\sigma(0<\phi<\frac{\pi}{2}) - d\sigma(\frac{\pi}{2}<\phi<\pi)}{d\sigma(0<\phi<\pi)} \quad \text{at } \theta = \frac{\pi}{2}$$

Figure 2

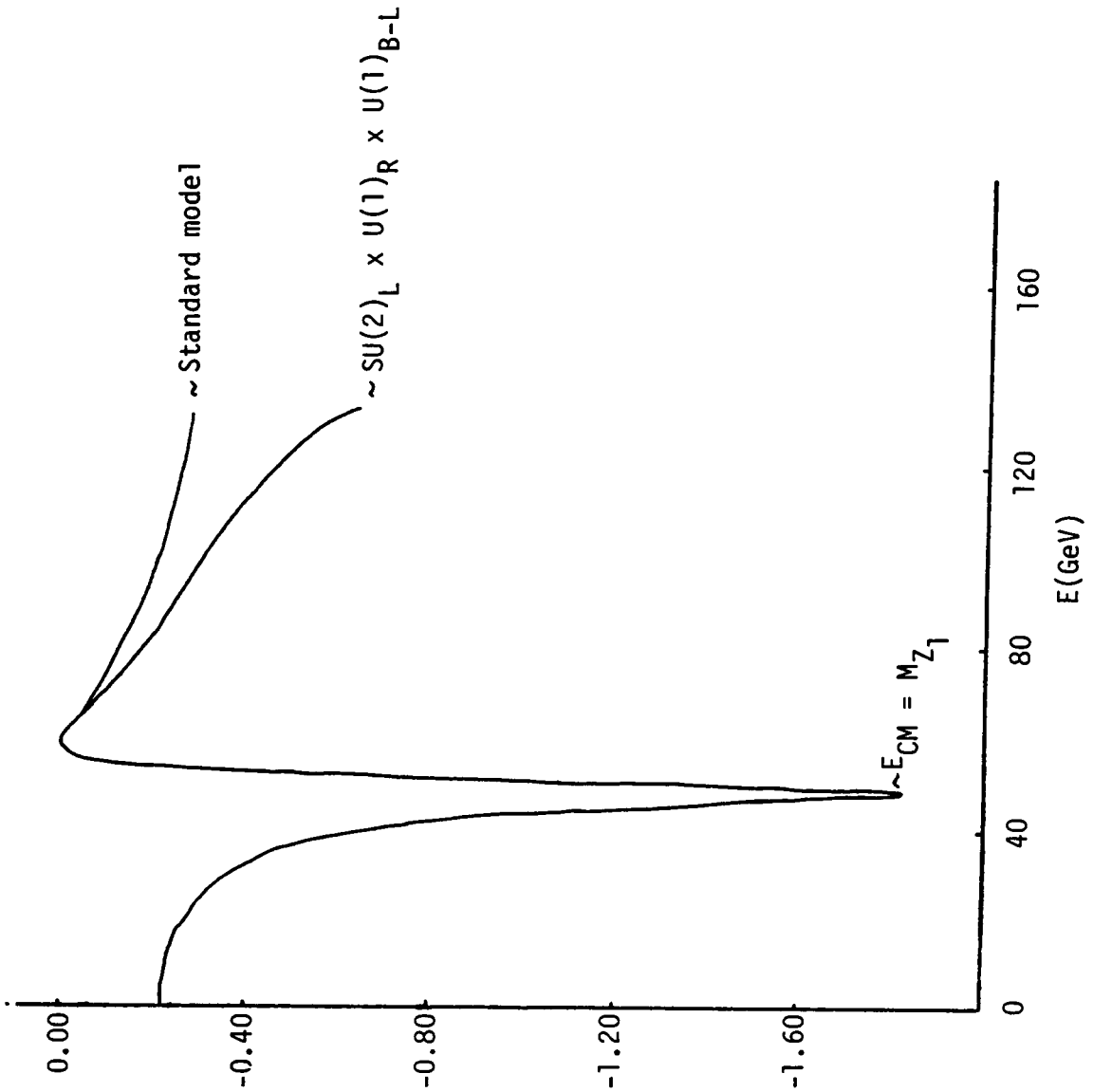

$d\sigma(e^+e^- \to e^+e^-)$ with naturally polarized beam

$$A = \frac{d\sigma(0<\phi<\frac{\pi}{2}) - d\sigma(\frac{\pi}{2}<\phi<\pi)}{d\sigma(0<\phi<\pi)} \quad \text{at } \theta = \frac{\pi}{2}$$

Figure 3

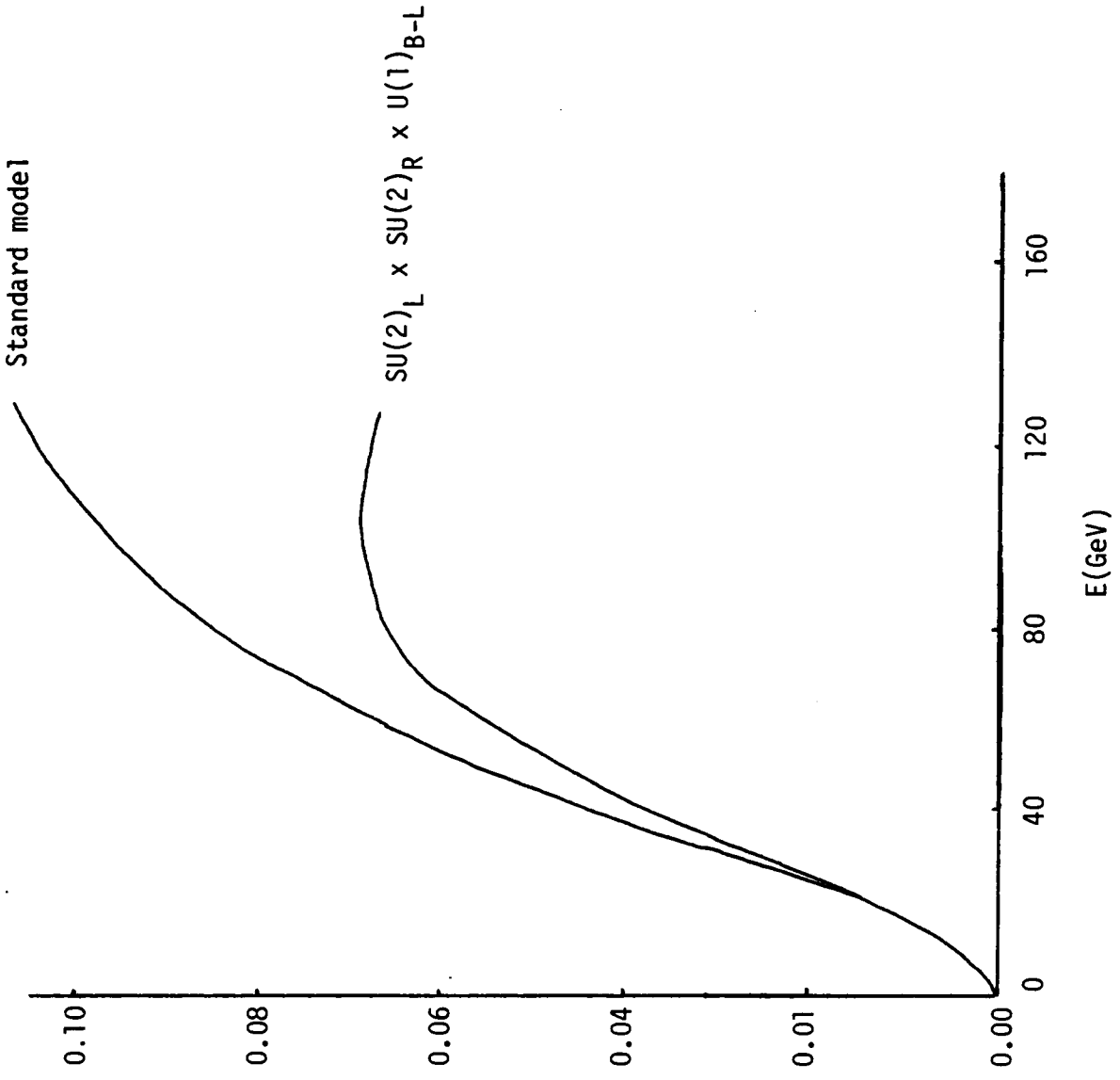

$$A = \frac{d\sigma(e_L^+e_L^- \to e^+e^-) - d\sigma(e_R^+e_R^- \to e^+e^-)}{d\sigma(e_L^+e_L^- \to e^+e^-) + d\sigma(e_R^+e_R^- \to e^+e^-)} \quad \text{at } \theta = \frac{\pi}{2}$$

Figure 4

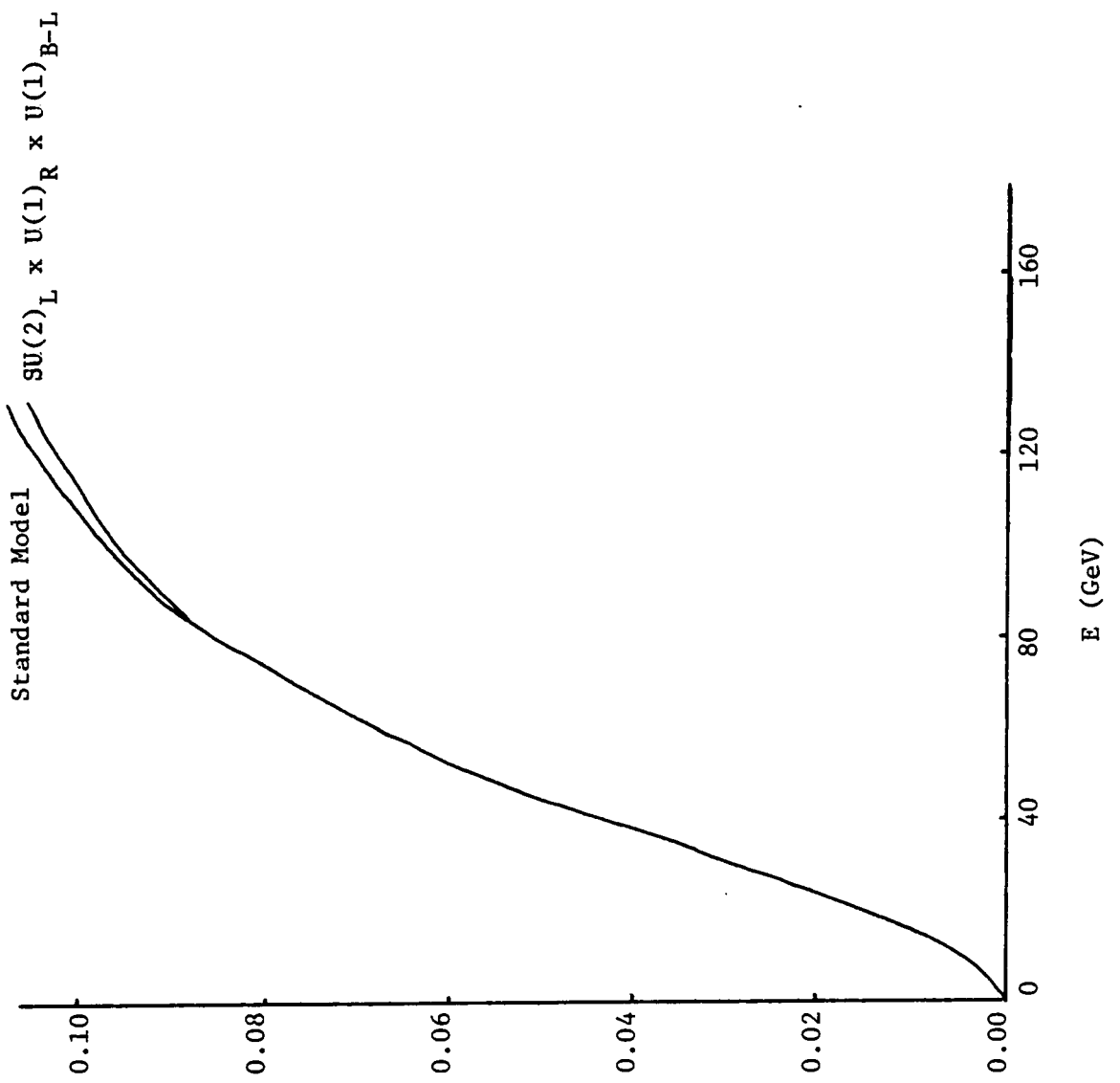

$$A = \frac{d\sigma(e_L^+ e_L^- \to e^+e^-) - d\sigma(e_R^+ e_R^- \to e^+e^-)}{d\sigma(e_L^+ e_L^- \to e^+e^-) + d\sigma(e_R^+ e_R^- \to e^+e^-)} \quad \text{at } \theta = \frac{\pi}{2}$$

Figure 5

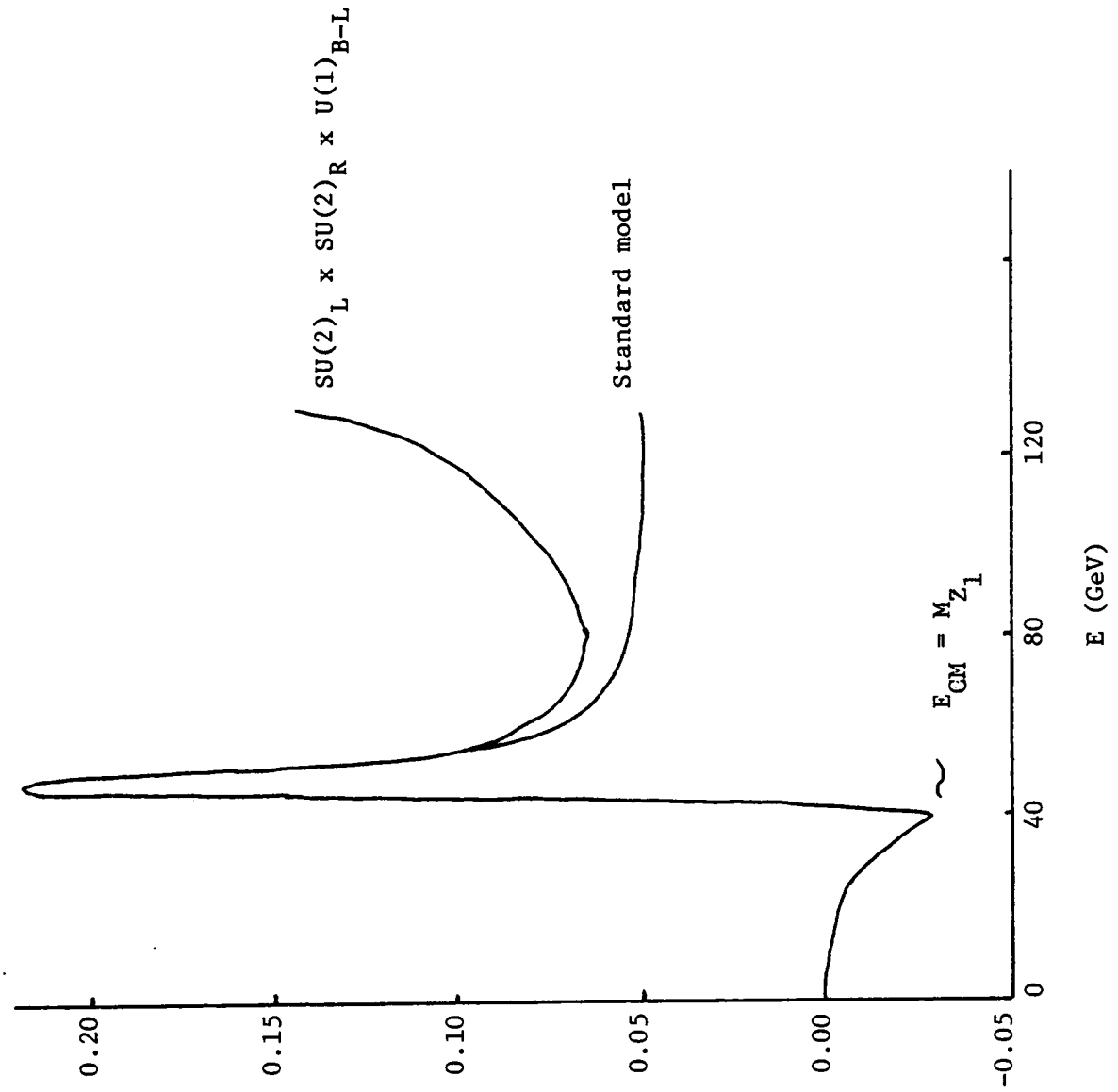
$SU(2)_L \times SU(2)_R \times U(1)_{B-L}$
Standard model
$E_{CM} = M_{Z_1}$
E (GeV)
0.20
0.15
0.10
0.05
0.00
-0.05
0
40
80
120
$A = \frac{d\sigma(e_L^+ e_R^- \to e^+e^-) - d\sigma(e_R^+ e_L^- \to e^+e^-)}{d\sigma(e_L^+ e_R^- \to e^+e^-) + d\sigma(e_R^+ e_L^- \to e^+e^-)}$ at $\theta = \frac{\pi}{2}$

Figure 6

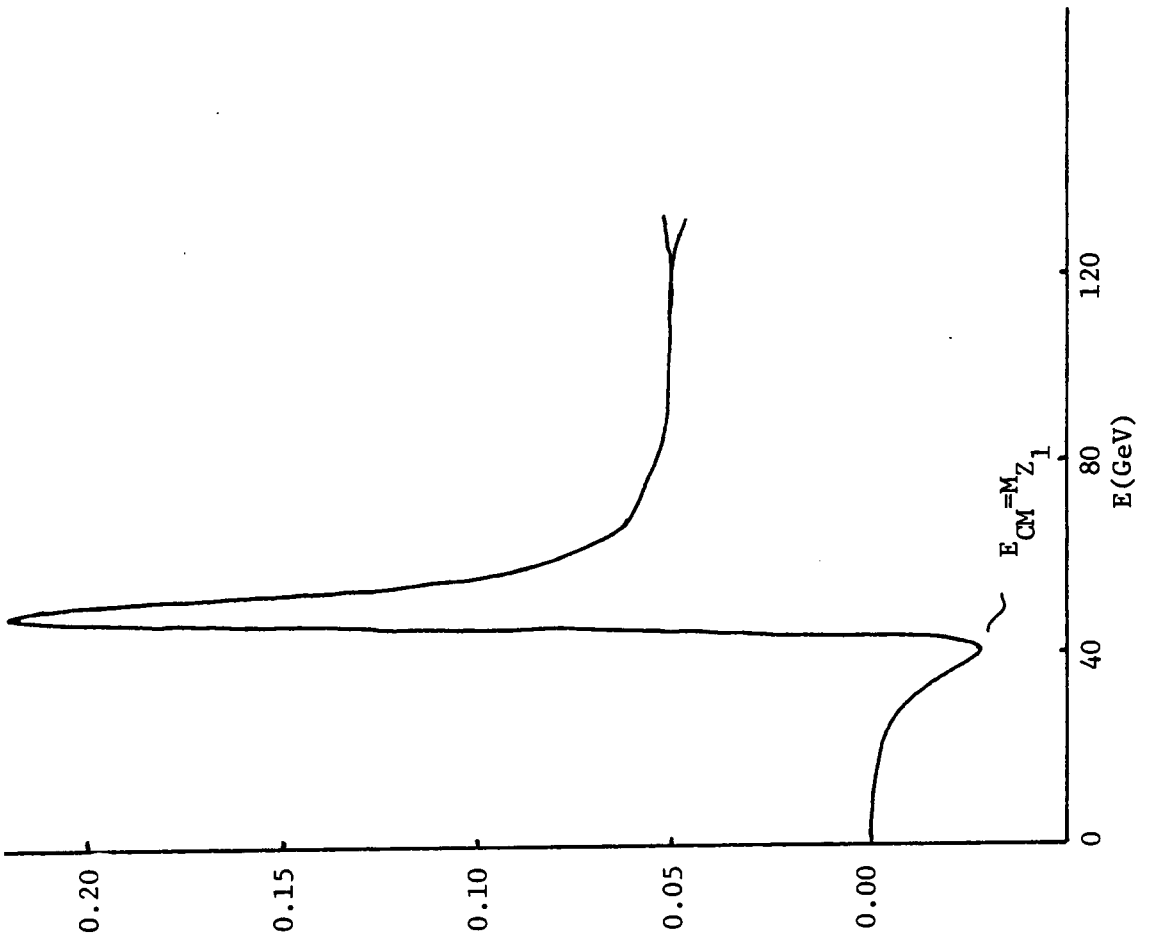

$$A = \frac{d\sigma(e_L^+e_R^- \to e^+e^-) - d\sigma(e_R^+e_L^- \to e^+e^-)}{d\sigma(e_L^+e_R^- \to e^+e^-) + d\sigma(e_R^+e_L^- \to e^+e^-)} \qquad \text{at } \Theta = \frac{\pi}{2}$$

in $SU(2)_L \times SU(2)_R \times U(1)_{B-L}$

Figure 7

$$g_L = g_V^{(3)} + g_A^{(3)} = 0.166$$
$$g_R = g_V^{(3)} + g_A^{(3)} = -0.164$$

In the $SU(2)_L xU(1)_R xU(1)_{B-L}$ model, the second Z boson couples equally to the left and right-handed currents. Therefore, it does not much affect the difference of the $e^+(L)e^-(R)$ and $e^+(R)e^-(L)$ cross sections.

Next we consider $e^+e^- \to q\bar{q}$. This process is calculated from the Feynman diagram in Fig 8. The initial beams can be naturally polarized, or longitudinally polarized. In the latter case, the cross section of $e^+(L)e^-(L) \to q\bar{q}$ and $e^+(R)e^-(R) \to q\bar{q}$ is proportional to the electron mass and quark masses, therefore at LEP energy they are many orders smaller than other cross sections.

Considering all the possible polarizations, the differential cross sections are:

for naturally polarized beams:

$$\begin{aligned}\frac{d\sigma}{d\Omega} = (E^2/8\pi^2) \sum_{i,j=1}^{N} & [(g_V^i g_V^j + g_A^i g_A^j)(f_V^i f_V^j + f_A^i f_A^j)(1+\cos^2\theta)/2 \\ & + (g_V^i g_A^j + g_A^i g_V^j)(f_V^i f_A^j + f_A^i f_V^j)\cos\theta \\ & + (g_V^i g_V^j - g_A^i g_A^j)(f_V^i f_V^j + f_A^i f_A^j)\frac{\sin^2\theta\cos 2\phi}{2}\ ] \\ & \mathrm{Re}[1/(4E^2 - M_{Z_j}^2 + iM_{Z_j}\Gamma_i)(4E^2 - M_{Z_j}^2 - iM_{Z_j}\Gamma_j)]\end{aligned} \tag{9}$$

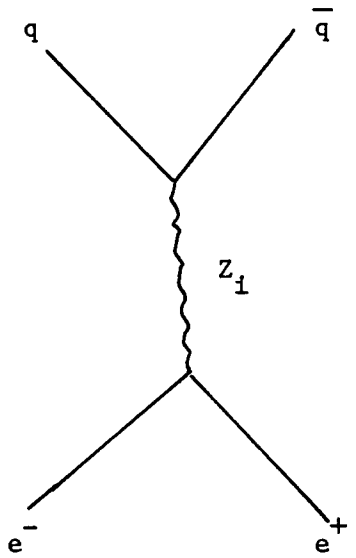

Figure 8

$e^+(L)e^-(R)\to q\,\bar{q}$

$$\frac{d\sigma}{d\Omega}=(E^2/4\pi^2)\sum_{i,j=1}^{N}[(g_V^i-g_A^i)(g_V^j-g_A^j)(f_V^i-f_A^i)(f_V^j-f_A^j)\cos^4(\theta/2)$$
$$+(g_V^i-g_A^i)(g_V^j-g_A^j)(f_V^i+f_A^i)(f_V^j+f_A^j)\sin^4(\theta/2)\,]$$
$$\mathrm{Re}[1/(4E^2-M_{Z_i}^2+iM_{Z_i}\Gamma_i)(4E^2-M_{Z_j}^2-iM_{Z_j}\Gamma_j)] \qquad (10)$$

$e^+(R)e^-(L)\to q\,\bar{q}$

$$\frac{d\sigma}{d\Omega}=(E^2/4\pi^2)\sum_{i,j=1}^{N}[(g_V^i+g_A^i)(g_V^j+g_A^j)(f_V^i+f_A^i)(f_V^j+f_A^j)\cos^4(\theta/2)$$
$$+(g_V^i+g_A^i)(g_V^j+g_A^j)(f_V^i-f_A^i)(f_V^j-f_A^j)\sin^4(\theta/2)\,]$$
$$\mathrm{Re}\,[1/(4E^2-M_{Z_i}^2+iM_{Z_i}\Gamma_i)(4E^2-M_{Z_j}^2-iM_{Z_j}\Gamma_j)] \qquad (11)$$

In the above expressions, $f_V^{\,i}$ is the coupling of Z_i to the vector part of the neutral weak quark current, and $f_A^{\,i}$ is the coupling of Z_i to the axial part of the neutral weak quark current.

In the standard model, for $I_3=+1/2$ quarks (u,c,t):

$$f_V^{(1)} = 2/3\ e = 2/3\ g\sin\theta_W$$
$$f_A^{(1)} = 0$$
$$f_V^{(2)} = (1/2\cos\theta_W)(1/2-4/3\cos^2\theta_W)$$
$$f_A^{(2)} = 1/4/\cos\theta_W$$

and for $I_3=-1/2$ quarks (d,s,b):

$$f_V^{(1)} = -1/3$$
$$f_A^{(1)} = 0$$
$$f_V^{(2)} = (1/2/\cos\theta_W)(-1/2+2/3\sin^2\theta_W)$$
$$f_A^{(2)} = -1/4/\cos\theta_W$$

In the $SU(2)_L x SU(2)_R x U(1)_{B-L}$ model, for the u,c,t quarks :

$$f_V^{(3)} = (g/4/\cos\theta_W)\ (1-8/3\sin^2\theta_W)\ /\sqrt{(1-2\sin^2\theta_W)}$$

$$f_A^{(3)} = (g/4/\cos\theta_W)\ (-1+2\sin^2\theta_W)\ /\sqrt{(1-2\sin^2\theta_W)},$$

and for the d,s,b quarks:

$$f_V^{(3)} = (g/4/\cos\theta_W)\ (-1+2\sin^2\theta_W)\ /\sqrt{(1-2\sin^2\theta_W)}$$

$$f_A^{(3)} = (g/4/\cos\theta_W)\ (1-4/3\sin^2\theta_W)\ /\sqrt{(1-2\sin^2\theta_W)}.$$

In the $SU(2)_L x U(1)_R x U(1)_{B-L}$ model, for the u, c, t quarks

$$f_V^{(3)} = (g/2/\cos\theta_W)\ [(1/\varepsilon/2)\sqrt{(\cos^2\theta_W-\varepsilon^2\sin^2\theta_W)}$$

$$-(1/3\varepsilon\sin^2\theta_W)/\sqrt{(\cos^2\theta_W-\varepsilon^2\sin^2\theta_W)}\ ]$$

$$f_A^{(3)} = (g/2/\cos\theta_W)\ (1/\varepsilon/2)\sqrt{(\cos^2\theta_W-\varepsilon^2\sin^2\theta_W)},$$

and for the d, s, b quarks:

$$f_V^{(3)} = (g/2/\cos\theta_W)\ [(1/\varepsilon/2)\sqrt{(\cos^2\theta_W-\varepsilon^2\sin^2\theta_W)}$$

$$-(1/3\varepsilon\sin^2\theta_W)/\sqrt{(\cos^2\theta_W-\varepsilon^2\sin^2\theta_W)}\ ]$$

$$f_A^{(3)} = (g/2/\cos\theta_W)\ (1/\varepsilon/2)\sqrt{(\cos^2\theta_W-\varepsilon^2\sin^2\theta_W)}.$$ The numerical results are given in Fig.9-20.

The backward-forward asymmetry of both the up quark and down quark serves as a good test to the two-Z-boson model.

Among the electron-positron colliding experiments, finally we consider $e^+e^- \to \ell^+\ell^-$. It is calculated from the Feynman diagram in Fig 21. The final state ℓ can be either the μ or the τ. The μ final state is easy to identify. The production of τ makes it possible to measure the polarization of the final state. We consider not only the polarization of the initial beam, but also the measurement of the final state polarization.

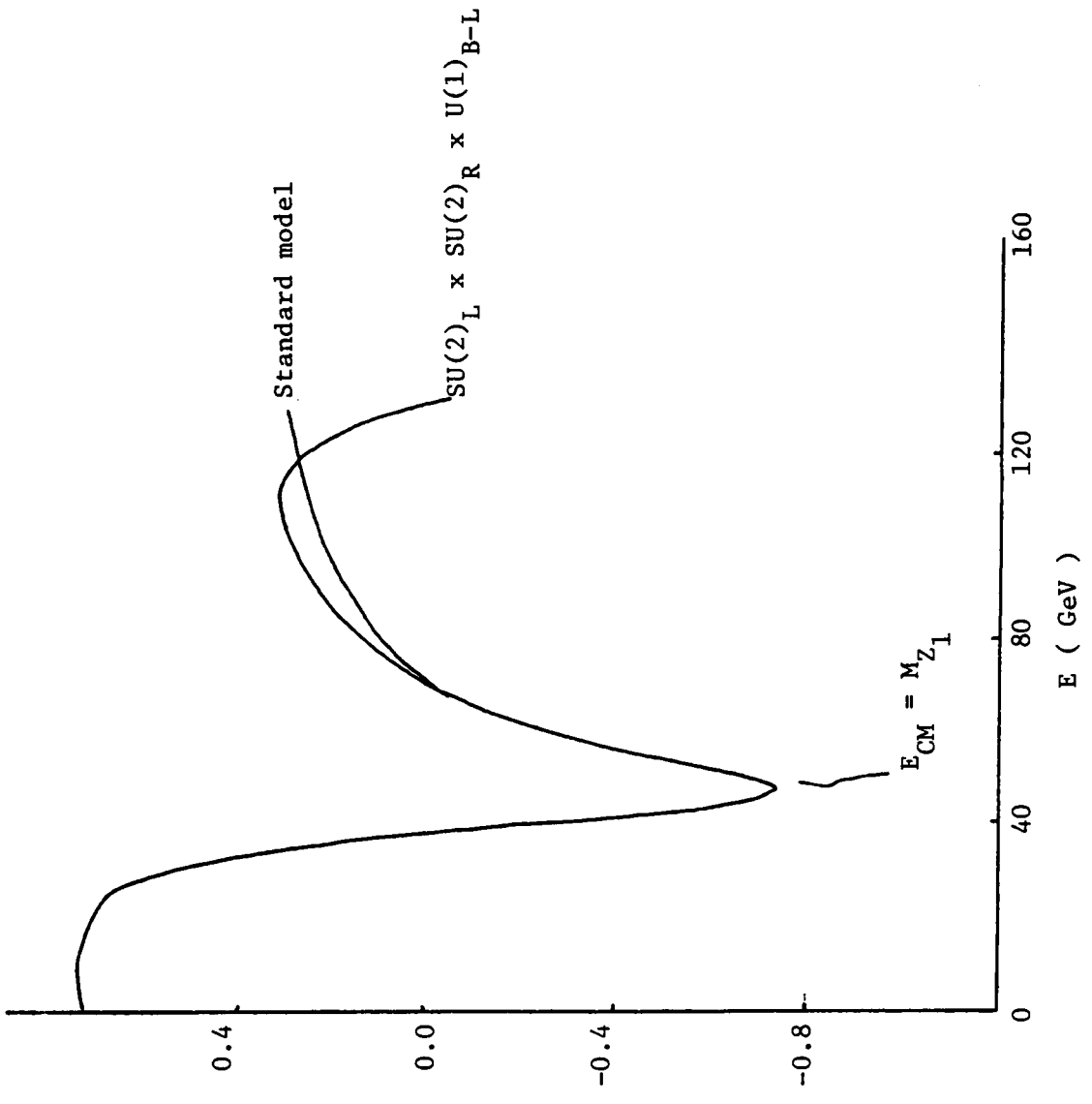

$e^+e^- \to u\bar{u}$ naturally polarized beam

$$A = \frac{d\sigma(0<\phi<\frac{\pi}{2}) - d\sigma(\frac{\pi}{2}<\phi<\pi)}{d\sigma(0<\phi<\pi)}$$

Figure 9

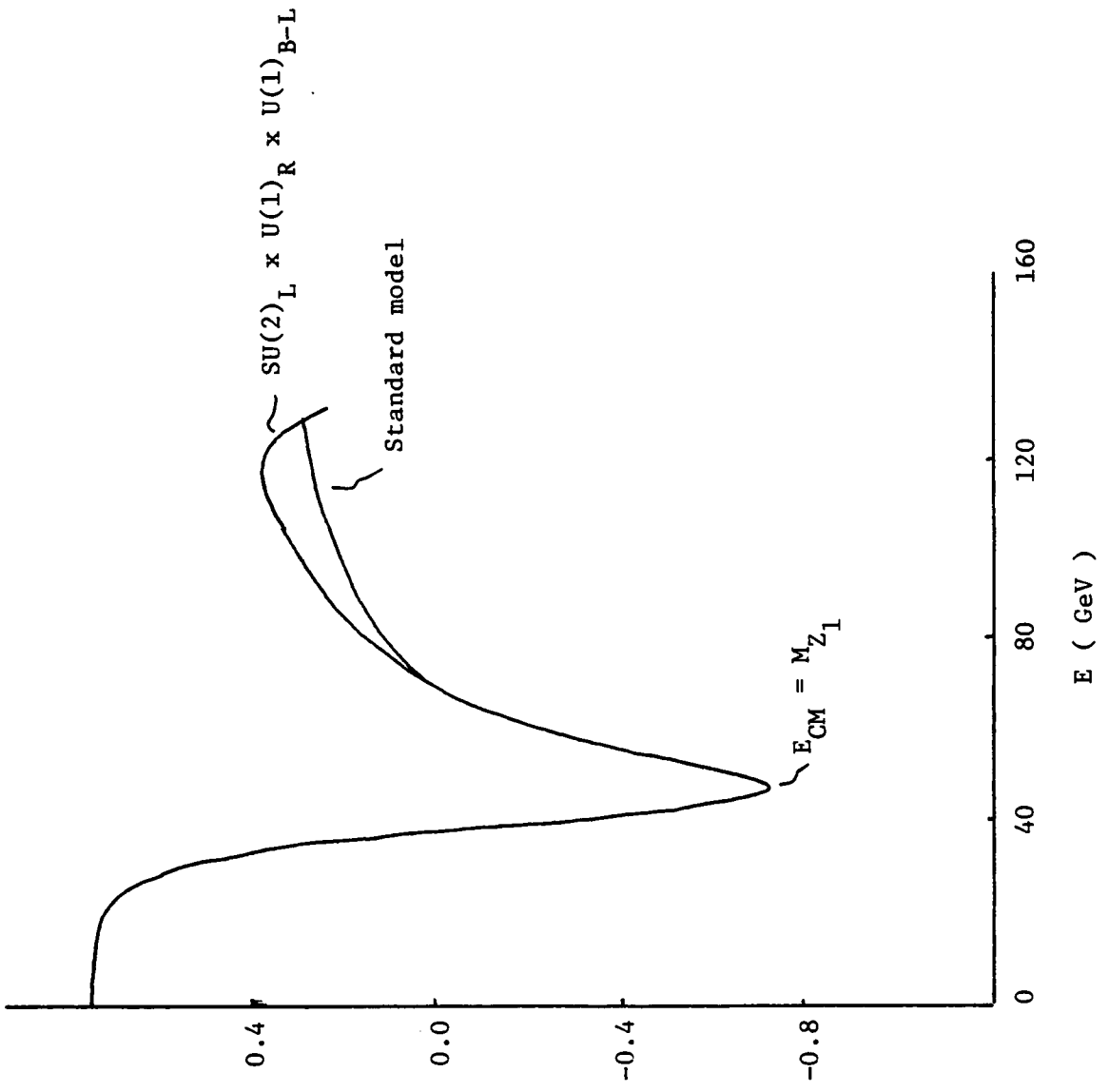

$e^+e^- \to u\bar{u}$ naturally polarized beam

$$A = \frac{d\sigma(0<\phi\frac{\pi}{2}) - d\sigma(\frac{\pi}{2}<\phi<\pi)}{d\sigma(0<\phi<\pi)}$$

Figure 10

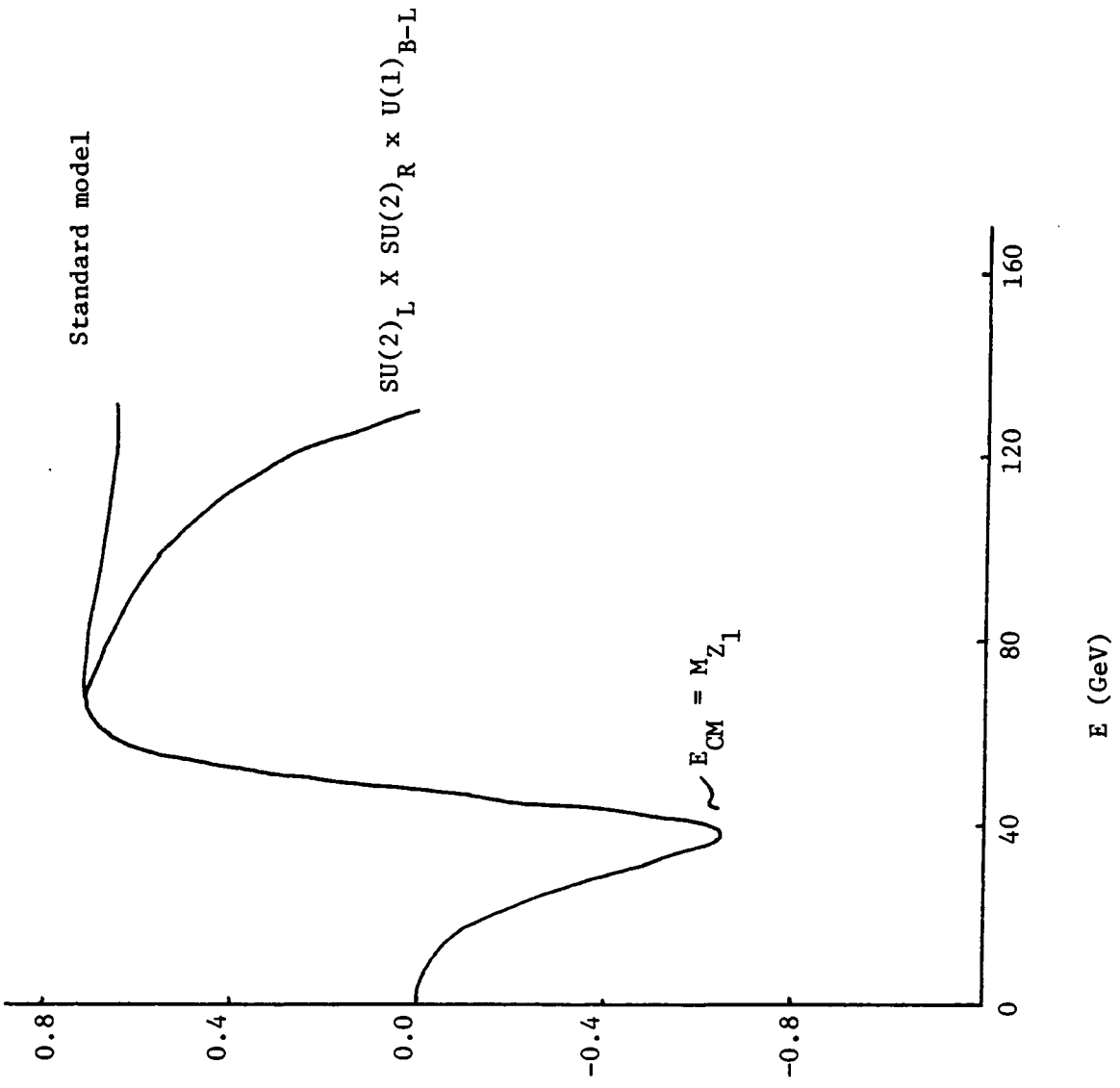

$e^+e^- \rightarrow u\,\bar{u}$ backward - forward asymmetry

Figure 11

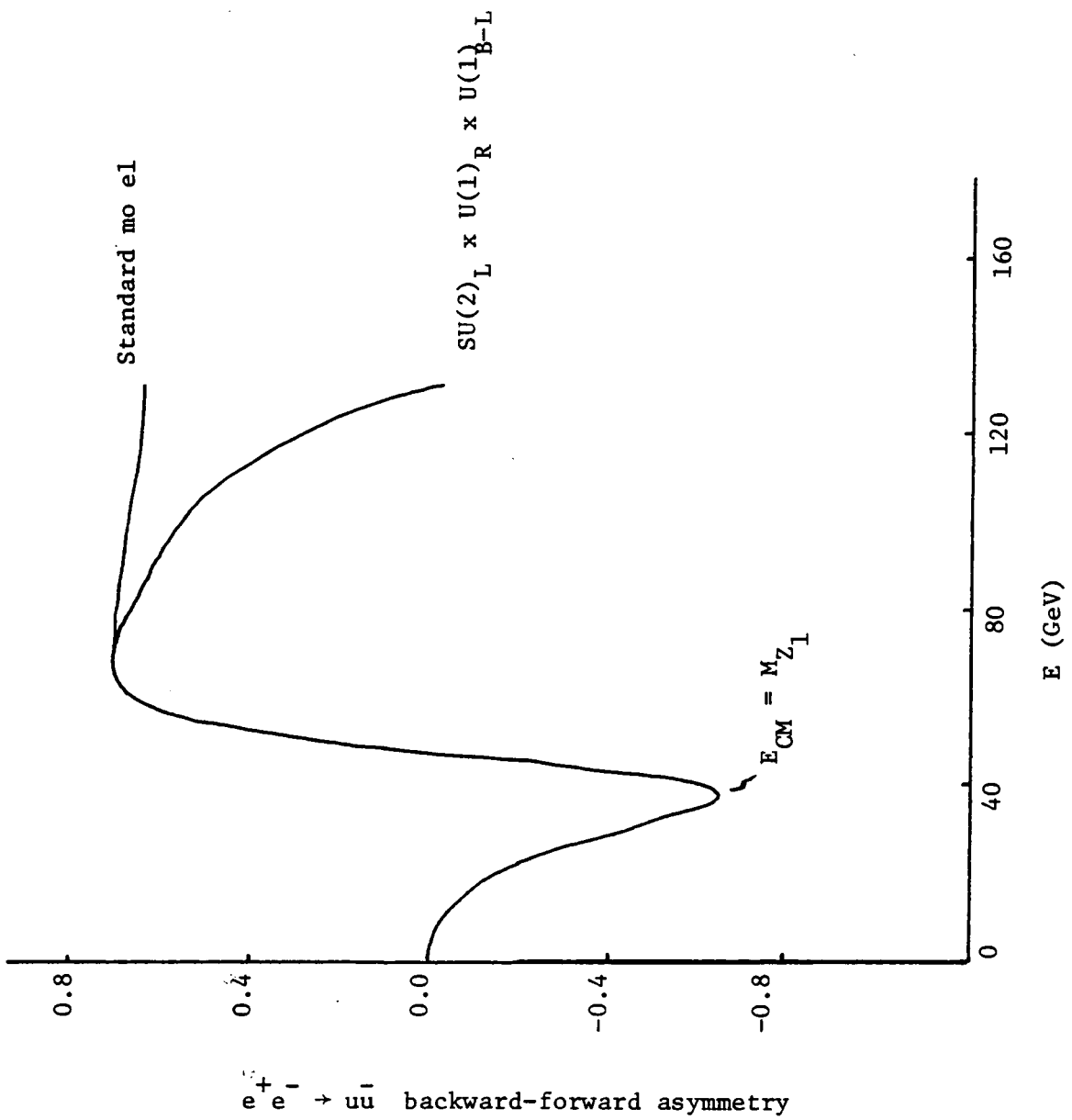
Standard mo el
$SU(2)_L \times U(1)_R \times U(1)_{B-L}$
$E_{CM} = M_{Z_1}$
0.8
0.4
0.0
-0.4
-0.8
0
40
80
120
160
E (GeV)
$e^+e^- \to u\bar{u}$ backward-forward asymmetry

Figure 12

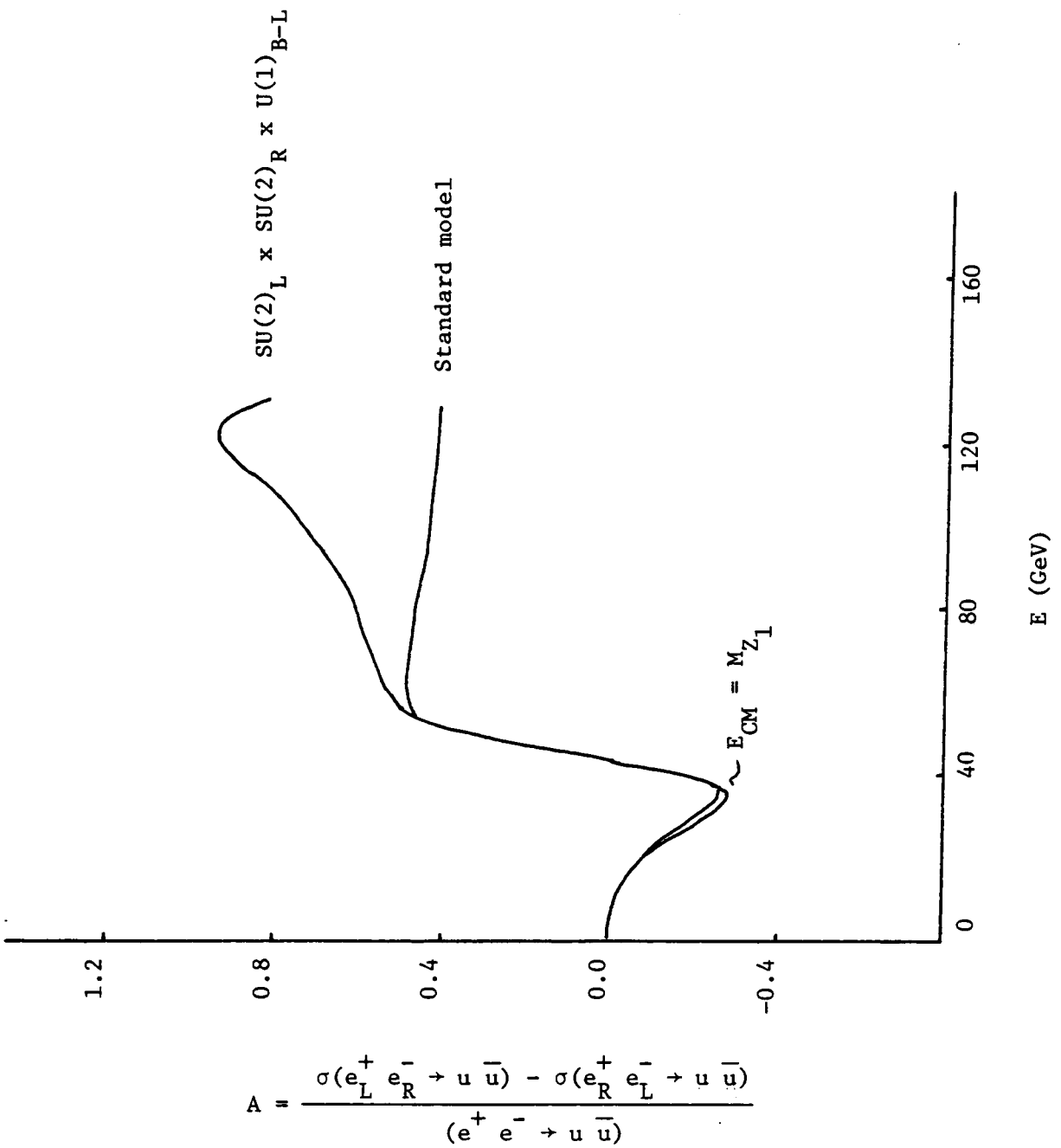
$SU(2)_L \times SU(2)_R \times U(1)_{B-L}$
Standard model
$E_{CM} = M_{Z_1}$
1.2
0.8
0.4
0.0
-0.4
0
40
80
120
160
E (GeV)
$A = \frac{\sigma(e_L^+ e_R^- \to u \bar{u}) - \sigma(e_R^+ e_L^- \to u \bar{u})}{(e^+ e^- \to u \bar{u})}$

Figure 13

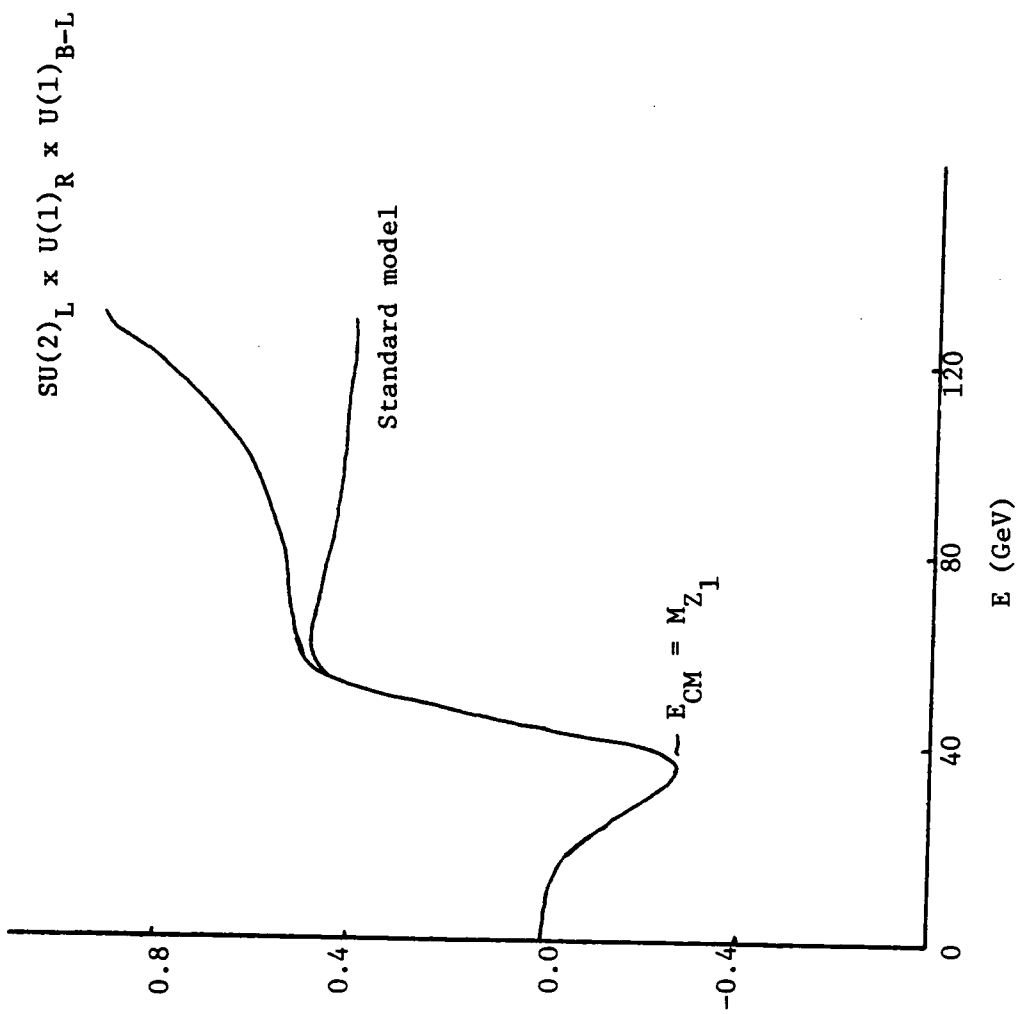
SU(2)L x U(1)R x U(1)B-L
Standard model
E (GeV)
0
40
80
120
0.8
0.4
0.0
-0.4
$E_{CM} = M_{Z_1}$
$A = \frac{\sigma(e_L^+ e_R^- \to u\,\bar{u}) - \sigma(e_R^+ e_L^- \to u\,\bar{u})}{(e^+ e^- \to u\,\bar{u})}$

Figure 14

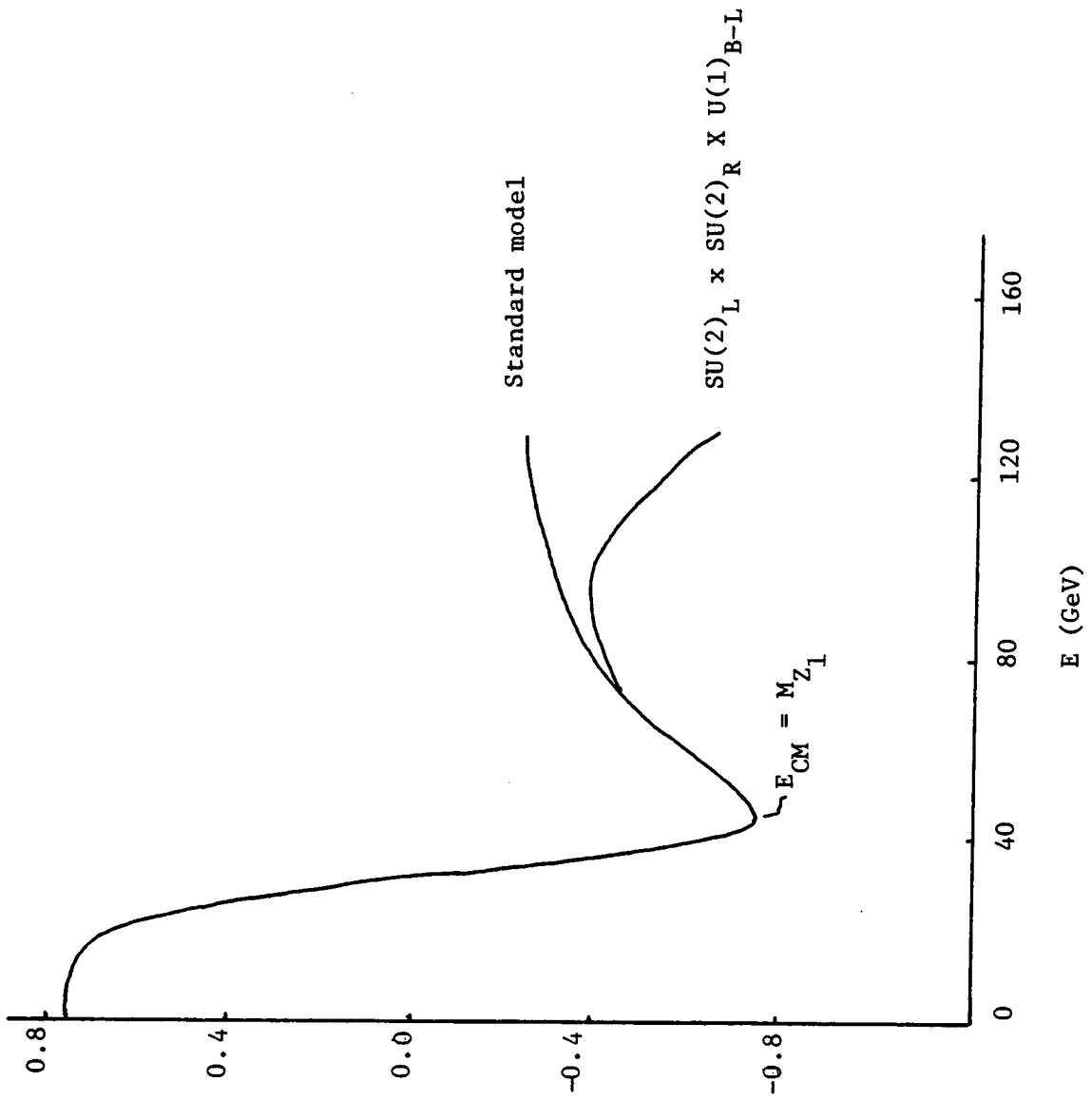

$e^+e^- \to d\bar{d}$ naturally polarized beam

$$A = \frac{d\sigma(0<\phi<\frac{\pi}{2}) - d\sigma(\frac{\pi}{2}<\phi<\pi)}{d\sigma(0<\phi<\pi)}$$

Figure 15

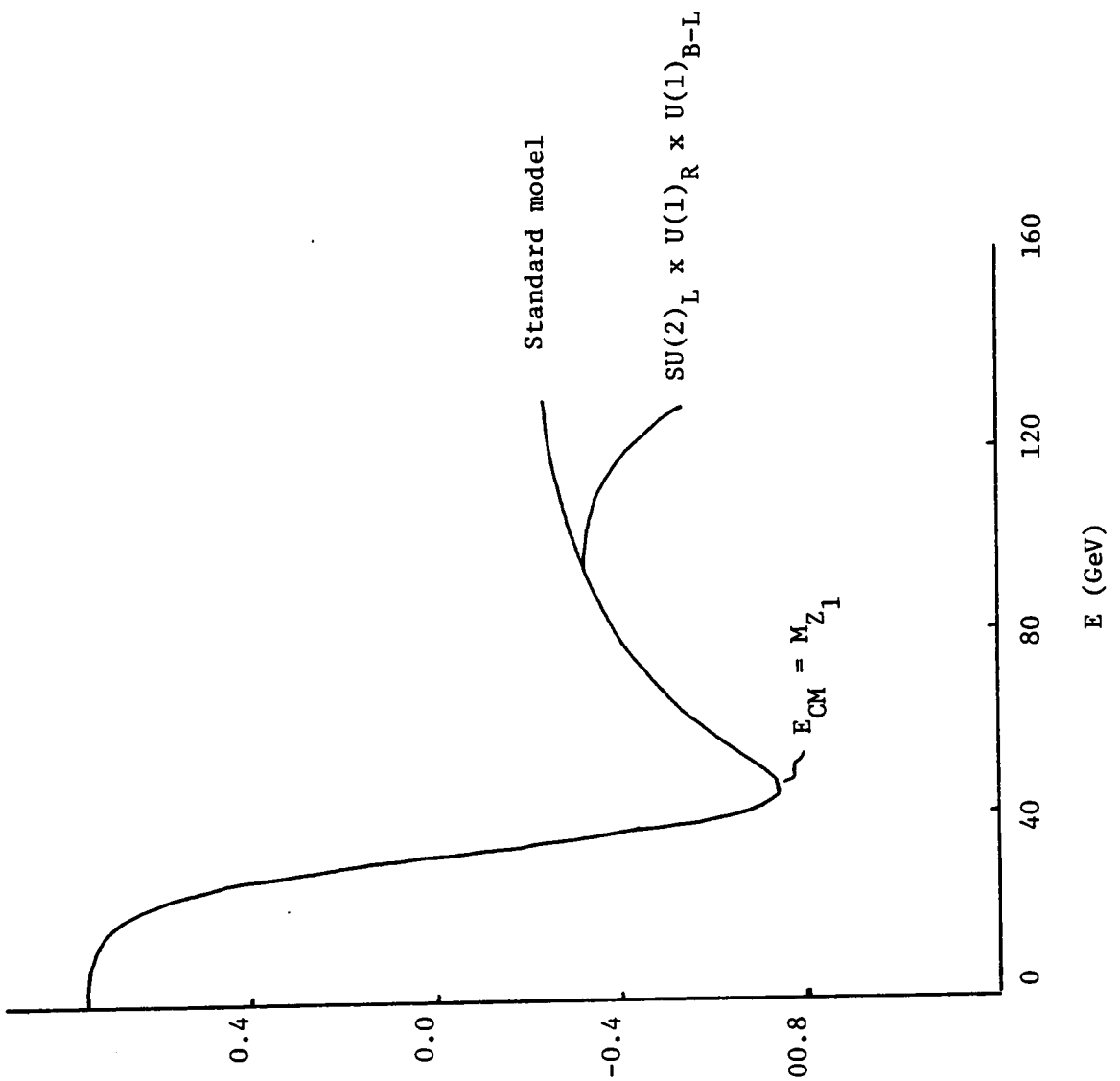

$e^+e^- \to d\bar{d}$ naturally polarized beam

$$A = \frac{d\sigma(0<\phi<\frac{\pi}{2}) - d\sigma(\frac{\pi}{2}<\phi<\pi)}{d\sigma(0<\phi<\pi)}$$

Figure 16

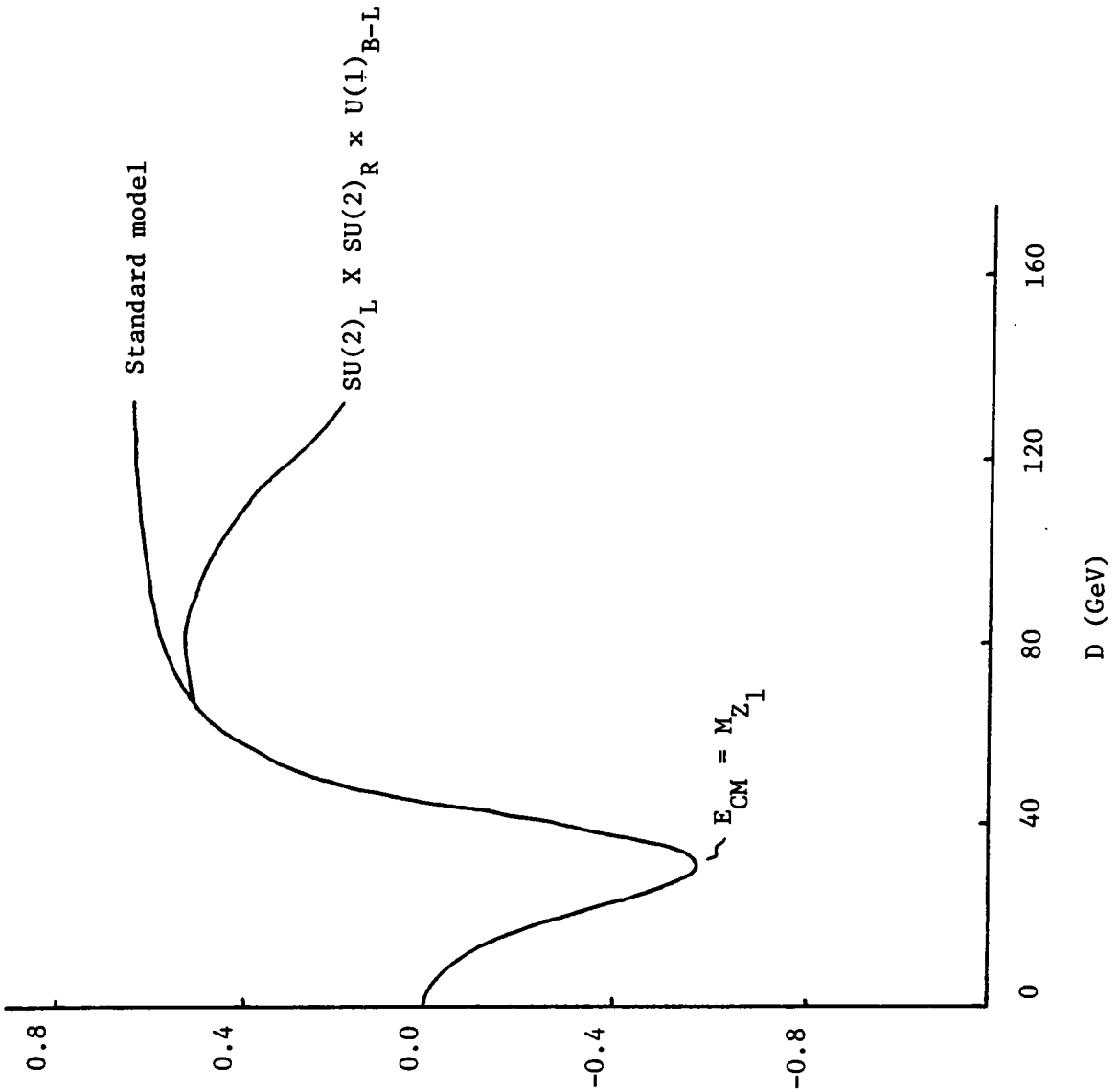

$e^+e^- \to d\bar{d}$ backward-forward asymetry

Figure 17

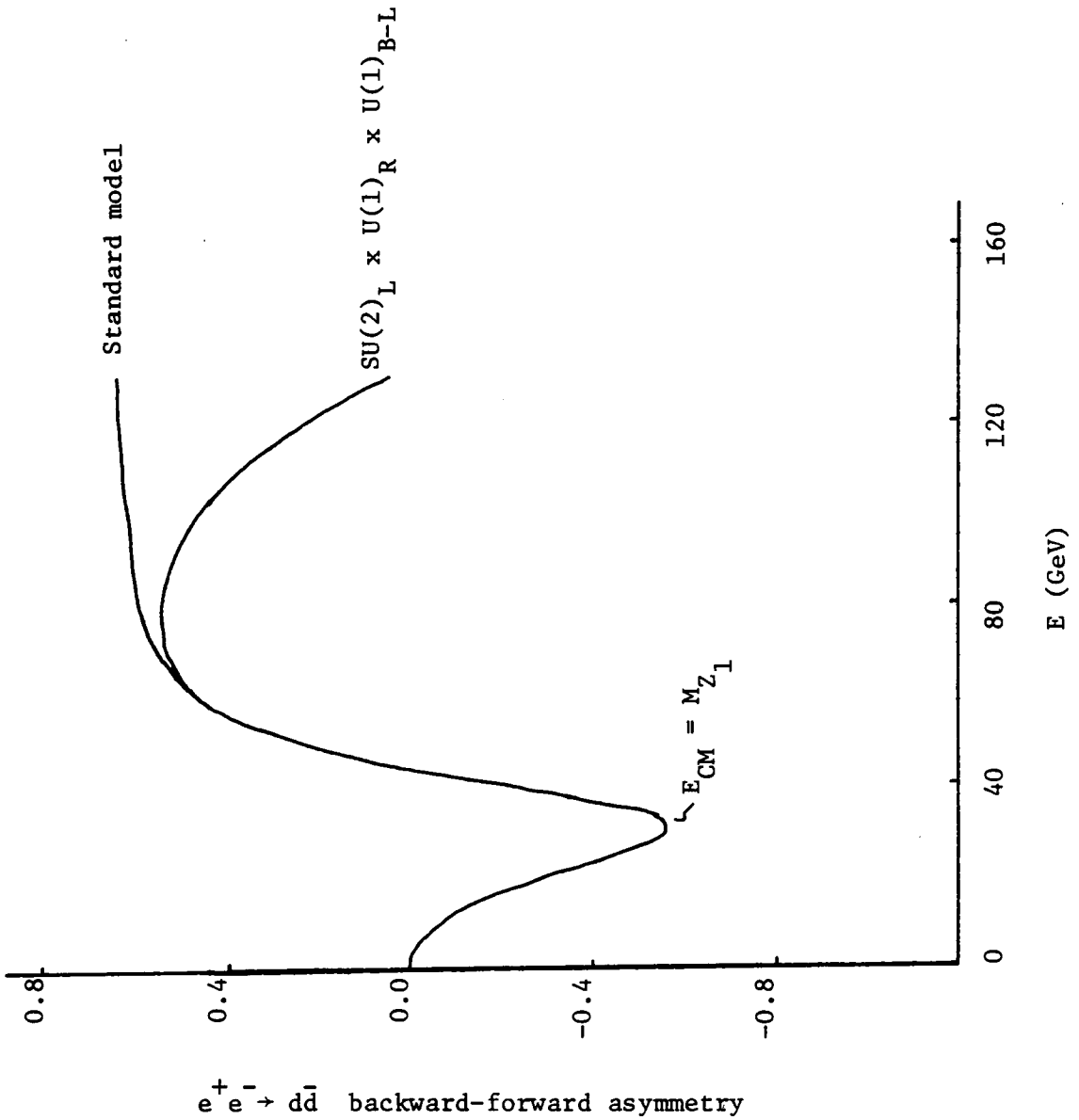
Standard model
$SU(2)_L \times U(1)_R \times U(1)_{B-L}$
$E_{CM} = M_{Z_1}$
0.8
0.4
0.0
-0.4
-0.8
0
40
80
120
160
E (GeV)
$e^+e^- \to d\bar{d}$ backward-forward asymmetry

Figure 18

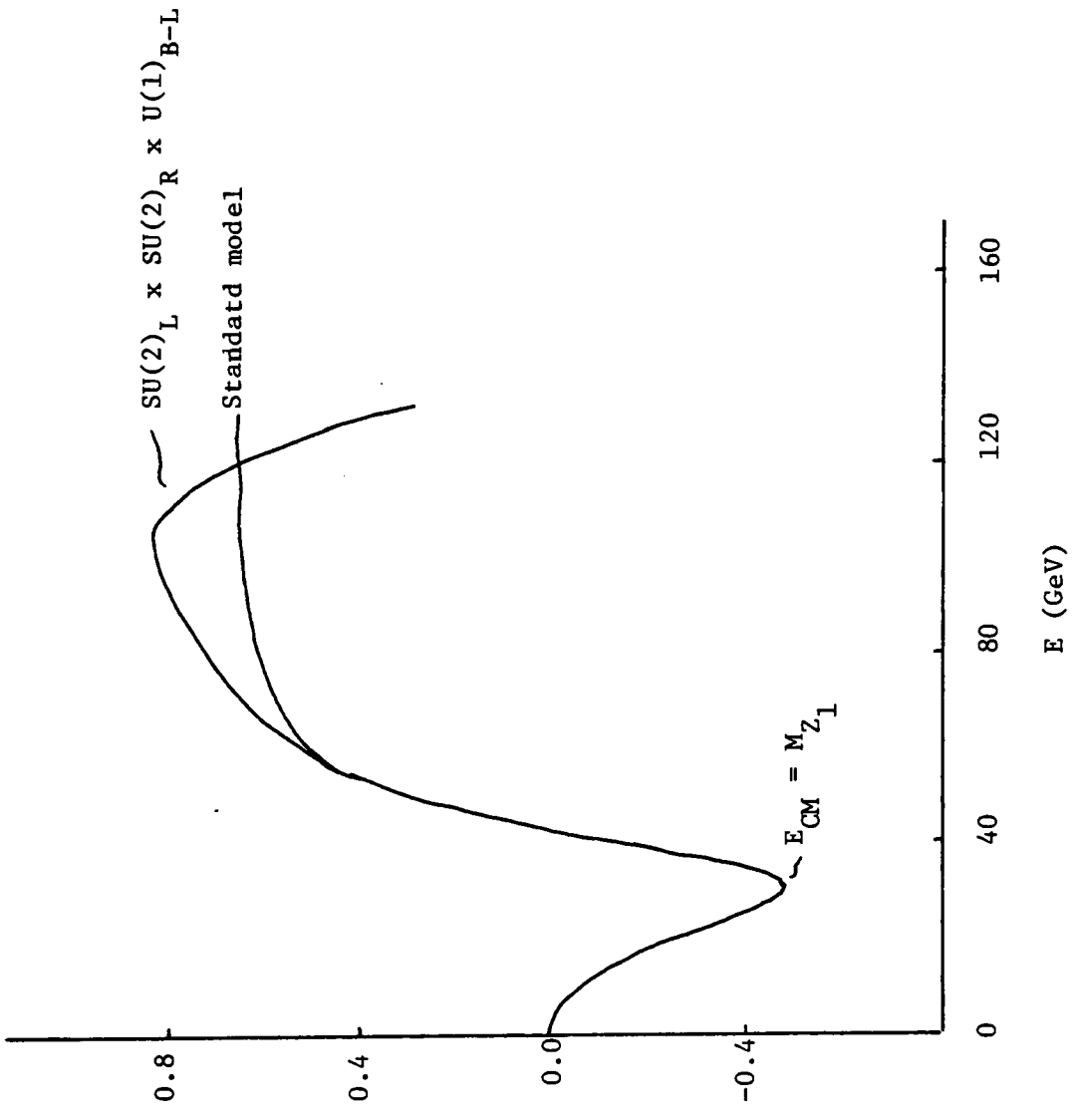

$$A = \frac{\sigma(e_L^+ e_R^- \to d\bar{d}) - \sigma(e_R^+ R_L^- \to d\bar{d})}{\sigma(e^+ e^- \to d\bar{d})}$$

Figure 19

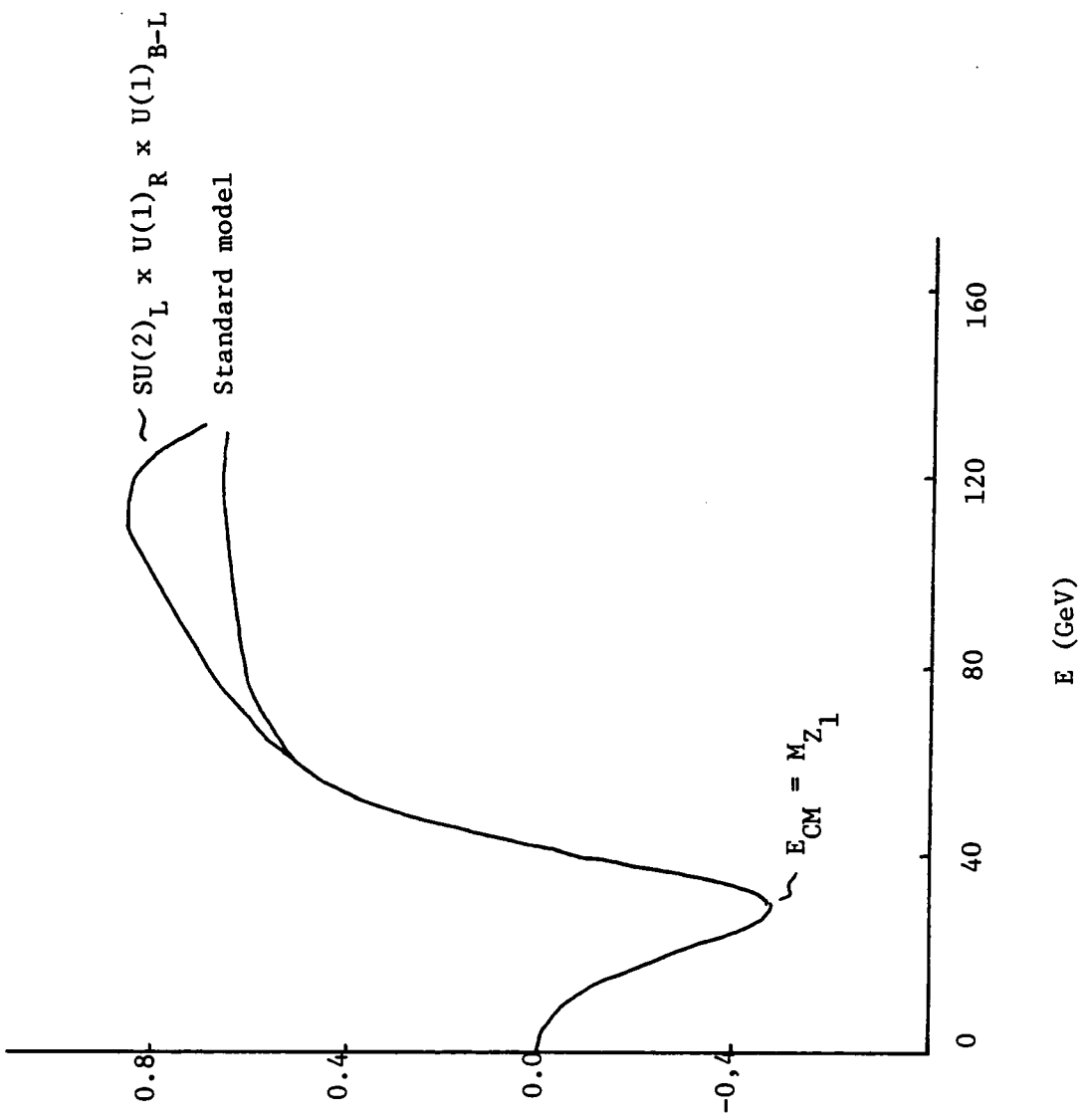

$$A = \frac{\sigma(e_L^+ e_R^- \to d\bar{d}) - \sigma(e_R^+ e_L^- \to d\bar{d})}{\sigma(e^+ e^- \to d\bar{d})}$$

Figure 20

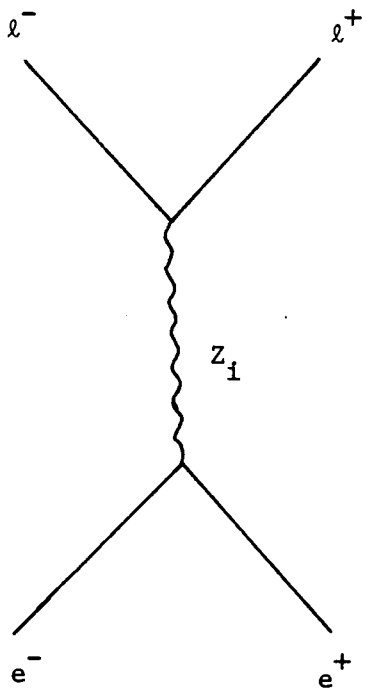

Figure 21

naturally polarized beams

$$\frac{d\sigma}{d\Omega}=(E^2/8\pi^2)\sum_{i,j=1}^{N}[(g_V^i g_V^j+g_A^i g_A^j)^2(1+\cos^2\theta)/2$$
$$+(g_V^i g_A^j+g_V^i g_A^j)^2\cos\theta$$
$$+(g_V^i g_V^j-g_A^i g_A^j)(g_V^i g_V^j+g_A^i g_A^j)\sin^2\theta\cos 2\phi\ ]$$
$$\mathrm{Re}\ [1/(4E^2-M_{Z_j}^2+iM_{Z_j}\Gamma_i)(4E^2-M_{Z_j}^2+iM_{Z_j}\Gamma_j)\ ] \qquad (12)$$

$e^+(L)e^-(R)\to\ell^+(L)\ell^-(R)$

$$\frac{d\sigma}{d\Omega}=(E^2/4\pi^2)\sum_{i,j=1}^{N}(g_V^i-g_A^i)^2(g_V^j-g_A^j)^2\cos^4(\theta/2) \qquad (13)$$
$$\mathrm{Re}\ [1/(4E^2-M_{Z_i}^2+iM_{Z_i}\Gamma_i)(4E^2-M_{Z_j}^2-iM_{Z_j}\Gamma_j)\ ]$$

$e^+(L)e^-(R)\to\ell^+(R)\ell^-(L)$

$$\frac{d\sigma}{d\Omega}=(E^2/4\pi^2)\sum_{i,j=1}^{N}(g_V^i-g_A^i)(g_V^j-g_A^j)(g_V^i+g_A^i)(g_V^j+g_A^j)\sin^4(\theta/2) \qquad (14)$$
$$\mathrm{Re}\ [(4E^2-M_{Z_i}^2+iM_{Z_i}\Gamma_i)(4E^2-M_{Z_j}^2-iM_{Z_j}\Gamma_j)\ ]$$

$e^+(R)e^-(L)\to\ell^+(R)\ell^-(L)$

$$\frac{d\sigma}{d\Omega}=(E^2/4\pi^2)\sum_{i,j=1}^{N}(g_V^i+g_A^i)^2(g_V^j+g_A^j)^2\cos^4(\theta/2) \qquad (15)$$
$$\mathrm{Re}\ [1/(4E^2-M_{Z_i}^2+iM_{Z_i}\Gamma_i)(4E^2-M_{Z_j}^2-iM_{Z_j}\Gamma_j)\ ]$$

$e^+(R)e^-(L)\to\ell^+(L)\ell^-(R)$

$$\frac{d\sigma}{d\Omega}=(E^2/4\pi^2)\sum_{i,j=1}^{N}(g_V^i+g_A^i)(g_V^j+g_A^j)(g_V^i-g_A^i)(g_V^j-g_A^j)\sin^4(\theta/2) \qquad (16)$$
$$\text{Re}\ [1/(4E^2-M_{Z_i}^2+iM_{Z_i}\Gamma_i)(4E^2-M_{Z_j}^2-iM_{Z_j}\Gamma_j)\ ]$$

The numerical results are given in Figures 22 to 31.

Of all the possible experiments on e^+e^- collider, the $e^+e^-\to\mu^+\mu^-$ backward-forward asymmetry and :

(I) $e^+(L)e^-(R)\to\ell^+(L)\ell^-(R)$

(II) $e^+(L)e^-(R)\to\ell^+(R)\ell^-(L)$

(III) $e^+(R)e^-(L)\to\ell^+(R)\ell^-(L)$

are the most sensitive to the deviation of the two-Z-boson model from the standard model. At the highest available LEP energy, the standard model and two-Z-boson model predict the opposite signs to $\sigma(I)-\sigma(II)$, $\sigma(II)-\sigma(III)$ and the $e^+e^-\to\mu^+\mu^-$ backward-forward asymmetry, if the Z_R mass is as low as 300 GeV. For these results, see Figures 24, 25, 28, 29, 30, and 31.

For the same reason as in $e^+e^-\to e^+e^-$ experiment, in some of the effects, i.e. the cross section difference betwwen $e^+(L)e^-(R)\to\ell^+(L)\ell^-(R)$ and $e^+(R)e^-(L)\to\ell^+(R)\ell^-(L)$, $SU(2)_L xSU(2)_R xU(1)_{B-L}$ model deviates largely from the standard model, whereas $SU(2)_L xU(1)_R xU(1)_{B-L}$ model does not.

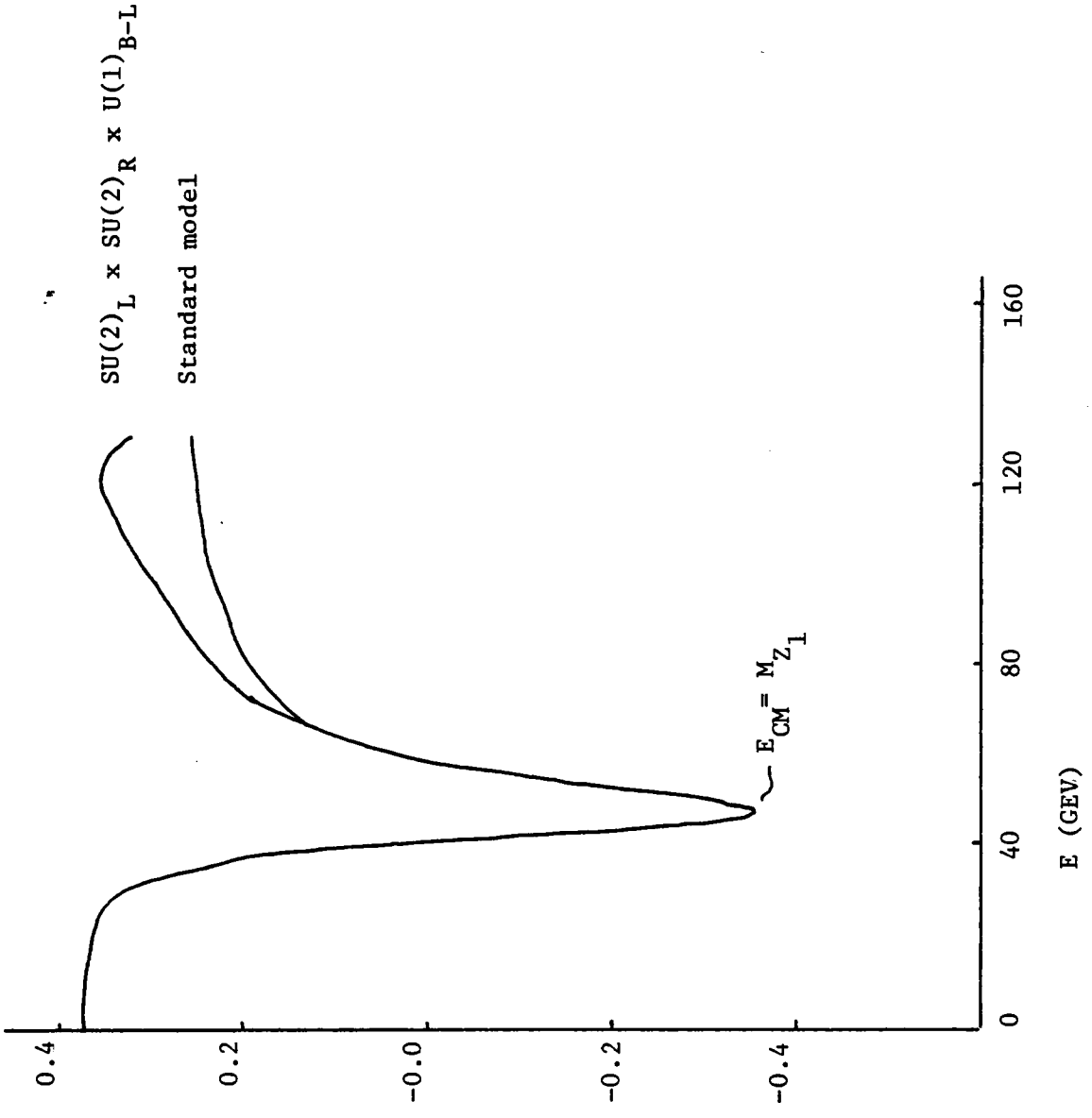

$e^+e^- \to u^+u^-$ naturally polarized beam

$$A = \frac{\sigma(0<\phi<\frac{\pi}{2}) - \sigma(\frac{\pi}{2}<\Phi<\pi)}{\sigma(0<\phi<\pi)}$$

Figure 22

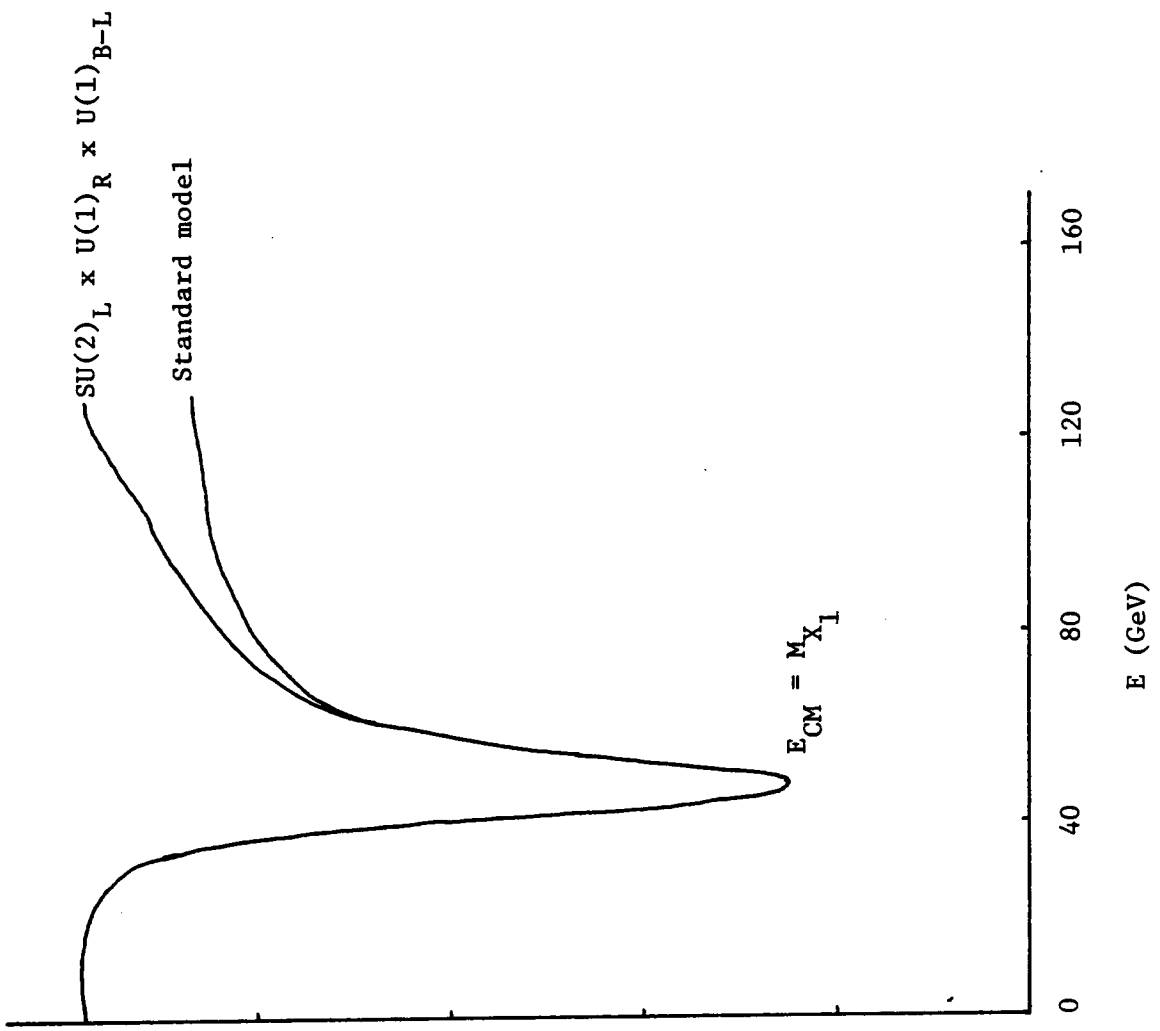

$e^+e^- \to u^+u^-$ initially naturally polarized geam

$$A = \frac{\sigma(0<\phi<\frac{\pi}{2}) - \sigma(\frac{\pi}{2}<\phi<\pi)}{\sigma(0<\phi<\frac{\pi}{2}) + \sigma(\frac{\pi}{2}<\phi<\pi)}$$

Fig. 23

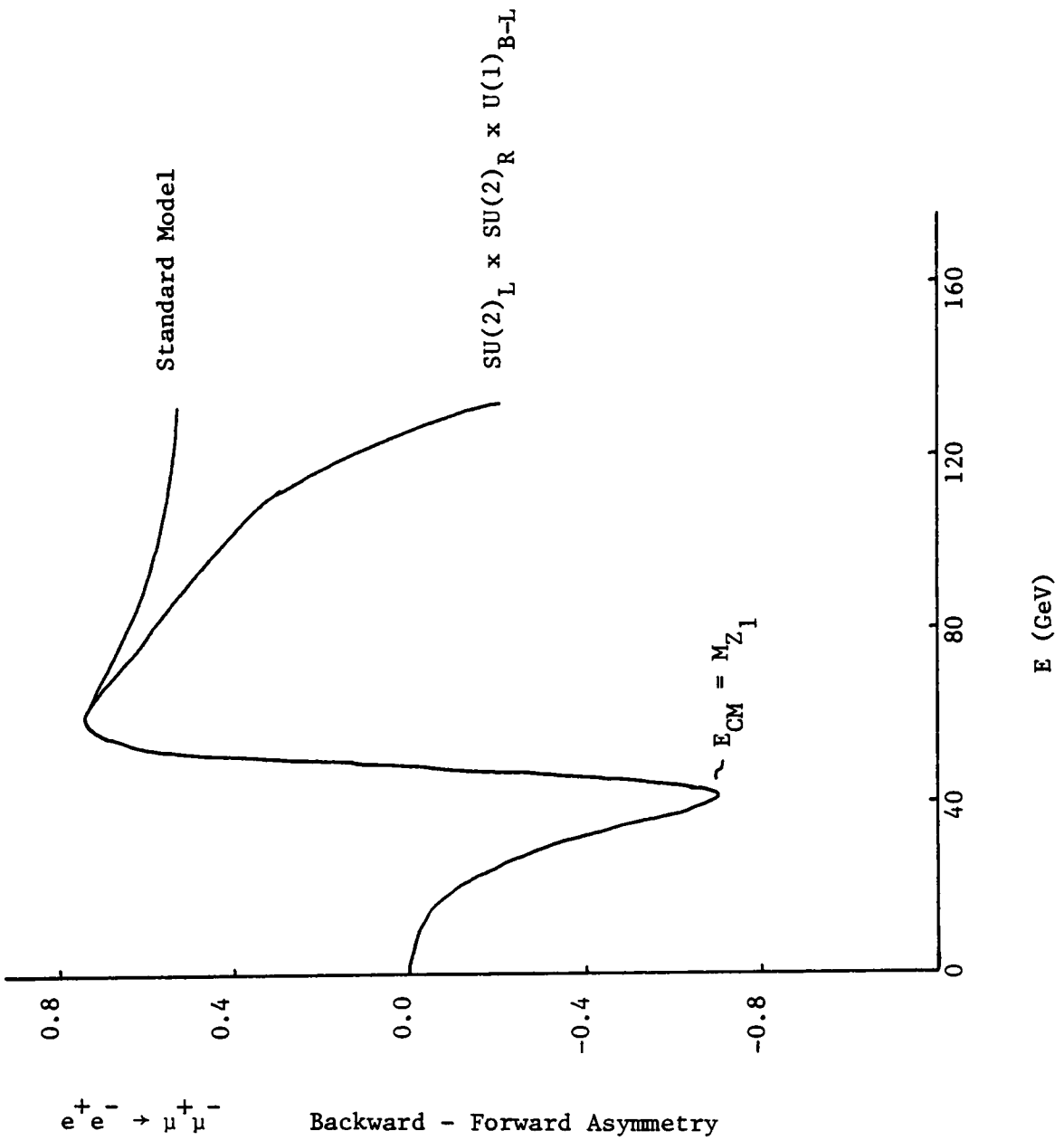
Standard Model
$SU(2)_L \times SU(2)_R \times U(1)_{B-L}$
$\sim E_{CM} = M_{Z_1}$
0.8
0.4
0.0
-0.4
-0.8
0
40
80
120
160
E (GeV)
$e^+e^- \to \mu^+\mu^-$
Backward - Forward Asymmetry

Figure 24

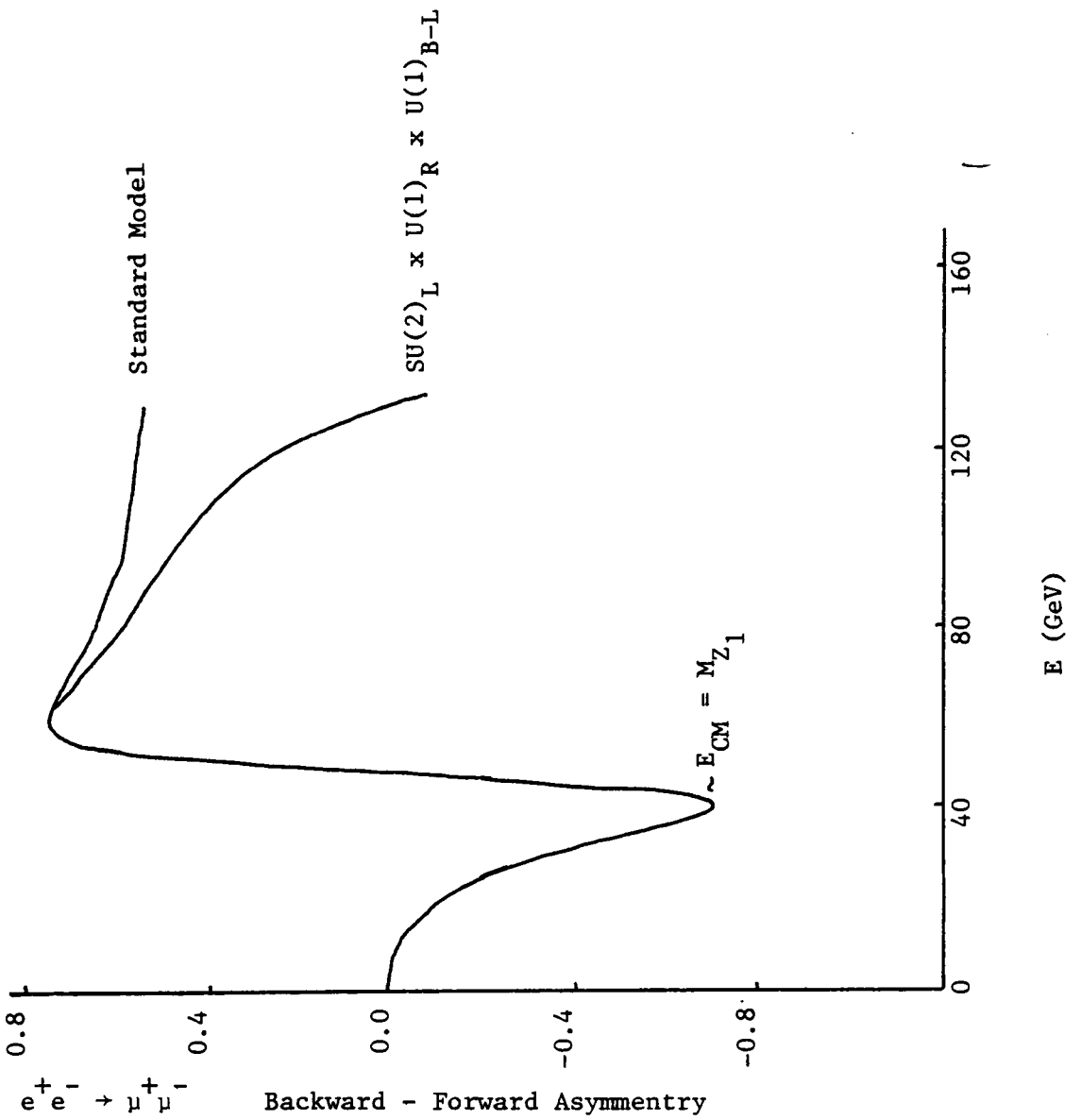
Standard Model
$SU(2)_L \times U(1)_R \times U(1)_{B-L}$
$\sim E_{CM} = M_{Z_1}$
0.8
0.4
0.0
-0.4
-0.8
0
40
80
120
160
E (GeV)
$e^+e^- \rightarrow \mu^+\mu^-$
Backward - Forward Asymmentry

Figure 25

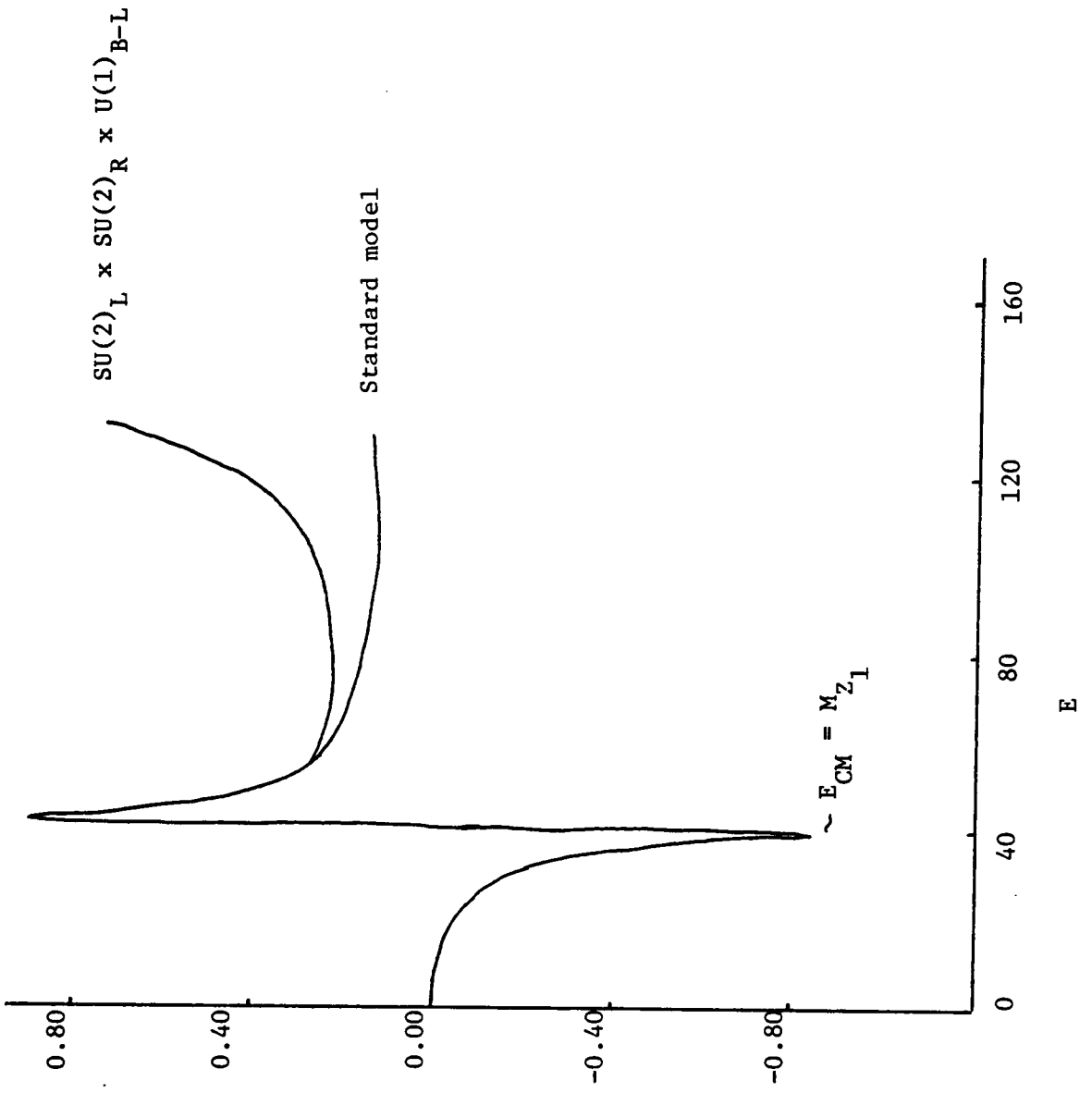

$$A = \frac{\sigma(e_L^+ e_R^- \to \tau_L^+ \tau_R^-) - \sigma(e_L^+ e_R^- \to \tau_R^+ \tau_L^-)}{\sigma(e_L^+ e_R^- \to \tau^+ \tau^-)}$$

Figure 26

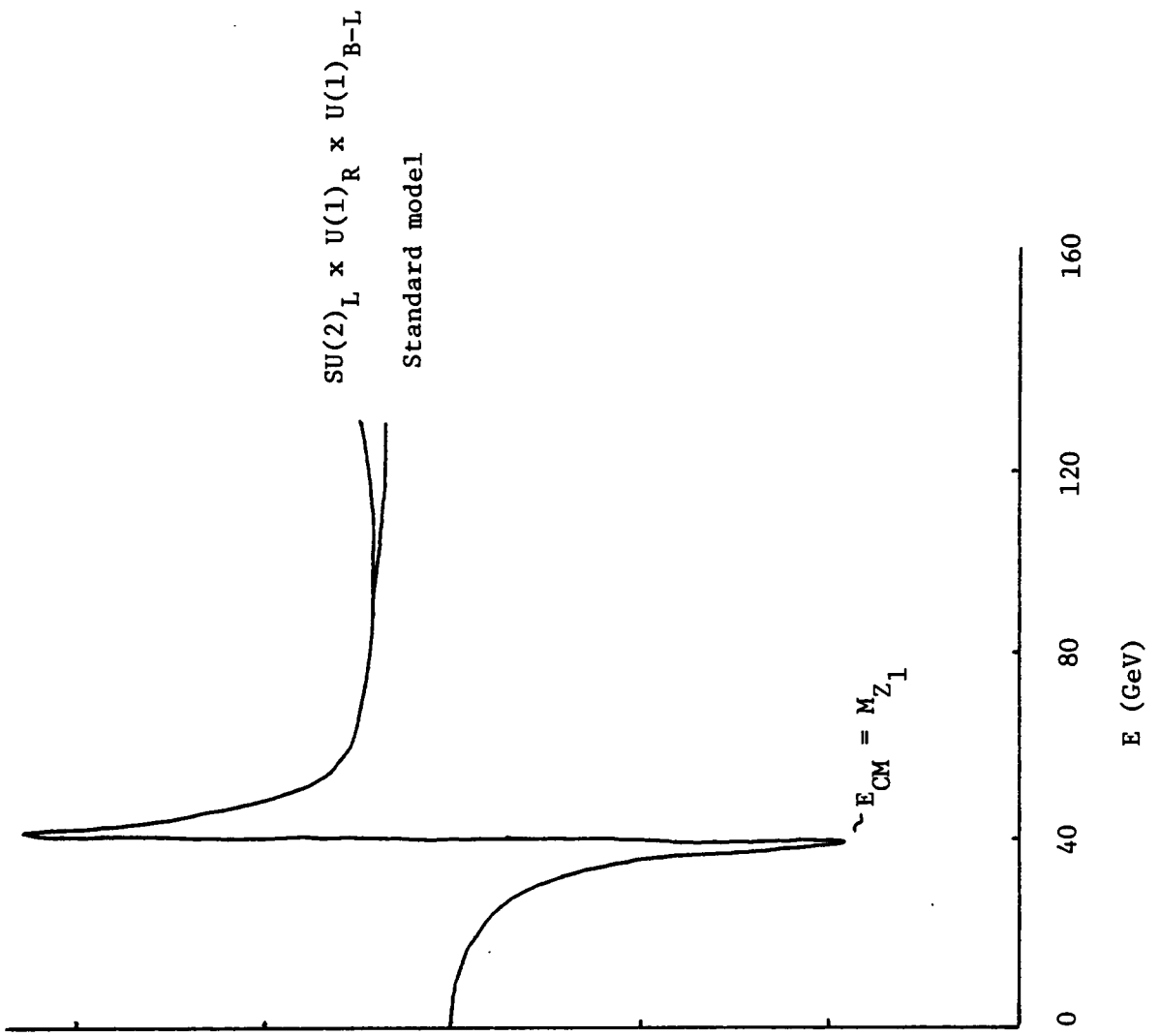

$$A = \frac{\sigma(e_L^+ e_R^- \to \tau_L^+ \tau_R^-) - \sigma(e_L^+ e_R^- \to \tau_R^+ \tau_L^-)}{\sigma(e_L^+ e_R^- \to \tau^+ \tau^-)}$$

Figure 27

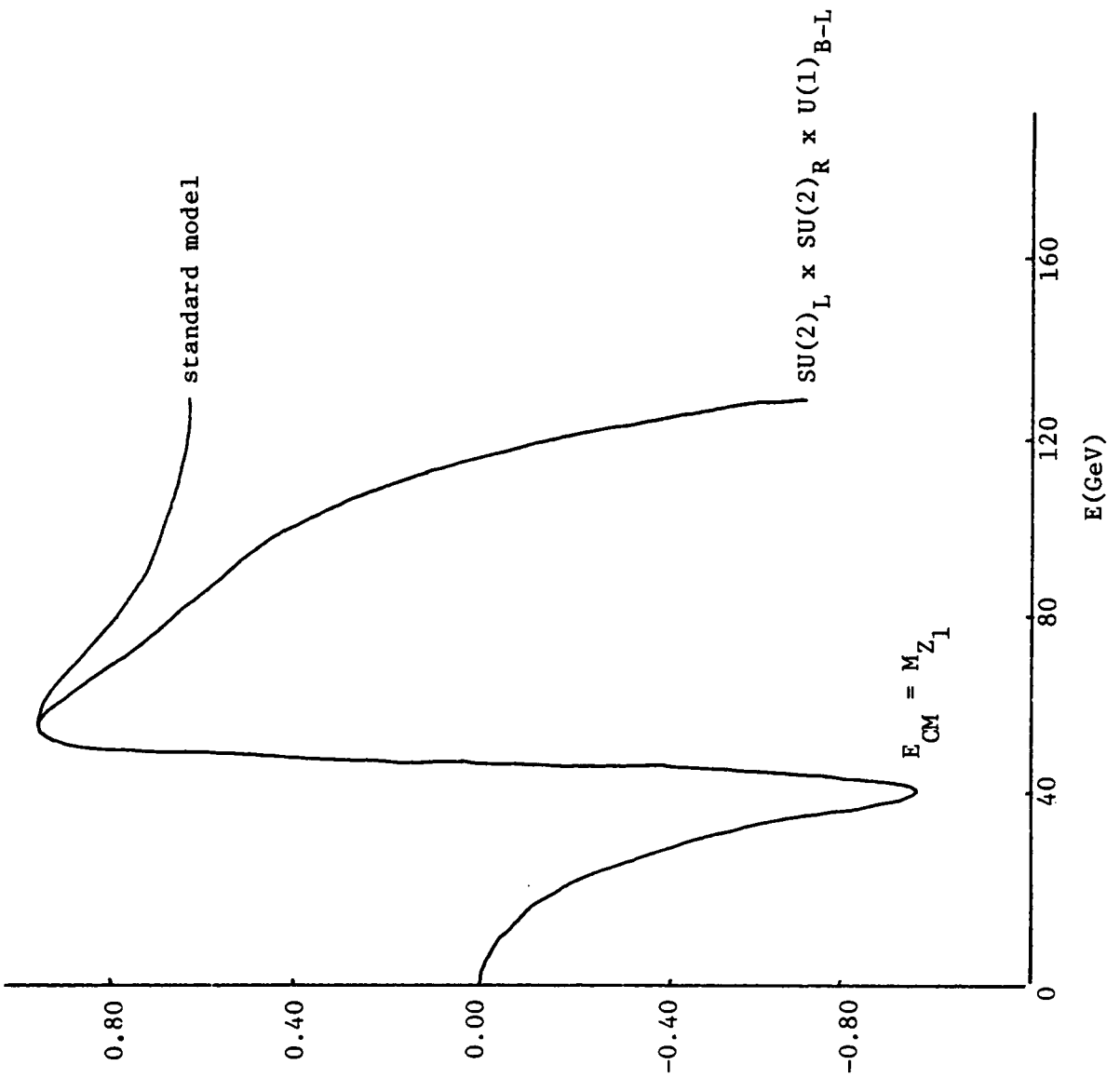

$$A = \frac{\sigma(e_R^+e_L^- \to \tau_R^+\tau_L^-) - \sigma(e_L^+e_R^- \to \tau_R^+\tau_L^-)}{\sigma(e_L^+e_R^- \to \tau_R^+\tau_L^-) + \sigma(e_L^+e_R^- \to \tau_R^+\tau_L^-)}$$

Figure 28

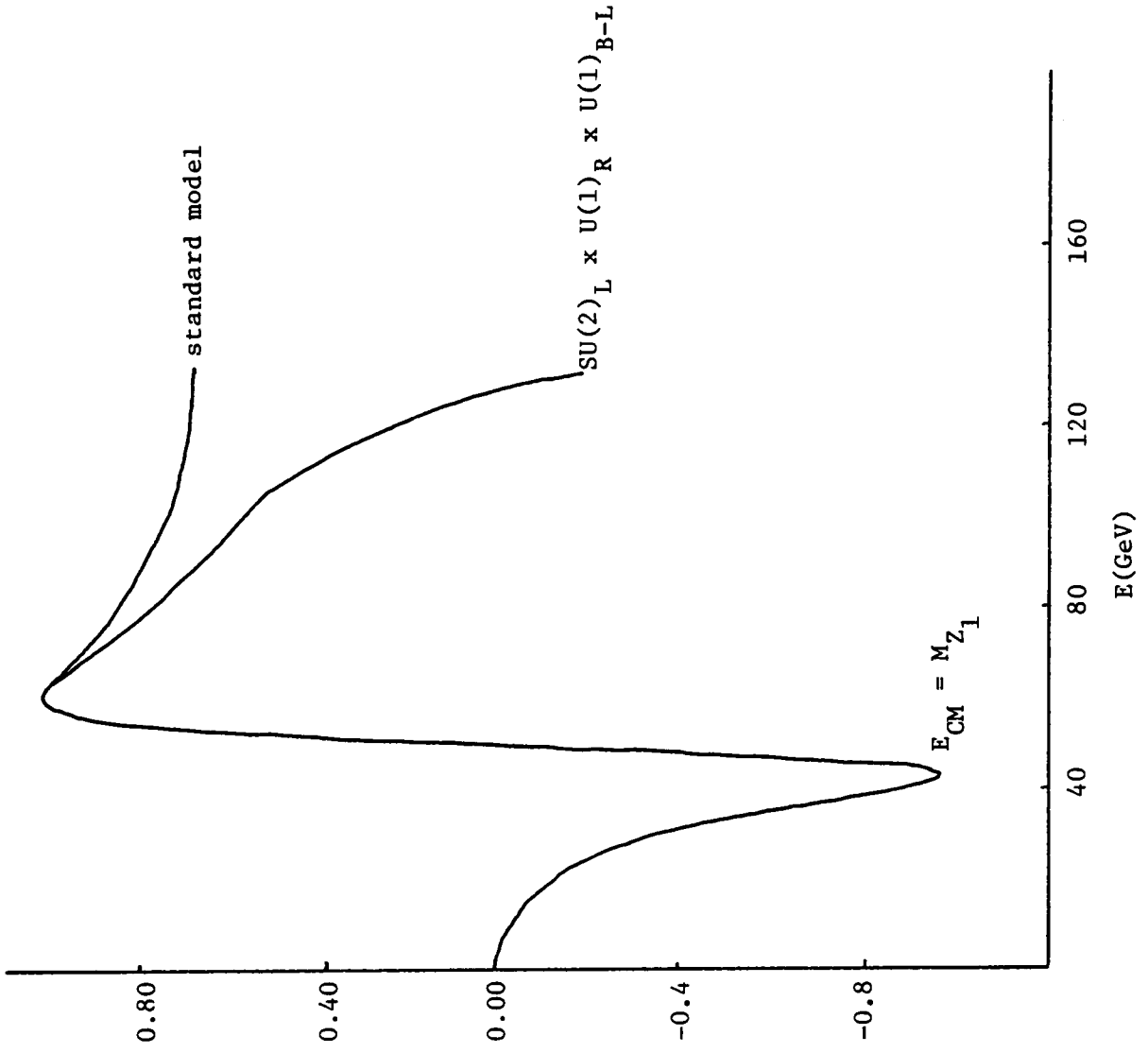

$$A = \frac{\sigma(e_R^+ e_L^- \to \tau_R^+ \tau_L^-) - \sigma(e_L^+ e_R^- \to \tau_R^+ \tau_L^-)}{\sigma(e_L^+ e_R^- \to \tau_R^+ \tau_L^-) + \sigma(e_R^+ e_L^- \to \tau_R^+ \tau_L^-)}$$

Figure 29

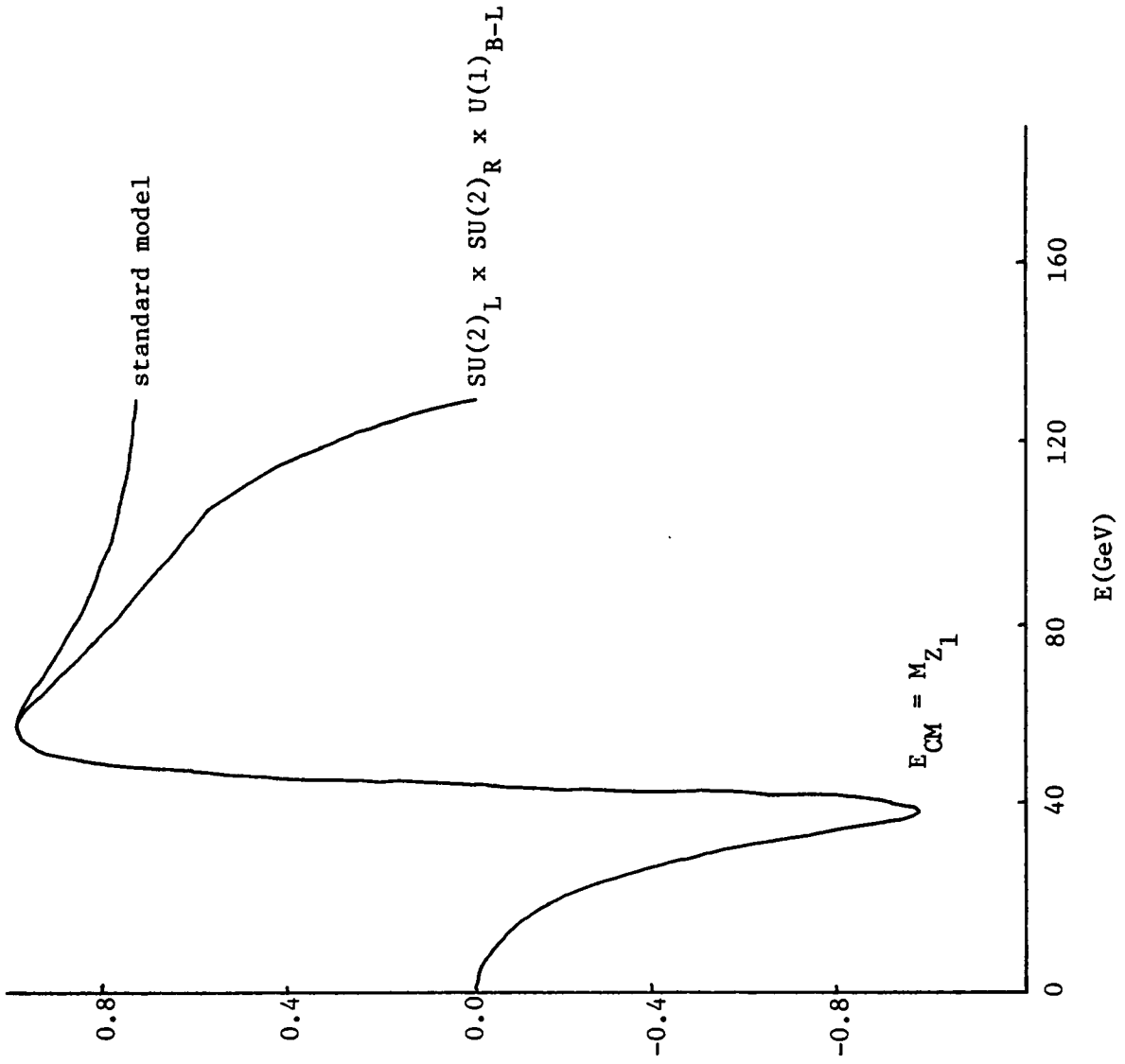

$$A = \frac{\sigma(e_L^+ e_R^- \to \tau_L^+ \tau_R^-) - \sigma(e_R^+ e_L^- \to \tau_R^+ \tau_L^-)}{\sigma(e_L^+ e_R^- \to \tau_L^+ \tau_R^-) + \sigma(e_R^+ e_L^- \to \tau_R^+ \tau_L^-)} \quad \text{in } SU(2)_L \times SU(2)_R \times U(1)_{B-L}$$

Figure 30

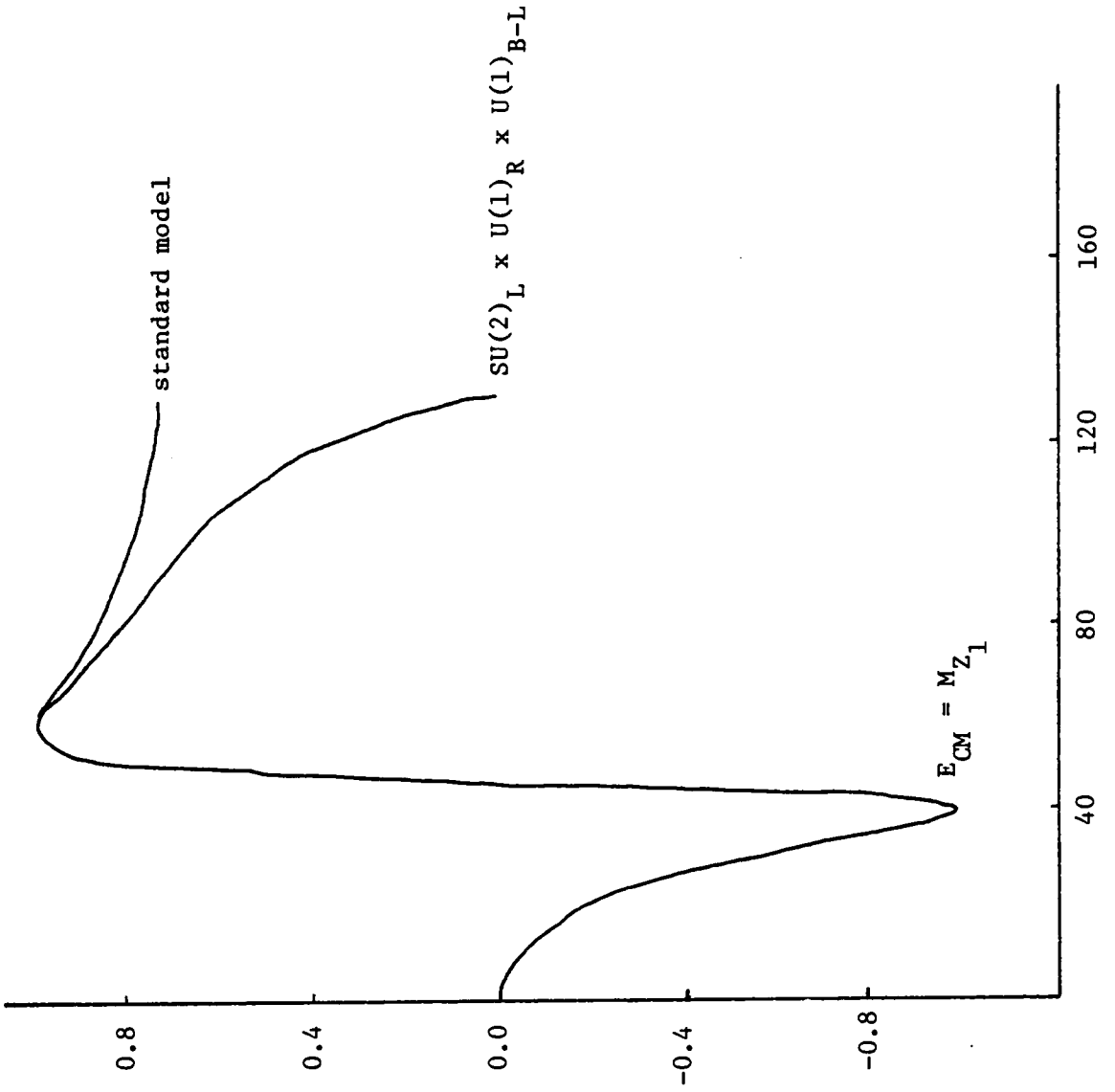

$$A = \frac{\sigma(e_L^+e_R^- \to \tau_L^+\tau_R^-) - \sigma(e_R^+e_L^- \to \tau_R^+\tau_L^-)}{\sigma(e_L^+e_R^- \to \tau_L^+\tau_R^-) + \sigma(e_R^+e_L^- \to \tau_R^+\tau_L^-)} \text{ is } SU(2)_L \times U(1)_R \times U(1)_{B-L}$$

Figure 31

EXPERIMENTAL TESTS ON ELECTRON-PROTON COLLIDER

The HERA electron-proton collider will have a (c.m. energy)^2 of 10^5 GeV^2. There are two experiments which can be done with the e-p collider. First, if the right-handed neutrino mass is less than 300 GeV, then the straightforward experiment is to detect the right-handed neutrino. Another experiment is deep inelastic scattering, i.e. a SLAC[5] type experiment. The difference between the cross sections using left- and right-handed electron beams reveals the neutral current, and this difference is sensitive to the second Z boson. Let us first consider the deep inelastic scatering.

e-p Deep Inelastic Scattering

This process is calculated from the Feynman diagram in Fig 32. The cross sections of e_L^--p and e_R^--p are given by:

$$\frac{ds(e_L)}{dxdy} = \frac{g^4 s}{32\pi} \sum_q \sum_{i=1}^{N} xq(x) \left[(g_V^i - g_A^i)^2 (f_V^i - f_A^i)^2 + (g_V^i - g_V^i)(f_A^i + f_A^i)^2 (1-y)^2\right] / (Q^2 + M_{Z_i}^2)^2 \quad (17)$$

$$\frac{ds(e_R)}{dxdy} = \frac{g^4 s}{32\pi} \sum_q \sum_{i=1}^{N} xq(x) \left[(g_V^i + g_A^i)^2 (f_V^i + f_A^i)^2 + (g_V^i + g_A^i)^2 (f_V^i - f_A^i)^2 (1-y)^2\right] / (Q^2 + M_{Z_i}^2)^2 \quad (18)$$

When $y \to 1$ and $x \to 1$, i.e. at the highest four-momentum transfer, the u quark contribution dominates, and the d quark can be neglected. The numerical results in this case are given in Figures 33 and 34. At the highest available energy at HERA, the difference between the cross sections using left and right handed incident electron beams is 71% in the standard model, whereas it is 62% in the $SU(2)_L xU(1)_R xU(1)_{B-L}$ model, and 50% in the $SU(2)_L xSU(2)_R xU(1)_{B-L}$ model.

Now we turn to the possible detection of the right-handed neutrino.

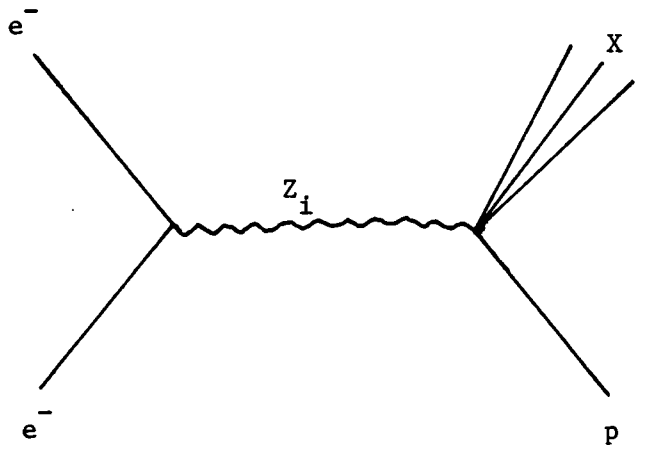

Figure 32

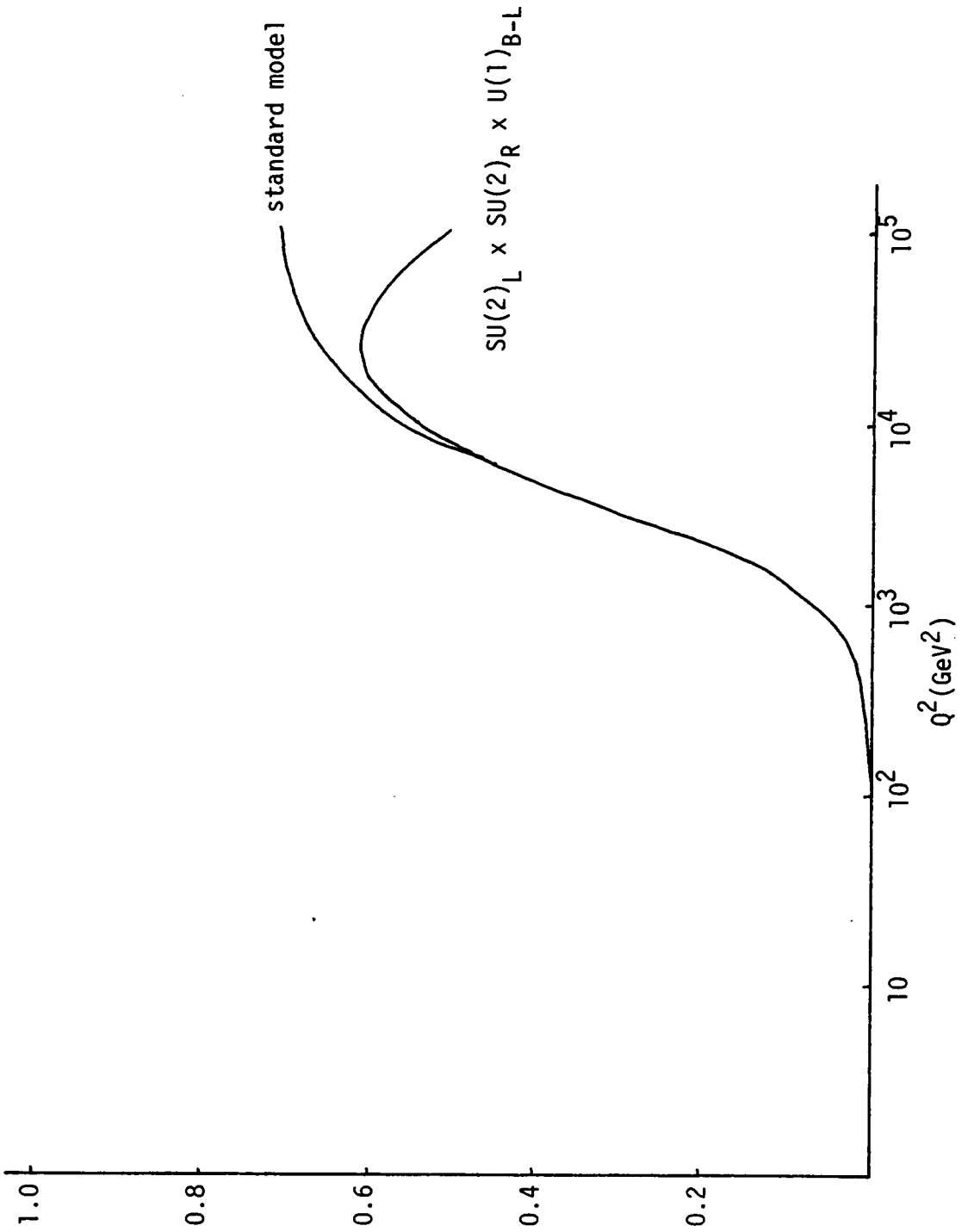

$$A = \frac{d\sigma(e_L p \to eX) - d\sigma(e_R p \to eX)}{d\sigma(ep \to eX)}$$

Figure 33

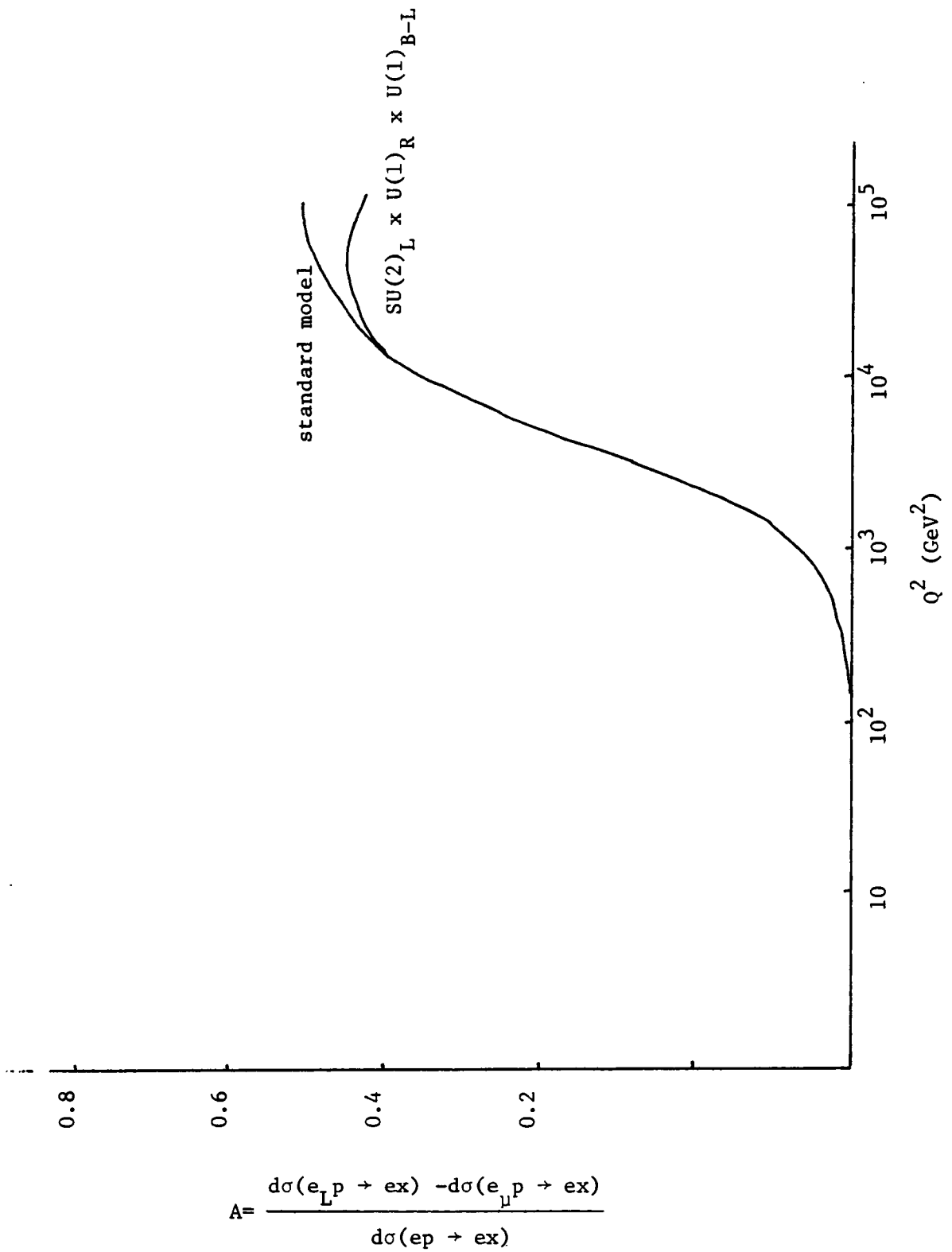
standard model
$SU(2)_L \times U(1)_R \times U(1)_{B-L}$
Q^2 (GeV^2)
10
10^2
10^3
10^4
10^5
0.8
0.6
0.4
0.2
$A = \frac{d\sigma(e_L p \to ex) - d\sigma(e_\mu p \to ex)}{d\sigma(ep \to ex)}$

Figure 34

$ep \to N_R + X$

Perhaps a more direct experiment to establish the existence of right-handed weak currents is to make use of the possibility of producing directly the right-handed neutrinos.

This process can be due to the exchange of W_R (Fig 35), or due to the exchange of W_L (Fig 36) if there is a mixing between the light neutrino and the heavy neutrino. If

$$U_{\nu N}^2 >> (M_L/M_R)^4$$

then the W_L diagram dominates. (The neutrino with mass 4~10 GeV produced by left-handed current was discussed by Chang et al [6].)

If

$$U_{\nu N}^2 << (M_L/M_R)^4$$

then the W_R diagram dominates.

where $U_{\nu N}$ is the light-heavy neutrino mixing matrix element, M_L and M_R are left and right W boson masses, respectively. These quantities depend on the Higgs structure of the model. The experimental limit on light-heavy neutrino mixing is[7]:

$$U_{\nu N}^2 \leq 0.043$$

for electron neutrinos. This inequality follows from the ratio:

$$\Gamma(\pi \to e\nu) : \Gamma(\pi \to \mu\nu)$$

The experimental limit on W_R mass is :

$$M_{W_R} > 1.6 \text{ TeV}.$$

In models in which B-L symmetry is spontaneously broken, (within a grand unification group or without the grand unification group), the neutrino has a Dirac mass at the electron mass scale and a Majorana mass at the B-L breaking scale. In this case,the mixing is :

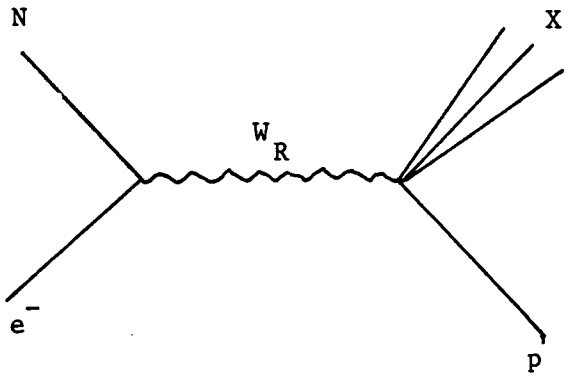

Figure 35

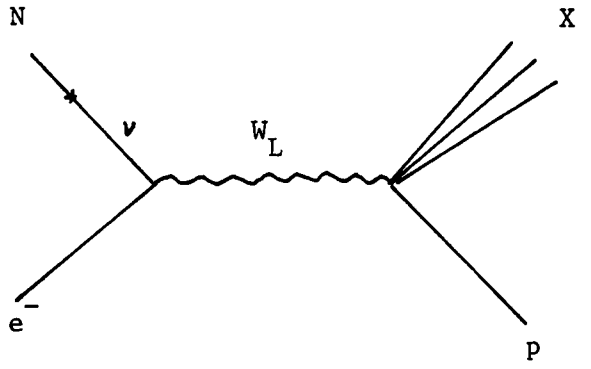

Figure 36

$$U_{\nu N} \sim -m_e/M_{B-L}$$

where m_e is the electron mass, and M_{B-L} is the B-L breaking scale.

In the SO(10) breaking chain as discussed by Chang et al, the B-L breaking scale is a few hundred GeV, whereas the W_R mass is 10^5 GeV. In this case, the W_L diagram dominates.

The total cross section of $ep \to N+X$ in the case of W_R dominance is:

$$\sigma=\frac{g^4}{2\pi} \int_L^U dy \int_A^1 dy \, (2MExy + M_W^2)^{-2} \qquad (19)$$

$$\{F_2(x)[\, ME\,(2-2y+y^2) - \frac{(2-y)m^2}{2x}\,]$$

$$+ xF_3(x)\,[\, MEy(2-y) - \frac{m^2 y}{2x}\,]\,\}$$

where m is the heavy neutrino mass, M_W is the W_R boson mass. M is the proton mass. The quantity E is defined by:

$$E=(E_{cm})^2/(2M)$$

The limits of integration U, L, A are given by:

$$A=1+\frac{1}{2MEy}\{-2ME-m^2+2E(E+M)(1-y)-2E[E^2(1-y)^2-m^2]^{-1/2}\} \qquad (20)$$

$$U=1-m(1+M/E)/\sqrt{(2EM+M^2)},$$

and

$$L = 1 - (1/2)(2EM+M^2)\{(2EM+m^2)(E+M)+E[(2EM-m^2)^2-4M^2m^2]^{-1/2}\} / E. \qquad (21)$$

The maximum of the neutrino mass which can be produced for a given beam energy is:

$$m^2 < 2M\ [E+M-(2EM+M^2\ )^{-1/2}\ ] \tag{22}$$

which implies $m < E_{cm} - M$. Finally, $F_2(x)$ and $F_3(x)$ are the proton structure functions. They are related to the quark distribution functions by the formulas:

$$F_2(x) = 2\ [xu(x)+x\bar{d}(x)+x\bar{s}(x)+xc(x)\ ] \tag{23}$$

$$xF_3(x) = 2\ [xu(x)-x\bar{d}(x)-x\bar{s}(x)+xc(x)\ ]$$

The quark distribution can be fitted using deep inelastic scattering data:

$$xu(x) = 1.14\ (1-x)^3$$

$$xc(x) = 0.03\ (1-x)^{10}$$

$$x\bar{d}(x) = 0.17\ (1-x)^7 \tag{24}$$

$$x\bar{s}(x) = 0.1\ (1-x)^{10}$$

If the W_L diagram dominates, in Eq.(18), M_W is replaced by W_L mass, and there is an extra factor $U_{\nu N}^{\ 2}$ multiplying the entire right-hand side.

In the case that the W_L diagram dominates, at the highest HERA energy ($E_{cm}^{\ 2}=10^5$ GeV^2), the neutrino production crossection vs the neutrino mass is plotted in Figure 37.

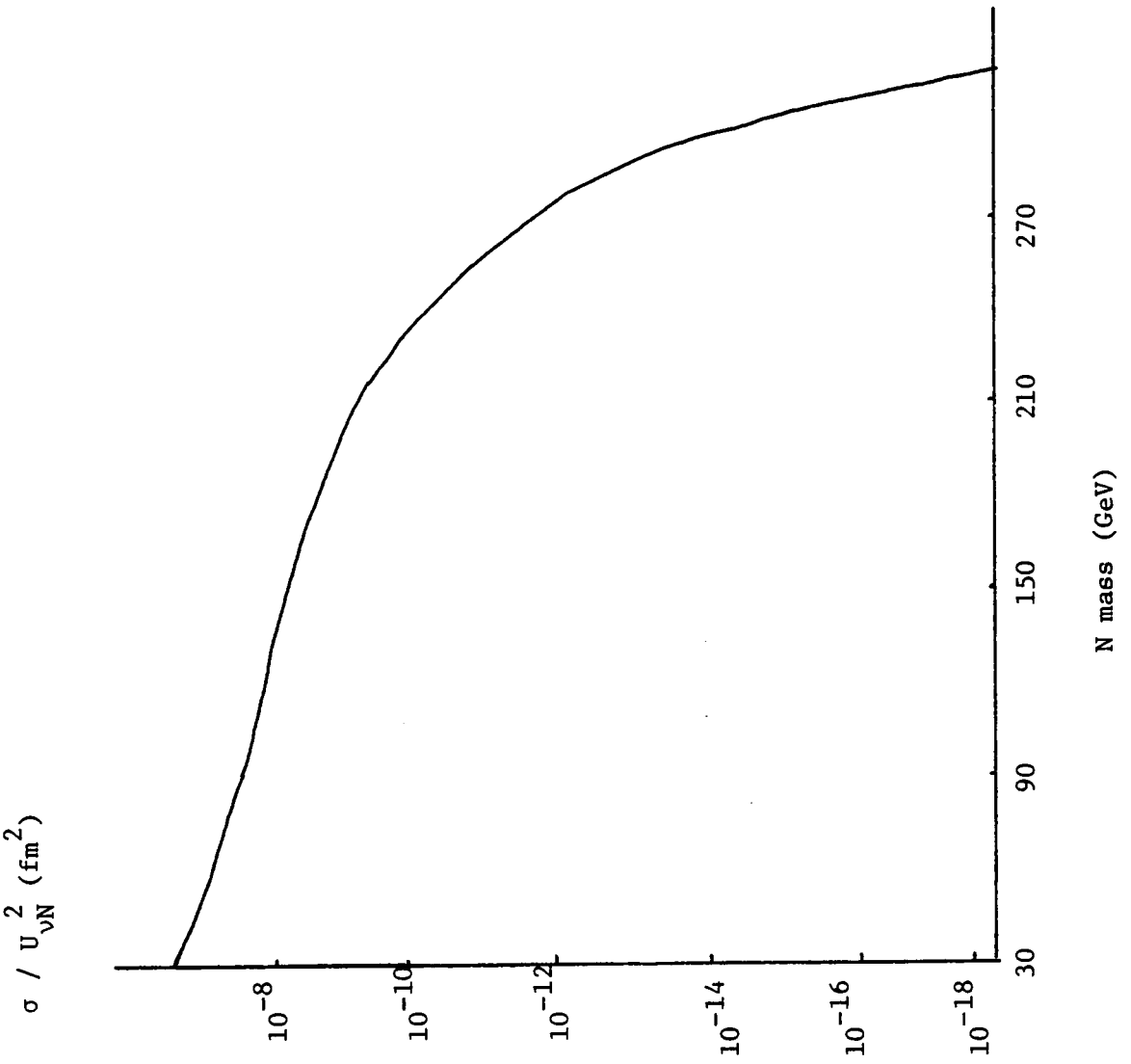

σ (e^- p → N + X) vs. N mass

Figure 37

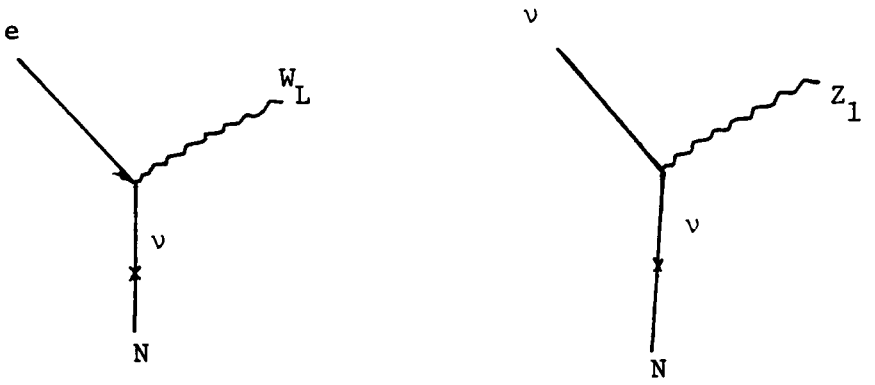

Figure 38

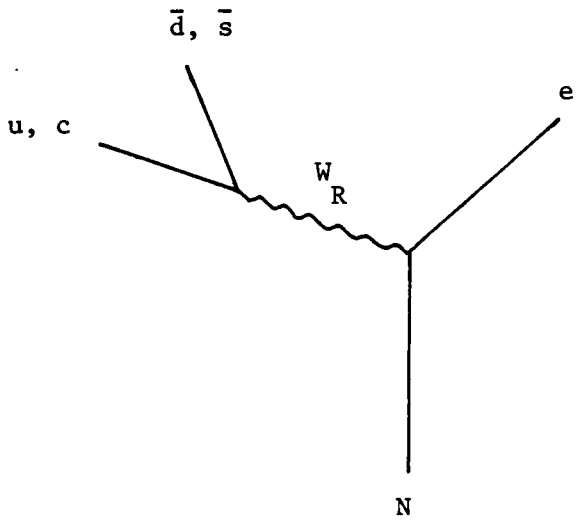

Figure 39

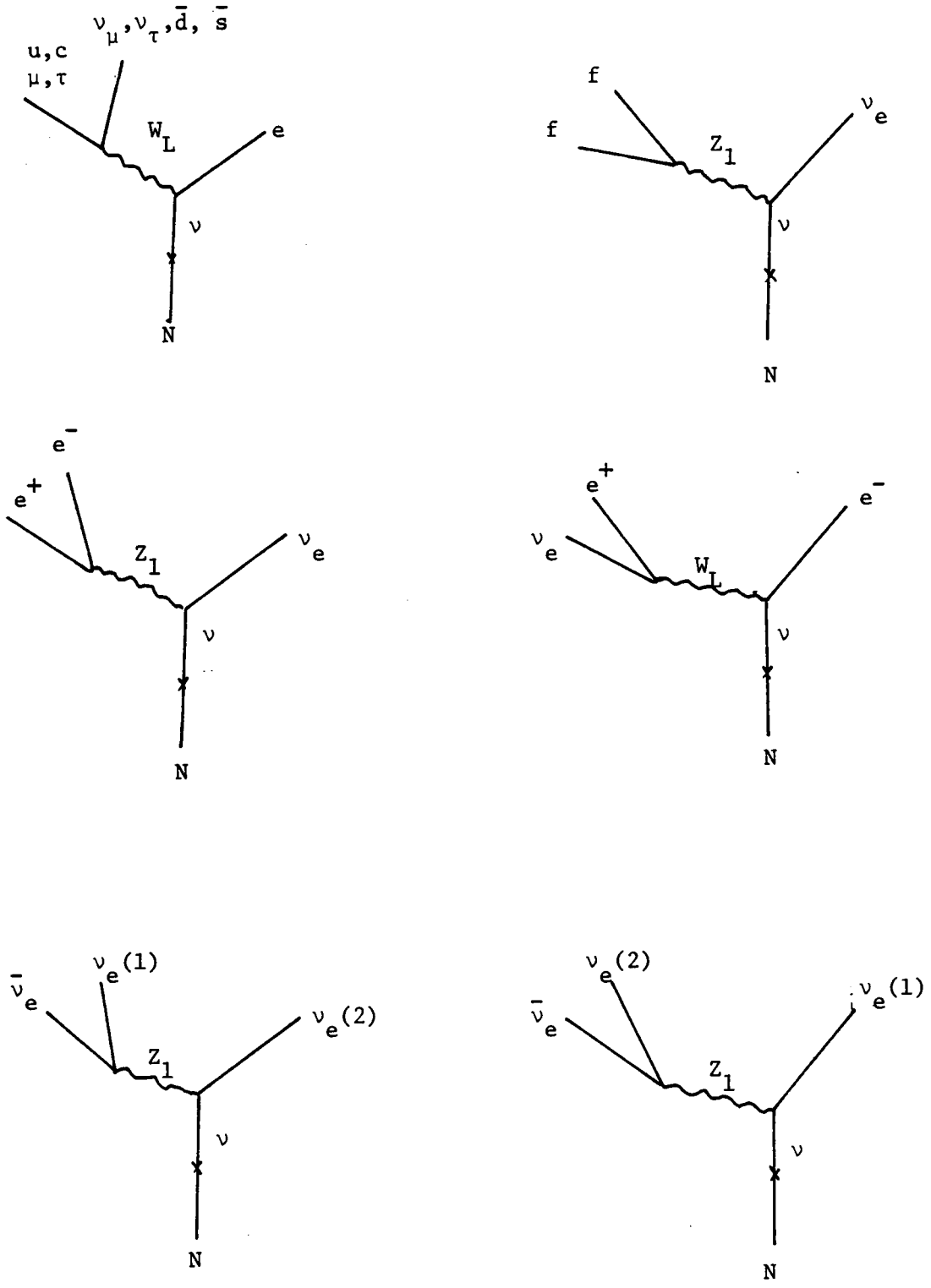
$\nu_\mu, \nu_\tau, \bar{d}, \bar{s}$
u,c
μ,τ
W_L
e
ν
N
f
f
Z_1
ν_e
ν
N
e^-
e^+
Z_1
ν_e
ν
N
e^+
ν_e
W_L
e^-
ν
N
$\bar{\nu}_e$
$\nu_e(1)$
Z_1
$\nu_e(2)$
ν
N
$\nu_e(2)$
$\bar{\nu}_e$
Z_1
$\nu_e(1)$
ν
N

Figure 40

Now we discuss the decay mode of the right-handed neutrino, because we can only identify it through its decay products. The decay of the heavy neutrino is calculated from the Feynman diagrams in Fig 38, 39 and 40; which channel dominates depends on the mixing angle of light and heavy neutrinos and the ratio of W_L and W_R masses.

If

$$U_{\nu N}^2 >> (M_L/M_R)^4$$

and $m_N > M_Z$, then the major decay channel is $N \to e\, W_L$ and $N \to \nu_e\, Z_1$. The partial width of $N \to e\, W_L$ is:

$$g^2\, U_{\nu N}^2\, (m_N^2+2M_W^2)(m_N^2-M_W^2)^2/(32\pi m_N^3 M_W^2)\ , \tag{25}$$

and the $N \to \nu_e\, Z_1$ width is:

$$g^2\, U_{\nu N}^2\, (m_N^2+2M_Z^2)(m_N^2-M_Z^2)^2/(64\pi \cos^2\theta_W m_N^3 M_Z^2)\ . \tag{26}$$

If $m_N < M_W$, there are four different types of channels:

The first type of channel is $N \to e\, \mu\, \nu_\mu$, $N \to e\, \tau\, \nu_\tau$, $N \to e\, u\, d$, or $N \to e\, c\, s$. Each of these processes has the partial width given by:

$$\Gamma = U_{\nu N}^2\ g^4 m_N^2/(768\pi^3)\ \{\ 1/(4m_N)+3(M_W^2-m_N^2)/(8m_N M_W^2)+(M_W^2-m_N^2)/(2m_N^3) \tag{27}$$
$$+(M_W^2-m_N^2)^2/(4M_W^2 m_N^3)-[3M_W^2(M_W^2-m_N^2)/(4m_N^5)]\log[M_W^2/(M_W^2-m_N^2)]\ \}\ .$$

The second type of channel is $N \to \nu_e\, f^+\, f^-$. Here f can be μ, τ, or any quark flavour. The partial width of each f is:

$$\Gamma = U_{\nu N}^2 \; g^2/(4\cos^2\theta_W)[(g_V^f+g_A^f)^2+(g_V^f-g_A^f)^2]m_N^2/(768\pi^3)$$
$$\{1/(4m_N)-[3M_Z^2(M_Z^2-m_N^2)/(4m_N^5)]\log[M_Z^2/(M_Z^2-m_N^2)]$$
$$+3(M_Z^2-m_N^2)/(8M_Z^2m_N)+(M_Z^2-m_N^2)/(2m_N^3)+(M_Z^2-m_N^2)^2/(4M_Z^3m_N^2) \quad \} \tag{28}$$

The third channel is $N \to e^+e^-\nu_e$ with the partial width:

$$\Gamma = U_{\nu N}^2 \; m_N^2 / (768 \pi^3) \; g^4$$
$$\{1/(4m_N)-[3M_W^2(M_W^2-m_N^2)/(4m_N^5)]\log[M_W^2/(M_W^2-m_N^2)]$$
$$+3(M_W^2-m_N^2)/(8M_W^2m_N) +(M_W^2-m_N^2)/(2m_N^3) + (M_W^2-m_N^2)^2/(4M_W^2m_N^3) \}$$
$$+ U_{\nu N}^2 \; g^2/(4\cos^2\theta_W)[(g_V^e+g_A^e)^2+(g_V^e-g_A^e)^2] \; m_N^2/(768\pi^3)$$
$$\{1/(4m_N)-[3M_Z^2(M_Z^2-m_N^2)/(4m_N^5)]\log[M_Z^2/(M_Z^2-m_N^2)]$$
$$+3(M_Z^2-m_N^2)/(8M_Z^2m_N) +(M_Z^2-m_N^2)/(2m_N^3) +(M_Z^2-m_N^2)^2/(4M_Z^2m_N^3) \}$$
$$- U_{\nu N}^2 \; g^3/(1024\pi^3\cos\theta_W)(g_V^e-g_A^e)$$
$$\int_0^{m_N/2} dE \; (m_N^2-2m_NE)E/m_N/(-2m_NE+M_Z^2-M_W^2)$$
$$[\log(-2m_N^2E+M_Z^2m_N) -\log(-2m_N^2E+M_Z^2m_N-2M_Z^2E+2m_N^2E)$$
$$-\log(M_W^2m_N) + \log(2Em_N^2-4m_NE^2-2M_W^2E+M_W^2m_N) \quad] \tag{29}$$

The fourth channel is $N \to \nu_e \nu_e \nu_e$, with the partial width:

$$\Gamma = U_{\nu N}^2 \; m_N^2 \, g^4 / (1536 \, \pi^3 \cos^4\theta_W)$$
$$\{1/(4m_N) - [3M_Z^2(M_Z^2-m_N^2)/(4m_N^5)]\log[M_Z^2/(M_Z^2-m_N^2)]$$
$$+3(M_Z^2-m_N^2)/(8M_Z^2m_N) + (M_Z^2-m_N^2)/(2m_N^3) + (M_Z^2-m_N^2)^2/(4M_Z^2m_N^3)\}$$
$$+ U_{\nu N}^2 \; g^4 / (2048 \, \pi^3 \cos^4\theta_W)$$
$$\int_0^{m_N/2} dE \; E \, (m_N^2 - 2m_N E) / (2m_N^2 E)$$
$$[\log(-2m_N^2E+M_Z^2m_N) - \log(-2m_N^2E+M_Z^2m_N-2M_Z^2E+2m_N^2E)$$
$$-\log(M_Z^2m_N) + \log(2Em_N^2-4m_NE^2-2M_Z^2E+M_Z^2m_N)] \qquad (30)$$

The numerical results are plotted in Figure 41.

If the neutrino mass is below the W_L mass, the decay branching ratios are:

$$B(e\ \mu\ \nu)=B(e\ \tau\ \nu)=B(e\ u\ d)=B(e\ c\ s)=B(e\ t\ b)=8.0\%$$

$$B(\nu\mu^+\mu^-)=B(\nu\tau^+\tau^-)=0.8\%$$

$$B(\nu_e\nu_\mu\nu_\mu)=1.6\%$$

$$B(\nu_e\nu_\tau\nu_\tau)=1.6\%$$

$$B(\nu\ u\ u)=B(\nu\ c\ c)=B(\nu\ t\ t)=2.7\%$$

$$B(\nu\ d\ d)=B(\nu\ s\ s)=B(\nu\ b\ b)=3.5\%$$

$$B(\nu_e\ e^+\ e^-)=9.1\%$$

$$B(\nu_e\nu_e\nu_e)=2.6\%$$

and if the neutrino mass is above the W_L mass, then the branching ratios are :

$$B(N \to \nu Z) \simeq 33\%$$

$$B(N \to e\ W) \simeq 67\%$$

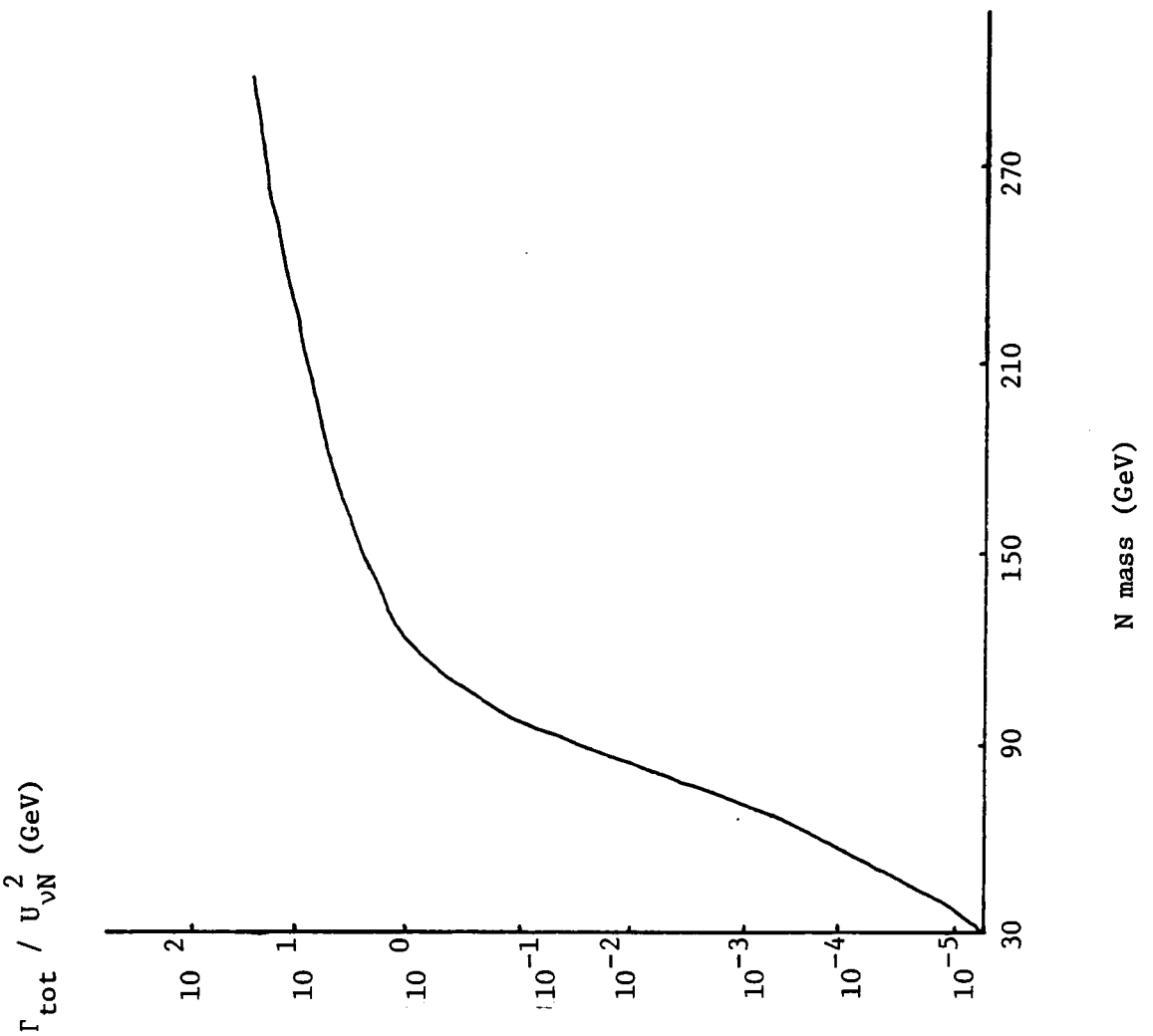

right-handed neutrino vs. mass

Figure 41

The decay of Z_2 and W_R

Finally, it is interesting to predict the decay of Z_2 and W_R bosons. The decay of Z_2 boson goes to fermion pairs, as calculated from the Feynman diagram in Fig.42, and has the partial width:

$$1/(12\pi M_Z^2)\sqrt{(M_Z^2-4m_f^2)}\{[(g_V^f)^2+(g_A^f)^2](M_Z^2-m_f^2)-3[(g_V^f)^2-(g_A^f)^2]m_f^2\} \quad (31)$$

Numerically $\Gamma \simeq 0.02M_R$ and,

$$B(\nu_e\nu_e)=B(\nu_\mu\nu_\mu)\simeq 0.7\%$$

$$B(\nu_\tau\nu_\tau)\simeq 0.7\%$$

$$B(e^+e^-)=B(\mu\mu)=B(\tau\tau)\simeq 2.5\%$$

$$B(u\ u)=B(c\ c)=B(t\ t)\simeq 11\%$$

$$B(d\ d)=B(s\ s)=B(b\ b)\simeq 19\%$$

In the $SU(2)_L xSU(2)_R xU(1)_{B-L}$ model, the decay of W_R to up-quark down-quark pairs, as calculated from Feynman diagram in Fig 43, has the partial decay width:

$$g^2 M_W /(48\pi) \quad (32)$$

Numerically, $\Gamma \simeq 0.02\ M_W$ with branching ratios :

$$B(u\bar{d})=B(c\bar{s})=B(t\bar{b})=33\%$$

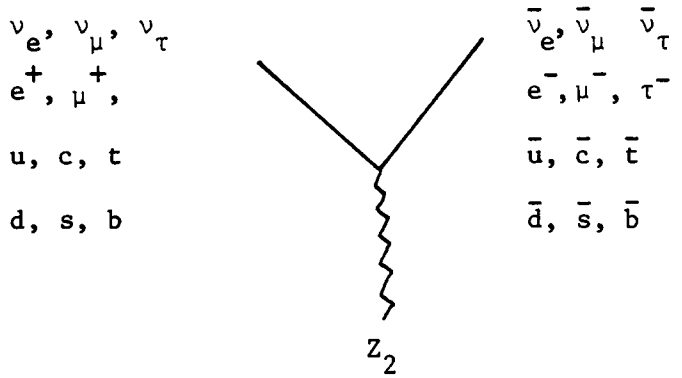

Figure 42

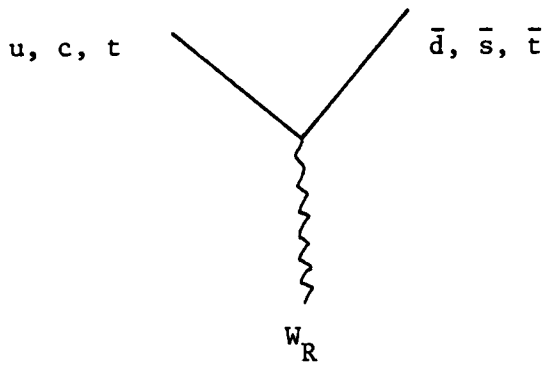

Figure 43

SUMMARY

Of all the possible experiments to test for the right-handed weak current, there are three which are most sensitive. The first expriment is the measurement of backward-forward asymmetry in the process $e^+e^- \rightarrow \mu^+\mu^-$. At the highest available LEP energy, i.e. E_{CM} = 260 GeV, the standard model predicts the asymmetry to be 53%, whereas the $SU(2)_L xU(1)_R xU(1)_{B-L}$ model predicts -2.6%, and the $SU(2)_L xSU(2)_R xU(1)_{B-L}$ model predicts -22%, if the M_{Z_2} mass is 300 GeV. This experiment has the advantage over experiments which require a polarized beam or which require observation of the final state polarization, because the process $e^+e^- \rightarrow \mu^+\mu^-$ has a greater count rate.

The second experiment is the measurement of the following cross sections:

$$\text{(I)}\quad e^+(L)e^-(R) \rightarrow \tau^+(L)\tau^-(R)$$

$$\text{(II)}\quad e^+(L)e^-(R) \rightarrow \tau^+(R)\tau^-(L)$$

$$\text{(III)}\quad e^+(R)e^-(L) \rightarrow \tau^+(R)\tau^-(L)$$

The quantity $[\sigma(I)-\sigma(II)]/[\sigma(I)+\sigma(II)]$ is predicted to be 74% by the standard model, whereas the $SU(2)_L xU(1)_R xU(1)_{B-L}$ model predicts -2.0%, and the $SU(2)_L xSU(2)_R xU(1)_{B-L}$ model predicts -1.9%. Furthermore the quantity $[\sigma(II)-\sigma(III)]/[\sigma(II)+\sigma(III)]$ is predicted to be 67% by the standard model, whereas the $SU(2)_L xU(1)_R xU(1)_{B-L}$ model predicts -21%, and the $SU(2)_L xSU(2)_R xU(1)_{B-L}$ model predicts -76%. However if the the initial beam is polarized, we loose beam intensity, and if the final state

polarization is measured, the count rate is diminished. Thus this experiment is very difficult.

The third experiment which would be the most definitive is the heavy neutrino production in e^-p collisions. Because of the uncertainty in the light-heavy neutrino mixing angle, the W_R boson mass and the heavy neutrino mass, it is difficult to predict the cross section. Under the most favorable circumstances, assuming that $U_{\nu N}^2 \simeq 0.01$ and $M_N \simeq 100$ GeV, the cross section is at the order of magnitude of 10^{-10} fm^2.

REFERENCES FOR PART I

1. Phys.Lett.122B (1983)103

2. Phys.Lett.129B (1983)130

3. T. G. Rizzo, G. Senjanovic, Phys.Rev.D24,704(1981); G. Senjanovic, R. N. Mohapatra, Phys.Rev. D 12,1502(1975)

4 D. Chang, R. N. Mohapatra, J. Gipson, R. E. Marshak, M. K. Parida, Phys. Rev. D31, 1718(1985)

5 C. Y. Prescott, Proc. Int. Conf. on High Energy Physics, Geneva 126(1979)

6 L. N. Chang, E. Derman, J. N. Ng, Phys.Rev.D12,3539(1975).

7 M. Gronau, C.N.Leung, J.L. Rosner, Phys. Rev. D29,2539(1984)

Part II SEMI-PHENOMINOLOGICAL THEORY OF $(Q\bar{q})$ SYSTEM

INTRODUCTION

In the years since 1974, two heavy quarks, charm and bottom were found. They enlarge the quark spectrum from the original 3 to 5. Recently, there appears to be evidence for the t quark with a mass in the neighborhood of 40 Gev.

The charm and bottom quarks were first found in the quarkonium state, i.e., a quark and an antiquark with the same flavour in a bound state. A few years later , the D meson, which contains a c quark and a light antiquark ($\bar{u}$ or $\bar{d}$) , and the B meson, which contains a b quark and a light antiquark ($\bar{u}$ or $\bar{d}$), were found in charmonium and bottomonium decay products. The F meson, which contains a c quark and an s antiquark, were discovered recently. Their properties are under experimental investigation. According to the quark model, we expect to have $(b\bar{s})$ and $(b\bar{c})$ mesons as well. If the existence of the t quark is confirmed, we should have another five mesons $(t\bar{u})$, $(t\bar{d})$, $(t\bar{s})$, $(t\bar{c})$, $(t\bar{b})$. The understanding of their properties is of great interest to particle theory.

In this paper, by $(Q\bar{Q})$, we mean quarkonium, i.e. the system composed of a quark and an antiquark of the same flavour. Whereas $(Q\bar{q})$ refers to the system composed of a quark and an antiquark of different flavour, with $m(Q) > m(q)$. This work is devoted to the study of the $(Q\bar{q})$ system.

In the $(Q\bar{q})$ system, there are many properties which can be measured experimentally. First of all, we can measure the 1^3S_1 and 1^1S_0 masses. We can also measure the total width and the branching ratios of the various channels. But for any $(Q\bar{q})$ system in which Q is a c or b quark, the

main decay products are hadrons. We do not know how to treat the hadron final state interactions. So there is no reliable way to predict the $(Q\bar{q})$ total width and the hadronic decay partial width other than by rough estimates. However, there is a decay channel which is simple from a theoretical point of view, i.e. the $(\ell,\bar{\nu}_\ell)$ final state. We know that $(\ell\ \bar{\nu}_\ell)$ comes from the annihilation of the quark-antiquark pair into a virtual W boson. There is no complexity of final state strong interactions. The production of $(\ell\ \bar{\nu}_\ell)$ from the virtual W boson can be calculated without any ambiguity. The problem is to estimate the annihilation probability of Q and $\bar{q}$ to virtual W. Mathematically, this is described by the leptonic decay constant f. In this work we limit ourselves to the calculation of three quantities: the masses of the 1^3S_1 state, and 1^1S_0 state, as well as f.

Up to now, we have sparse experimental information about $(Q\bar{q})$ particles. We only know the masses of the D ($c\bar{u}$ or $c\bar{d}$ systems) and F ($c\bar{s}$ system) mesons in the 1^1S_0 state and in the 1^3S_1 state. We also know the mass of the B meson ($b\bar{u}$ and $b\bar{d}$ system) in the 1^1S_0 state. On the other hand, we have much richer experimental information about $(Q\bar{Q})$ systems. We know the whole spectrum of charmonium and bottomonium. We also know their e^+e^- decay widths, which is from the annihilation of the quark and antiquark into a virtual photon. It is like the $(\ell\bar{\nu})$ decay channel of $(Q\bar{q})$ system, because it is simple theoretically. For them $(Q\bar{Q})$ system, we also limit ourselves to the mass spectrum and e^+e^- decay width since we do not know how to calculate the hadronic decay channel. Because of the similarities between $(Q\bar{q})$ and $(Q\bar{Q})$ systems, we expect one theory to describe both. According to QCD, which is generally believed to be the

correct theory of quark-quark interactions, the strong force which binds the quarks together is flavour independent. The leptonic decay process $Q\bar{Q} \rightarrow e^+e^-$ is caused by the electromagnetic interaction, whereas $Q\bar{q} \rightarrow \ell\bar{\nu}_\ell$ is caused by the weak interaction. Both electromagnetic and weak interactions can be derived from $SU(2)_L xU(1)_Y$ gauge theory (GWS model). Therefore, we expect that a model which gives the correct $(Q\bar{Q})$ spectrum and e^+e^- decay width should also predict the mass of $(Q\bar{q})$ state and its $\ell\ \bar{\nu}$ decay width.

The general strategy of this work is: first try to calculate the quarkonium states, using the experimental information we already have, then apply the same model and the same parameters to $(Q\bar{q})$ states.

THE POTENTIAL MODEL

There are two ways to do quantitative calculations based on the quark model. After the initial quark model with only three flavours was suggested, the MIT bag model was introduced. The bag model gives many results concerning baryons composed of light quarks. These results agree with the experiments to a surprisingly good degree for such a simple and naive model which has only a few parameters. But unfortunately, it can not treat the π meson and the K meson due to the failure to take into account chiral symmetry. Neither does it give a good description of charmonium and bottomonium systems.

After the discovery of charmonium, the non-relativistic potential model was developed. The potential model assumes that the charmonium and bottomonium systems can be treated as non-relativistic systems, because their constituent quarks are heavy. It explains virtually all the properties of the charmonium and bottomonium states. On the other hand, it is not justified for mesons with light quarks. There is some work done with three quark states based on the potential model, but it is unclear whether or not it works for baryons and what to assume for the pair-wise potentials.

For the F meson, in which we are interested, the c quark can be treated as a non-relativistic particle. The s quark is at the border line between the relativistic and non-relativistic regime. Because of the c quark, we do not expect the bag model to give good predictions, since the bag model has already failed with charmonium. As an alterna-

tive, we propose to calculate the properties of the F meson using the potential model. As for the ($b\bar{c}$) meson state, the non-relativistic appoximation is well justified, because both constituents are heavy. The results should lead to good agreement with future experiments.

There are several different types of potentials. Some of them are totally phenomenological. Charmonium and bottomonium can be described by a power law potential, like the one suggested by Martin[1]:

$$V=-8.064+6.870\ r^{0.1}$$

$$M_b = 5.174$$

$$M_c = 1.8$$

$$M_s = 0.518\ .$$

All quantities are in terms of GeV. Martin et al calculated the entire charmoniun and bottomonium spectra with good success. Even more amazing, they can treat the ($s\bar{s}$) states as well, giving correct masses for the 1S, 1P and 2S states. Their prediction of the F meson mass is in good agreement with the recent measurement. There is no explanation from first priciples as to why the potential should have a power law dependence, though some people believe that it is in no way an accident. Even a simple linear potential can give the quarkonium spectra to reasonable accuracy, e.g. :

$$V = gr - V_0$$

These two approaches treat singlet-triplet mass splitting by introducing additional parameters. For example, in Martin's power law potential, a Fermi term is put in with the coefficient as an extra free parameter.

There is another type of potential which is motivated by QCD considerations which is generally believed to be the correct theory of strong

interactions[2]. The simplest among them is the Coulomb plus linear potential, first worked out by the Cornell group[3]. The Coulomb part is due to the short distance one-gluon exchange, and the linear term is implied by long distance confinement, which is indicated by lattice QCD; however the proof does not exist. There are many modifications to the Coulomb plus linear potential, for example a logarithmic potential in the intermediate range. They give essentially the same results for charmonium and bottomonium with limited improvement.

THE COULOMB PLUS LINEAR POTENTIAL

The most general Coulomb + linear potential has four terms. The first term is the Coulomb term.

$$-(4/3)\ \alpha_s\ /\ r$$

where α_s is the QCD fine structure constant, which varies from quark to quark according to the QCD renormalization group equation:

$$\alpha_s(M) = 4\pi/\beta_0/\log(M^2/\Lambda\overline{\overline{MS}}^2)-4\pi\beta_1\log\ \log(M^2/\Lambda\overline{\overline{MS}}^2)/\beta_0^3/\log(M^2/\Lambda\overline{\overline{MS}}^2) \qquad (33)$$

where

$$\beta_0 = 11 - (2/3)\ n_f$$

$$\beta_1 = 102 - (38/3)\ n_f$$

and n_f is the number of quark flavors with masses less than M. Therefore α_s is fixed by the parameter $\Lambda_{\overline{MS}}$.

The value of $\Lambda_{\overline{MS}}$ is usually derived from the ratio of quarkonium 3-gluon decay to leptonic pair decay[4], i.e. :

$$\Gamma_g\ /\ \Gamma_{\mu\mu} = 10(\pi^2-9)\alpha_s^3(M)\ /\ (81\pi\ e_q^2\ \alpha_e^2\ ) \qquad (34)$$

However, there is some theoretical ambiguity in this ratio. The correction factor is not close to one. So we obtain $\Lambda_{\overline{MS}}$ by fitting the quarkonium spectrum.

The second term in the potential is the linear term:

kr.

The coefficient k is obtained from quarkonium data fitting. It agrees in terms of order of magnitude with the one from lattice QCD. We must also take into account the mass splitting between singlet and triplet states due to the spin-spin interaction, namely:

$$\Delta M = M(^3S_1) - M(^1S_0) \tag{35}$$

The spin-spin interaction is described by the Fermi-Breit term:

$$(\frac{32\pi}{9})\ \alpha_s\ \psi^2(0)\ \sigma_1 \cdot \sigma_2\ /\ (m_1 m_2) \tag{36}$$

where m_1 and m_2 are the masses of the constituent quarks. $\psi(0)$ is the wave function at the origin. Note that Eq. (36) does not introduce any new parameters.

We also consider the relativistic corrections. This correction is particularly important for light quarks because of their low masses. In the original Coulomb+linear potential model of the Cornell group, a "Uehling" term was put in as an extra parameter. It varies from the c to the b quark. Later on, some theoretical work was done on the relativistic correction to the long range forces. Some authors have suggested that this correction term is proportional to the string tension k and inversely proportional to the quark masses.

One such work was done by Gromes[5] . He used a gauge invariant approach to the potential via a generalied Wilson loop, replacing static

sources by Dirac currents. The resulting expression is expanded with respect to 1/m. His final formula is:

$$V = \{1-(1/2)(1/m_1+1/m_2) + \Delta_1/(8m_1^2) + \Delta_2/(8m_2^2) \}\ kr \qquad (37)$$

where Δ is the Laplacian operator. m_1 and m_2 are the masses of the quarks of the system.

Work parallel with the above was done by Barnes and Ghandour[6]. They looked for an interaction operator which gives the known momentum space scattering amplitude (Feynman diagram) when sandwiched between initial and final nonrelativistic Pauli plane wave states. Their work yields:

$$\begin{aligned} V = \quad & +(1/2)m_1^{-2}\ [(1/4)(\Delta_1 S) + (\nabla_1)\cdot\nabla_1 + S\Delta_1\ ] \\ & +(1/2)m_2^{-2}\ [(1/4)(\Delta_2 S) + (\nabla_2)\cdot\nabla_2 + S\Delta_2\ ] \end{aligned} \qquad (38)$$

where ∇ is the differentiation operator, and S(r) is kr in Eq.(37).

In both Eq.(37) and Eq.(38), the correction term does not introduce any new parameters. We will use both formulas, and compare their predictions. We shall see, that the two different relativistic correction terms use slightly different parameters, and give slightly different predictions. We give two sets of predictions, those with the Gromes correction term, and the ones with the Barnes and Ghandour (B-G) correction term.

Altogether, there are only two parameters in the four terms of the potential, which are $\Lambda_{\overline{MS}}$ and k, besides the masses of the quarks. We

can deduce these two parameters and the two quark masses, M_c and M_b, from the charmonium and bottomonium spectra.

THE CALCULATION OF ($Q\bar{Q}$) STATES

Now we fit the charmonium and bottomonium states by means of this model and deduce the values of the parameters. As we know, the potential model is a very crude model, and we have severely limited the number of parameters, so we can not get very precise fits to the entire spectrum. All we want to do is to see how this simple QCD motivated nonrelativistic model can perform and what it predicts.

The parameters giving a good fit to the experimental quantities are:

$$\Lambda_{\overline{MS}} = 301 \text{ MeV}$$

$$k = 0.1965 \text{ GeV}^2$$

$$M_c = 1.3882 \text{ GeV}$$

$$M_b = 4.646 \text{ GeV}$$

with the Gromes correction term; and

$$\Lambda_{\overline{MS}} = 228.3 \text{ MeV}$$

$$k = 0.2567 \text{GeV}^2$$

$$M_c = 1.289 \text{ GeV}$$

$$M_b = 4.582 \text{ GeV}$$

with the B-G correction term.

The theoretical fitting compared with experiments are as shown in Table 1a, 1b, 2a, and 2b. In these tables, th I denotes the leptonic width without the QCD correction factor (Eq.40 below), and th II denotes the width with the QCD correction. By c.o.g. we mean center of gravity of the 1P state.

Table 1a

ψ	mass(MeV)		$M(^3S_1)-M(^1S_0)$		$\Gamma(e^+e^-)$(KeV)		
family	th	exp	th	exp	th I	th II	exp
1^3S_1	3097	3097	113	113	3.3	7.4	4.6±0.39
2^3S_1	3686	3686	84	92	1.8	4.0	2.05±0.21
3^3S_1	4123	4030	76		1.3	2.9	
4^3S_1	4492	4415	71				
1P	3488	3524					
c.o.g.							

Table 1b

Υ	mass(MeV)		$M(^3S_1)-M(^1S_0)$		$\Gamma(e^+e^-)$(KeV)		
family	th	exp	th	exp	th I	th II	exp
1^3S_1	9460	9460	34		0.66	1.0	1.26
2^3S_1	9908	10023	22		0.39	0.61	0.54
3^3S_1	10230	10355					
4^3S_1	10501	10573					
1P	9779	9904					
c.o.g.							

with the Gromes term.

Table 2a

ψ	mass(MeV)		$M(^3S_1)-M(^1S_0)$		$\Gamma(e^+e^-)$(KeV)		
family	th	exp	th	exp	th I	th II	exp
1^3S_1	3097	3097	113	113	3.7	7.3	4.6±0.39
2^3S_1	3686	3686	93	92	2.1	4.1	2.05±0.21
3^3S_1	4062	4030	83		1.6	3.1	
4^3S_1	4328	4415	79				
1P	3587	3524					

c.o.g.

Table 2b

T	mass(MeV)		$M(^3S_1)-M(^1S_0)$		$\Gamma(e^+e^-)$(KeV)		
family	th	exp	th	exp	th I	th II	exp
1^3S_1	9460	9460	33		0.71	1.1	1.26±0.06
2^3S_1	9961	10023	23		0.45	0.67	0.54±0.03
3^3S_1	10322	10355	20				
4^3S_1	10623	10573	19				
1P	9821	9903					

c.o.g.

with the B-G term.

We proceed to comment on the results given in Tables 1 and 2. The QCD cutoff parameter $\Lambda_{\overline{MS}}$ is determined by α_s for charmonium which, in turn, is mainly determined by the 1S state triplet-singlet splitting associated with the Fermi-Breit term. The string tension k is fixed by the masses of the 2S, 3S, and 4S states relative to the 1S state. The coulomb term does not contribute very much except for the 1S state. The linear term does not give a precise fit for the exited states, unless we put in an extra additive parameter and let it vary from charmonium to bottomonium. To get a better fit, the string tension in the potential has to vary from c quark to b quark, so that the k for bottom is larger than the k for charm. In the above, we have used the same k for all quark-antiquark potentials. Actually, from the point of view of QCD, k is related to $\Lambda_{\overline{MS}}$ by a flavour-dependent coefficient C[7]:

$$\Lambda_{\overline{MS}}^{\ 2} = C\ k$$

$$C = 3.320 \text{ for c}$$

$$C = 2.614 \text{ for b}$$

$$C = 1.914 \text{ for t}$$

For the set of C's here, we can not get the correct relation between k and $\Lambda_{\overline{MS}}$. But nevertheless, if we only use the ratio of the C's to fix the ratio of k between c quark and b quark, there is remarkable improvement of the fitting to the T family (cf Table 1b' and Table 2b'). In the calculation with the Gromes term we use $M_b = 4.619$ GeV, and in the calculation with the B-G term $M_b = 4.544$ GeV is used.

The Gromes and B-G terms require slightly different parameters and quark masses, and the results they give do not differ significantly.

Table 1b'

T family	mass(MeV) th	mass(MeV) exp	$M(^3S_1)-M(^1S_0)$ th	$M(^3S_1)-M(^1S_0)$ exp	$\Gamma(e^+e^-)$(KeV) th I	$\Gamma(e^+e^-)$(KeV) th II	$\Gamma(e^+e^-)$(KeV) exp
1^3S_1	9460	9460	39		0.75	1.2	1.26
2^3S_1	9973	10023	26		0.45	0.71	0.54
3^3S_1	10346	10355	23				
4^3S_1	10662	10501	21				
1P	9820	9903					

c.o.g.

with the Gromes term.

Table 2b'

T family	mass(MeV) th	mass(MeV) exp	$M(^3S_1)-M(^1S_0)$ th	$M(^3S_1)-M(^1S_0)$ exp	$\Gamma(e^+e^-)$(KeV) th I	$\Gamma(e^+e^-)$(KeV) th II	$\Gamma(e^+e^-)$(KeV) exp
1^3S_1	9460	9460			0.8	1.2	1.26
2^3S_1	10036	10023			0.52	0.78	0.54
3^3S_1	10452	10355					
4^3S_1	10798	10573					
1P	9874	9904					

c.o.g.

with the B-G term.

Table 3

ψ	coulomb	linear	KE	Gromes
1S	-293	392	348	-155
2S	-181	765	484	-178
3S	-141	1060	616	-208
4S	-120	1330	734	-242
T				
1S	-319	239	285	-44
2S	-182	496	344	-47
3S	-141	695	431	-51
4S	-118	874	505	-56

with the Gromes term.

Table 4

ψ	Coulomb	linear	KE	B-G
1S	-264	501	390	-136
2S	-167	957	567	-270
3S	-132	1320	733	-457
4S	-112	1635	888	-679
T				
1S	-303	301	308	-18
2S	-180	605	400	-33
3S	-140	844	506	-56
4S	-118	1058	596	-81

with the B-G term.

To give some sense of the relative contributions of the various terms in the potential to the binding energy, we list the contribution of each term (KE is the kinetic energy term) in Tables 3 and 4. From these two tables we see that, in bottomonium states, a non-relativistic calculation is justifiable, because the kinetic energy is small compared with the bottom quark mass. The relativistic corrections calculated from either the Gromes term or B-G term are small. It should be pointed out that the kinetic energy contributions are comparable to the linear terms for the lowest states.

To this point, we accept the view of people working on potential models. In many of these kinds of calculations, v/c is not really small. Thus Martin's treatment of the ϕ particle is on shaky ground, since it is obviously not a non-relativistic system. But, given how well the simple model works with so few parameters, and how difficult it is to improve on these potential models, we just go ahead and solve the non-relativistic Schrödinger equation, and see what results come out.

The leptonic decay width is another piece of information for the charmonium and bottomonium systems. Later on we shall estimate the leptonic decay width of the $(Q\bar{q})$ mesons. The decay width is calculated by means of the Weisskopf-Van Royen formula[8]

$$\Gamma(e^+e^-) = 16\ \pi\ e_q^2\ \alpha_e^2\ \psi^2(0)\ /\ M_V^2 \qquad (39)$$

Here e_q is the quark electric charge. M_V is the mass of the original state.

The QCD correction due to one-gluon exchange is :

$$1 - \frac{16}{3\pi}\alpha_s \tag{40}$$

For the QCD fine structure constant, Eq.(40) changes the width by about a factor of two. Some theoretical work has been done to estimate this correction more precisely[9]. But ambiguities exist due to the fact that the bound state field equation has to be solved approximately. The most interesting one among these calculations is only slightly different from the one-gluon exchange correction given by Eq.(40) for charmonium and bottomonium states. In our fitting , the experimentally measured decay width is in between the calculated width with and without the QCD correction factor. We will use these two values as the estimated limits for the $(Q\bar{q})$ mesons.

One further piece of experimental information which can be compared with the potential model is the rate of electro-magnetic radiative transitions. The magnetic dipole transition width is given by:

$$\Gamma_{M1} = (e_q M_q/2)^2 \alpha E^3 M_{if}^2 (2J+1) \tag{41}$$

where J is the final state angular momentum, E is the photon energy , and

$$M_{if} = \int_0^\infty R_i(r) R_f(r) j_0(Er/2) r^2 dr \tag{42}$$

$R_i(r)$ and $R_f(r)$ are the radial wavefunctions of the initial and final states. j_0 is the zeroth order spherical Bessel function.

The comparison between theory and experiment is given in Table 5. The calculation of $\Gamma(J/\psi \to \gamma\eta_c)$ and $\Gamma(\psi' \to \gamma\eta_c')$ only depends on the quark

Table 5

decay mode	th (Gromes term)	th (B-G term)	exp(KeV)
$\Gamma(J/\psi \to \gamma\eta_c)$	0.61	0.7	0.80±0.20
$\Gamma(\psi' \to \gamma\eta_c')$	0.35	0.40	0.43~2.6
$\Gamma(\psi' \to \gamma\eta_c)$	0.87	0.98	0.60±0.15

mass, since $M_{if} \simeq 1.0$. The calculation of $\Gamma(\psi' \to \gamma\eta_c)$ depends on the overlap of the 1S and 2S wave functions. For all of those transitions, the agreement is reasonable.

THE PREDICTIONS FOR $(Q\bar{q})$ SYSTEM

Now we come to $(Q\bar{q})$ states. According to QCD , to the first order of approximation, the force binding $(Q\bar{q})$ is the same which binds $(Q\bar{Q})$ together. Thus we use the same potential and the same parameters to calculate the $(Q\bar{q})$ states. Experimentally, $(c\bar{u})$, $(c\bar{d})$, $(c\bar{s})$, $(b\bar{u})$, $(b\bar{d})$ are known, as well as the 1S triplet-singlet splitting of the D and F states. With regard to the parameters, the s, u, and d quark masses can be fitted by D and F meson masses. Here we use the same mass for u and d quarks. Because this model is so crude, we cannot distinguish this small mass difference.

The other problem is the QCD running coupling constant. The light quark masses are close to the cut off parameter $\Lambda_{\overline{MS}}$, and so we can not use Eq.(33) to determine $\alpha_s(M_q)$. Fortunately, we have experimental data for the D and F triplet-singlet mass splitting:

$$M(D^0) = 1865 \text{ MeV}$$

$$M(D^*) - M(D^0) = 135 \text{ MeV}$$

$$M(F^{\pm}) = 1971 \text{ MeV}$$

$$M(F^*) - M(F) = 139 \text{ MeV}$$

This helps to fix α_s for light quarks, as well as their masses. To get the correct masses and mass splitting of D and F, in addition to M_c, k, we need to set (note that we are really dealing with the constituent masses):

$$M_s = 362 \text{ MeV}$$

$$\alpha_s(M_s) = 0.365$$

$$M_{u,d} = 295 \text{ MeV}$$

$$\alpha_s(M_{u,d}) = 0.380$$

with the Gromes term, and

$$M_s = 422 \text{ MeV}$$

$$\alpha_s(M_s) = 0.307$$

$$M_{u,d} = 381 \text{ MeV}$$

$$\alpha_s(M_{u,d}) = 0.315$$

with the B-G term.

The contribution of each term in the potential is shown in Tables 6 and 7.

We find for the leptonic decay constants without the QCD corrections:

$$f_F = 323 \text{ MeV}$$

$$f_D = 298 \text{ MeV}$$

with the Gromes term,and

$$f_F = 367 \text{ MeV}$$

$$f_D = 360 \text{ MeV}$$

with the B-G term.

If we include the QCD corrections, then we find:

$$f_F = 199 \text{ MeV}$$

$$f_D = 178 \text{ MeV}$$

with the Gromes term, and

$$f_F = 254 \text{ MeV}$$

$$f_D = 246 \text{ MeV}$$

with the B-G term.

It should be noted that these values M_s and α_s predict the properties of the ϕ meson as in Tables 8 and 9. Also with the Gromes term, the 2S

Table 6

	Coulomb	linear	KE	Gromes
F	-225	565	402	-416
D	-220	602	417	-506

with the Gromes term.

Table 7

	Coulomb	linear	KE	B-G
F	-209	667	444	-536
D	-208	686	453	-625

with the B-G term.

All numbers are in MeV.

Table 8

	mass(MeV)	$M(^3S_1)-M(^1S_0)$	$\Gamma(e^+e^-)$ (KeV)
calculation	1065	284	th I 0.9 th II 2.4
experiment	1020		1.43±0.12

with Gromes term.

Table 9

	mass(MeV)	$M(^3S_1)-M(^1S_0)$	$\Gamma(e^+e^-)$ (KeV)
calculation	1166	249	th I 1.4 th II 2.9
experiment	1020		1.43±0.12

with the B-G term.

state mass is 1713 MeV, whereas the B-G term predicts the 2S mass as 1231 MeV, compared with the experimental value of 1685 MeV. With Gromes term, the c.o.g. of 1P state is 1525 MeV, compared with the experimentally observed 1420 MeV. The 1S, 1P, and 2S masses calculated with the Gromes term are close to the experimentally observed values. This is an encouragement to the potential model calculation involving s quarks.

With the same parameters, in addition to M_c, we can predict the properties of the B and B_s state. They are shown in Table 10. The contribution of each term in the potential is in Table 11.

The B mass is about 100 MeV below the experimentally reported value, but compared with the magnitude of the contribution of each term in the potential, the disagreement is not too bad. We expect that the B_s state is also 100 MeV higher than the prediction here, at a mass of about 5350 MeV. This agrees with the prediction of the Martin potential. With his parameters, we get $M(B_s) = 5380$ MeV. Note that the predicted B_s state is fairly close to what one gets from a simple estimate:

$$M(B_s) \leq [M(\Upsilon)+M(\phi)]/2 \simeq 5240 \text{ MeV}$$

We still need further experimental confirmation of the B_s mass.

As for the leptonic decay constant of the B meson, we find, without the QCD correction:

$$f_B = 196 \text{ MeV}$$

with the Gromes term, and

$$f_B = 245 \text{ MeV}$$

with the B-G term. If we include the QCD correction, it is

$$f_B = 117 \text{ MeV}$$

with the Gromes term, and

Table 10

	calculated	exp	calculated
	MeV	MeV	$M(^3S_1)-M(^1S_0)$
B	5191	5270	52
B_s	5283	not known yet	52

with the Gromes term.

B	5158	5270	52
B_s	5256	not known yet	51

with the B-G term.

All numbers are in MeV.

Table 11

	Coulomb	linear	KE	Gromes
B	-232	572	406	-457
B_s	-241	531	389	-365

with the Gromes term.

	Coulomb	linear	KE	B-G term
B	-224	640	437	-618
B_s	-227	616	429	-527

with the B-G term.

$$f_B = 167 \text{ MeV}$$

with the B-G term. There is no similar quantity for the $B\bar{s}$ state.

We can calculate the $(b\bar{c})$ states using the parameters deduced only from charmonium and bottomonium data. Thus, we get,

$$M(B_c) = 6180 \text{ MeV}$$

$$M(B_c^*) - M(B_c) = 71 \text{ MeV}$$

with the Gromes term, and

$$M(B_c) = 6193 \text{ MeV}$$

$$M(B_c^*) - M(B_c) = 65 \text{ MeV}$$

with the B-G term.

The contribution from each term in the potential is listed in Tables 12 and 13. Evidently, the non-relativistic calculation is well justified. So we expect the predicted mass to be close to the correct value. It should be noted that this prediction is about the same as that obtained by the rough estimate:

$$M(B_c) = [M(T)+M(\eta_c)]/2 \simeq 6220 \text{ MeV}$$

The predicted $f_{b\bar{c}}$, without QCD correction, is

$$f_{b\bar{c}} = 496 \text{ MeV}$$

with the Gromes term, and

$$f_{b\bar{c}} = 480 \text{ MeV}$$

with the B-G term. If we include the QCD correction, we get

$$f_{b\bar{c}} = 332 \text{ MeV}$$

with the Gromes term, and

$$f_{b\bar{c}} = 342 \text{ MeV}$$

with the B-G term.

We expect the correct value to lie between these two.

Table 12

Coulomb	linear	KE	Gromes
-365	319	345	-100

with the Gromes term.

Table 13

Coulomb	linear	KE	B-G term
-326	409	376	-89

with the B-G term.

All quantities are in MeV.

For all the leptonic decay constants f , and from the calculated charmonium and bottomonium leptonic decay widths compared with experiment, we expect that the correct value is between the one without QCD correction and the one with it. One interesting conclusion is the inequality of the f's of the different ($Q\bar{q}$) mesons.

$$f_{B_c} \geq f_F \geq f_D \geq f_B \geq f_K \geq f_\pi$$

THE STATES WITH T QUARKS

To complete the discussion of the $(Q\bar{Q})$ and $(Q\bar{q})$ systems, we calculate the $(t\bar{t})$ and $(t\bar{q})$ states, q is u, d, s, c, or b. Assuming that M_t = 40 GeV, the predictions of the toponium states are in Tables 14 and 15. The t-lighter antiquark states are predicted in Tables 16 and 17. In the table, T^* is the 1^3S_1 state, T is the 1^1S_0 state.

Table 14

	mass(MeV)	$M(^3S_1)-M(^1S_0)$	$\Gamma(e^+e^-)$ I	$\Gamma(e^+e^-)$ II
1^3S_1	79763	22.5	4.3	3.2
2^3S_1	80271	8.05	1.5	1.1
3^3S_1	80547	5.84	1.1	0.82
4^3S_1	80765	4.93	0.91	0.69
1P c.o.g.	80201			

with the Gromes term. And

Table 15

	mass(MeV)	$M(^3S_1)-M(^1S_0)$	$\Gamma(e^+e^-)$ I	$\Gamma(e^+e^-)$ II
1^3S_1	79844	20.3	4.0	3.1
2^3S_1	80385	8.2	1.6	1.2
3^3S_1	80700	6.2	1.2	0.93
4^3S_1	80952	5.3	1.0	0.78
1P c.o.g.	80287			

with the B-G term.

Table 16

	mass(MeV)	$M(T^*)-M(T)$	f I(KeV)	f II(KeV)
$t\bar{b}$	44682	15	553	442
$t\bar{c}$	41518	13		
$t\bar{s}$	40662	6.6	83	52
$t\bar{u}$ (or $t\bar{d}$)	40572	6.5	73	44

with the Gromes term. And

Table 17

	mass(MeV)	$M(T^*)-M(T)$	f I(KeV)	f II(KeV)
$t\bar{b}$	44702	13	540	441
$t\bar{c}$	41570	11		
$t\bar{s}$	40667	6.5	97	68
$t\bar{u}$ (or $t\bar{d}$)	40563	6.6	92	63

with the B-G term.

CONCLUSION

We have calculated the leptonic decay widths of the unequal quarkonium states with the decay constants calculated above. We take the larger of the two values determined by using the Gromes term, and by using the B-G term without QCD corrections to set the upper limit. The lower limit is set by the smaller of these two values with QCD correction. These results are given in Table 18. In Table 18, "Γ I" refers to the upper limit, and "Γ II" refers to the lower limit. We only consider the $\tau\bar{\nu}$ channel. The other two leptonic channels, i.e. the $\mu\bar{\nu}$ and $e\bar{\nu}$ channels have branching ratios which are negligible compared to the $\tau\bar{\nu}$ branching ratio, due to the V-A structure of the weak current and the small masses of e or μ. In Table 18, V_{bu}, V_{ts} and V_{td} are the elements of the KM matrix which we do not know yet. The other KM matrix element V_{bc}, is in the range:

$$0.036 < V_{bc} < 0.070,$$

so we can give limits on B_c leptonic decay width:

$$10^{-4}\ \text{eV} < \Gamma(B_c \to \tau\bar{\nu}_\tau) < 10^{-5}\text{eV}.$$

The total width estimated by the spectator picture is between 1.5×10^{-3} eV and 5×10^{-4} eV, so the branching ratio of $\tau\nu$ is between 6% and 2%. In the spectator picture, we assume that the b quark decays freely, without the participation of the c quark, that is, the c quark is only a spectator in the decay process. This picture can only give an order of magnitude estimate.

Among all these particles, only F, D and B_c have relatively large $\tau\bar{\nu}_\tau$ branching ratios; this is due to the fact that according to the spec-

Table 18

	Γ(tot)	$\Gamma(\tau\bar{\nu})$ I	$\Gamma(\tau\bar{\nu})$II	B($\tau\bar{\nu}$) I	B($\tau\bar{\nu}$) II
cs	3.5×10^{-3}	1.0×10^{-4}	3.9×10^{-3}	3.0%	1.1%
cd	7.2×10^{-4}	1.5×10^{-6}	3.7×10^{-7}	0.21%	0.05%
bc	$\sim10^{-4}$	$2.2\times10^{-2}V_{bc}$	$1.0\times10^{-2}V_{bc}$		
bu	4.7×10^{-4}	$4.3\times10^{-3}V_{bu}$	$9.8\times10^{-4}V_{bu}$		
tb	$\sim10^{4}$	3.7×10^{-1}	2.4×10^{-1}		
ts	$\sim10^{4}$	$6.8\times10^{-3}V_{ts}$	$1.9\times10^{-3}V_{ts}$		
td	$\sim10^{4}$	$6.0\times10^{-3}V_{td}$	$1.4\times10^{-3}V_{td}$		

All decay widths are in terms of eV.

tator picture, the total width is proportional to the fifth power of the Q quark mass, whereas the $\tau\bar{\nu}_\tau$ partial width is proportional to the $(Q\bar{q})$ state mass which is close to the Q quark mass. So when we go to quarks of heavy masses, this branching ratio decreases rapidly. In the case of the D meson, the $\tau\bar{\nu}$ partial width is supressed by the Cabbibo angle, but the total width is not, because the D meson can decay to Cabbibo favoured strange mesons, so that the $\tau\bar{\nu}$ branching ratio is suppressed by the factor $\sin^2\theta_c$, which is about 0.05. For the F meson, the $\tau\bar{\nu}_\tau$ channel is favoured by the Cabbibo angle, however the experimentally measured total width is several times wider than the estimate given by the spectator picture. The observed $\Gamma_{total}(F)$ is about five times $\Gamma_{total}(D^{\pm})$, but the spectator picture predicts that they should be equal. Thus the $\tau\bar{\nu}_\tau$ partial width is several times smaller than we would have otherwise expected from simple considerations.

To conclude the discussion, we would like to compare the predicted masses of the $(Q\bar{q})$ states and triplet-singlet state mass splitting with Martin's empirical relation:

$$[M(1^3S_1)]^2 - [M(1^1S_0)]^2 \simeq 0.56\ \text{GeV}^2$$

For example,

$$M_\rho{}^2 - M_\pi{}^2 = 0.57\ \text{GeV}^2$$

$$M_K{}^{*2} - M_K{}^2 = 0.55\ \text{GeV}^2$$

$$M_D{}^{*2} - M_D{}^2 = 0.55\ \text{GeV}^2$$

$$M_F{}^{*2} - M_F{}^2 = 0.57\ \text{GeV}^2$$

Martin's relation also holds for the predicted B meson splitting:

$$M(B^*) = 5320\ \text{MeV}$$

$$M(B\ ) = 5270\ \text{MeV}$$

$$M^2(B^*) - M^2(B) = 0.53 \text{ GeV}^2$$

and also for $(b\bar{s})$ splitting:

$$M(B_s^*) \simeq 5420 \text{ MeV}$$

$$M(B_s) \simeq 5370 \text{ MeV}$$

$$M^2(B_s^*) - M^2(B_s) \simeq 0.54 \text{ GeV}^2$$

However for our predicted $(b\bar{c})$ states, the relation are given by:

$$M(B_c) \simeq 6200 \text{ MeV}$$

$$M(B_c^*) \simeq 6265 \text{ MeV}$$

$$M^2(B_c^*) - M^2(B_c) \simeq 0.8 \text{ GeV}^2$$

and the predicted $(t\bar{q})$ states, the relations are given by:

$$M(T^*) - M(T) \simeq 0.54 \text{ GeV}^2$$

$$M(T_s^*) - M(T_s) \simeq 0.53 \text{ GeV}^2$$

$$M(T_c^*) - M(T_c) \simeq 0.91 \text{ GeV}^2$$

$$M(T_b^*) - M(T_b) \simeq 1.2 \text{ GeV}^2$$

According to the potential model calculation in this work, only T and T_s still obey Martin's relation, but T_c and T_b violate it badly. If Martin's relation is valid for all the quark-light-antiquark systems, then the singlet-triplet splitting of B_c, T_c, and T_b would be smaller than the predictions given by our potential model. It is interesting to see the experimental results. In the $(Q\bar{q})$ system, the potential model does not give Martin's relation.

The potential model can not explain two important properties of the quarkonium system. The first is the mass difference between 2^3S_1 and 1^3S_1 states approximately given by 500 ~ 600 MeV. For example, this is 589 MeV for charmonium and 563 MeV for bottomonium. The potential model can not explain this approximate constant. But, incidently, for toponium,

we predict that the mass difference between the 1^3S_1 state and the 2^3S_1 state is 508 MeV using Gromes term, and 541 MeV using B-G term, this tends to support the calculation. The second property is the constancy of the leptonic decay width divided by the charge squared, i.e.

$$\Gamma(^3S_1 \to e^+e^-) \; / \; e_q^2 \simeq 11 \text{ KeV} \tag{43}$$

It is difficult to explain Eq (43) by any potential if we also want to get the correct mass spectrum. However, in the potential model calculations of $(s\bar{s})$, $(c\bar{c})$ and $(b\bar{b})$ e^+e^- decay widths, if we take the prediction without QCD correction as the upper limit, and take the prediction with the QCD correction as the lower limit, the experimental values, which agree with Eq.(43), are always in this range. In the prediction of the $(t\bar{t})$ system, the 1^3S_1 state leptonic decay width is expected to be equal to the charmonium 1^3S_1 state leptonic decay width, which is 4.6±0.39 KeV experimentally, if Eq.(43) is valid for the t quark. Our prediction is close to this value, at about 4 KeV.

So far in this work, we have seen that the Coulomb+linear potential gives a good approximation to many properties of the quarkonium systems. We expect this potential will also give reasonable approximations to the $(Q\bar{q})$ systems. By comparing the predictions of the $(Q\bar{q})$ systems with future experiments, it will bring some light to a better understanding of the quarks and hadrons.

REFERENCES FOR PART II

1. A. Martin, Phys. Lett.100B,511(1981)

2. W. Buchmuller, S. H. H. Tye, Phys.Rev.D24,132(1981);

3. E. Eichten, K. Gottfried, T. Kinoshita, K. D. Lane, T. M. Yan, Phys. Rev. D21,203(1980)

4. Paul B. Mackenzie, G. P. Lepage, Phys. Rev. Lett. 47,1244(1981);

5. D. Gromess, Z.Phys.C 22,265(1984);

6. T. Barnes, G. I. Ghandour, Phys. Lett.118B,411(1982);

7. A. A. Bykov, I. M. Dremin, A. V. Leonidov, Sov. J. Nucl. Phys. 39(4),618(1984);

8. R. Van Royen, V. F. Weisskopf, Nuovo Cim.50,617(1967);

9. E. C. Poggio, H. J. Schnitzer, Phys. Rev. D20, 1175(1979);

The vita has been removed from the scanned document